Electronic Supplementary Material (ESI) for RSC Advances.

First efficient synthesis of SF_5-substituted pyrrolidines using 1,3-dipolar cycloaddition of azomethine ylides with pentafluorosulfanyl-substituted acrylic esters and amides

E. Falkowska, [a] V. Tognetti, [a] L. Joubert, [a] P. Jubault [a] *, J.-P. Bouillon, [a] * X. Pannecoucke [a]

[a]*Normandie Univ., COBRA, UMR 6014 & FR 3038, Univ. Rouen, INSA Rouen, CNRS, 1 rue Tesnière, F-76821 Mont-Saint-Aignan Cedex, France.*

E-mail: philippe.jubault@insa-rouen.fr, jean-philippe.bouillon@univ-rouen.fr

Supporting Information

Table of Contents

1. General Remarks

All reactions were carried out in oven dried reaction glassware under argon. Reaction temperatures are reported as the temperature of the bath surrounding the vessel. Dry dichloromethane used was purified by distillation over CaH_2 and was transferred under argon. Commercially available chemicals were obtained from Acros Organics, Aldrich Chemical Co., ABCR (SF_5Cl), Alfa Aesar, Fischer Scientific and were used without further purification. NMR spectra were recorded on a Bruker DXP 300. Chemical shifts (δ) are quoted in ppm relative to TMS (^1H) and $CFCl_3$ (^{19}F). Coupling constants (*J*) are quoted in Hz. The following abbreviations were used to show the multiplicities: s singlet, d doublet, t triplet, q_t quintuplet, dd: doublet of doublet, m: multiplet. The residual solvent signal was used as reference ($CDCl_3$: δH = 7.26 ppm, δC = 77.00 ppm). High-Resolution Mass Spectra (HRMS) were recorded on Waters LCT Premier. Infrared spectra were recorded on a Perkin Elmer FT-IR spectrometer Paragon 100 (ATR) ; the wave numbers (ν) of recorded IR-signals are quoted in cm^{-1}. Melting points were recorded on Kofler bench and are uncorrected. Analytical thin layer chromatography was performed on precoated 200 µm layer thickness silica gel 60 Alugram® Xtra SIL G/UV_{254}. Visualization was accomplished with short wave UV light, phosphomolybdenic acid staining solution followed by heating. Flash chromatography was performed on Merck silica gel (40-63 mesh) either by standard technique or a Biotage Isolera One Flash Purification System (gradient of solvents).

2. General Procedure for the Synthesis of Pyrrolidines 5

To a stirred solution of ester **2** or amide **3** (1 equiv, 0.31 mmol) in dry CH_2Cl_2 (1.8 mL) under argon, was added dipole precursor **4** (1.2 equiv, 0.37 mmol or 2 equiv, 0.62 mmol, depending on the substrate). The mixture was cooled to 0 °C and 1M solution of trifluoroacetic acid (TFA) (0.1 equiv, 0.03 mmol) in CH_2Cl_2 was added at this temperature. After 2 h of stirring at room temperature, a saturated solution of sodium bicarbonate (1 mL) was added to the reaction mixture until pH = 7. The organic phase was separated, washed with brine (1 mL) and dried over $MgSO_4$. After removal of solvent under reduced pressure, the crude product was purified by silica gel column chromatography leading to pyrrolidine **5**.

(±)-N-Benzyl-3-(benzyloxycarbonyl)-4-pentafluorosulfanylpyrrolidine (5a)

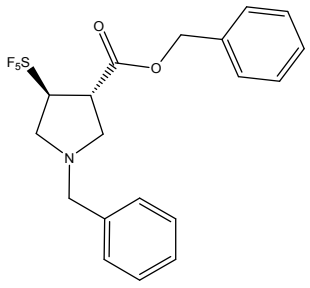

The title compound was prepared according to the general procedure as described above. The resulting crude product was purified by silica gel column chromatography (PE/AcOEt: 92/8)

to afford **5a** in 69% yield as a colourless oil. R*f* (PE/AcOEt: 94/6) = 0.27. ^{19}F NMR ($CDCl_3/CFCl_3$, 282 MHz): δ 59.2 (dd, $^2J_{F,F}$ = 143.9 Hz, $^3J_{F,H}$ = 5.2 Hz, 4F), 84.7 (m, 1F). ^{1}H NMR ($CDCl_3$, 300 MHz): δ 2.9-3.0 (m, 3H), 3.23 (m, 1H), 3.6-3.7 (m, 3H), 5.03 (m, 1H), 5.20 (s, 2H), 7.3-7.4 (m, 10H). ^{13}C NMR ($CDCl_3$, 75 MHz): δ 46.7 (q_t, $^3J_{F,C}$ = 3.6 Hz), 55.8, 56.4 (q_t, $^3J_{F,C}$ = 4.7 Hz), 58.9, 67.3, 83.3 (q_t, $^2J_{F,C}$ = 11.1 Hz), 127.3, 128.0 (2C), 128.3, 128.37 (2C), 128.38 (2C), 128.5 (2C), 135.3, 137.4, 171.6. ATR-FTIR (cm^{-1}): 3033, 2807, 1738, 1173. HRMS (ESI$^+$): *m/z* calcd for $[M+H]^+$ $C_{19}H_{21}F_5NO_2S$ 422.1213, found 422.1197.

(±)-N,N-Dibenzyl-1-benzyl- 4-pentafluorosulfanylpyrrolidinyl-3-carboxamide (5b)

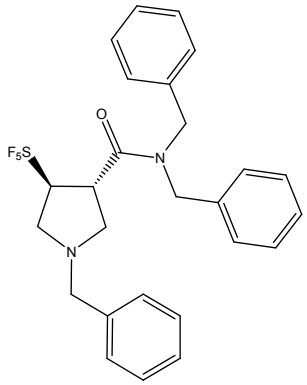

The title compound was prepared according to the general procedure as described above. The resulting crude product was purified by silica gel column chromatography (PE/AcOEt: 88/12) to afford **5b** in 79% yield as a white solide. M.p. 80 °C. R*f* (PE/AcOEt: 90/10) = 0.16. ^{19}F NMR ($CDCl_3/CFCl_3$, 282 MHz): δ 59.6 (dd, $^2J_{F,F}$ = 145.7 Hz, $^3J_{F,H}$ = 5.2 Hz, 4F), 85.6 (m, 1F). ^{1}H NMR ($CDCl_3$, 300 MHz): δ 2.64 (m, 1H), 2.80 (m, 1H) 3.17 (m, 2H), 3.53 (d, $^2J_{H,H}$ = 13.3 Hz, 1H), 3.71 (d, $^2J_{H,H}$ = 13.3 Hz, 1H), 3.88 (m, 1H), 4.30-4.50 (m, 3H), 4.89 (d, $^2J_{H,H}$ = 14.7 Hz, 1H), 5.48 (m, 1H), 7.1-7.2 (m, 5H), 7.3-7.4 (m, 10H). ^{13}C NMR ($CDCl_3$, 75 MHz): δ 44.7 (q_t, $^3J_{F,C}$ = 3.3 Hz), 48.7, 49.7, 56.2 (q_t, $^3J_{F,C}$ = 5.0 Hz), 56.4, 59.0, 84.3 (q_t, $^2J_{F,C}$ = 10.3 Hz), 126.4 (2C), 127.3, 127.5, 127.9, 128.0 (2C), 128.4 (4C), 128.7 (2C), 129.0 (2C), 135.7, 136.8, 137.5, 171.4. ATR-FTIR (cm^{-1}): 3030, 2807, 1648. HRMS (ESI$^+$): *m/z* calcd for $[M+H]^+$ $C_{26}H_{28}F_5N_2OS$ 511.1843, found 511.1837.

(±)-N-Benzyl-3-[(2'-nitro)benzyloxycarbonyl)]-4-pentafluorosulfanylpyrrolidine (5c)

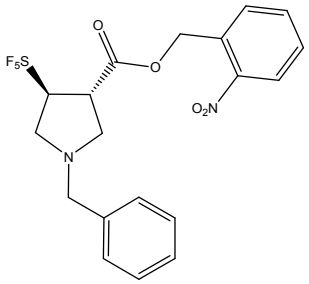

The title compound was prepared according to the general procedure as described above. The resulting crude product was purified by silica gel column chromatography (PE/AcOEt: 86/14)

to afford **5c** in 88% yield as a yellow oil. R*f* (PE/AcOEt: 86/14) = 0.29. ^{19}F NMR ($CDCl_3/CFCl_3$, 282 MHz): δ 59.2 (dd, $^2J_{F,F}$ = 143.9 Hz, $^3J_{F,H}$ = 5.2 Hz, 4F), 84.6 (m, 1F). ^{1}H NMR ($CDCl_3$, 300 MHz): δ 2.9-3.0 (m, 3H), 3.25 (m, 1H), 3.63 (d, $^2J_{H,H}$ = 13.2 Hz, 1H), 3.69 (d, $^2J_{H,H}$ = 13.2 Hz, 1H), 3.71-3.78 (m, 1H), 5.03 (m, 1H), 5.61 (s, 2H), 7.3-7.4 (m, 5H), 7.5-7.6 (m, 2H), 7.67 (dd, $^3J_{H,H}$ = 7.4 Hz, $^3J_{H,H}$ = 7.4 Hz, 1H), 8.15 (d, $^3J_{H,H}$ = 8.2 Hz, 1H). ^{13}C NMR ($CDCl_3$, 75 MHz): δ 46.7 (q_t, $^3J_{F,C}$ = 3.5 Hz), 55.8, 56.4 (q_t, $^3J_{F,C}$ = 4.7 Hz), 58.9, 64.0, 83.2 (q_t, $^2J_{F,C}$ = 11.6 Hz), 125.1, 127.4, 128.41 (2C), 128.44 (2C), 128.9, 129.0, 131.3, 133.8, 137.4, 147.4, 171.3. ATR-FTIR (cm^{-1}): 2919, 1705, 1522, 1342. HRMS (ESI$^+$): *m/z* calcd for $[M+H]^+$ $C_{19}H_{20}F_5N_2O_4S$ 467.1064, found 467.1064.

(±)-N-Benzyl-3-(dodecyloxycarbonyl)-4-pentafluorosulfanylpyrrolidine (5d)

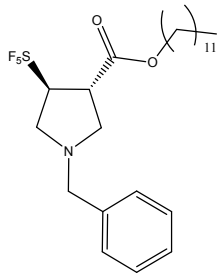

The title compound was prepared according to the general procedure as described above. The resulting crude product was purified by silica gel column chromatography (PE/AcOEt: 96/4) to afford **5d** in 62% yield as a colourless oil. R*f* (PE/AcOEt: 96/4) = 0.26. ^{19}F NMR ($CDCl_3/CFCl_3$, 282 MHz): δ 59.1 (dd, $^2J_{F,F}$ = 143.9 Hz, $^3J_{F,H}$ = 5.2 Hz, 4F), 84.8 (m, 1F). ^{1}H NMR ($CDCl_3$, 300 MHz): δ 0.89 (m, 3H), 1.2-1.4 (m, 18H), 1.5-1.6 (m, 2H) 2.89 (d, $^3J_{H,H}$ = 6.8 Hz, 2H), 2.98 (m, 1H), 3.21 (m, 1H), 3.6-3.7 (m, 3H), 4.15 (t, $^3J_{H,H}$ = 6.6 Hz, 2H) 5.00 (m, 1H), 7.3-7.4 (m, 5H). ^{13}C NMR ($CDCl_3$, 75 MHz): δ 14.1, 22.7, 25.7, 28.5, 29.2, 29.3, 29.45, 29.52, 29.6 (2C), 31.9, 46.8 (q_t, $^3J_{F,C}$ = 3.7 Hz), 56.0, 56.5 (q_t, $^3J_{F,C}$ = 4.4 Hz), 59.1, 65.8, 83.4 (q_t, $^2J_{F,C}$ = 11.6 Hz), 127.4, 128.41 (2C), 128.45 (2C), 137.5, 171.9. ATR-FTIR (cm^{-1}): 2924, 2854, 1740, 1457, 1189. HRMS (ESI$^+$): *m/z* calcd for $[M+H]^+$ $C_{24}H_{39}F_5NO_2S$ 500.2622, found 500.2621.

(±)-N-Benzyl-3-(benzyloxycarbonyl)-3-methyl-4-pentafluorosulfanylpyrrolidine (5e)

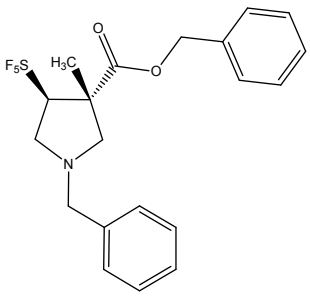

The title compound was prepared according to the general procedure as described above. The resulting crude product was purified by silica gel column chromatography (PE/AcOEt: 98/2)

to afford **5e** in 46% yield as a colourless oil. R*f* (PE/AcOEt: 96/4) = 0.28. ^{19}F NMR ($CDCl_3/CFCl_3$, 282 MHz): δ 65.7 (d, $^2J_{F,F}$ = 143.9 Hz, 4F), 85.0 (m, 1F). ^{1}H NMR ($CDCl_3$, 300 MHz): δ 1.69 (s, 3H), 2.83 (d, $^2J_{H,H}$ = 8.8 Hz, 1H), 2.95 (d, $^2J_{H,H}$ = 8.8 Hz, 1H), 3.21 (m, 1H), 3.47 (m, 1H), 3.74 (m, 2H), 5.20 (s, 2H), 5.2-5.3 (m, 1H), 7.3-7.4 (m, 10H). ^{13}C NMR ($CDCl_3$, 75 MHz): δ 19.5 (m), 52.9, 53.3 (q_t, $^3J_{F,C}$ = 5.0 Hz), 60.0, 64.4, 67.6, 86.1 (q_t, $^2J_{F,C}$ = 10.5 Hz), 127.4, 128.2 (2C), 128.4 (2C), 128.45, 128.51 (2C), 128.6 (2C), 135.4, 137.9, 172.9. ATR-FTIR (cm^{-1}): 1734, 1455, 1263, 1212, 1107. HRMS (ESI$^+$): *m/z* calcd for $[M+H]^+$ $C_{20}H_{23}F_5NO_2S$ 436.1370, found 436.1367.

(±)-N-Benzyl-1-benzyl-4-pentafluorosulfanylpyrrolidinyl-3-carboxamide (5f)

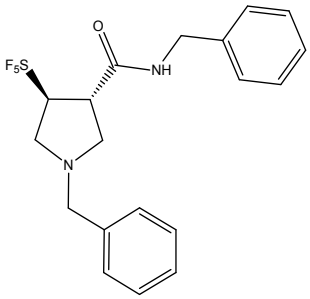

The title compound was prepared according to the general procedure as described above. The resulting crude product was purified by silica gel column chromatography (cyclohexane/AcOEt: 82/18) to afford **5f** in 92% yield as a white solid. M.p. 126-128 °C. R*f* (cyclohexane/AcOEt: 82/18) = 0.12. ^{19}F NMR ($CDCl_3/CFCl_3$, 282 MHz): δ 59.3 (dd, $^2J_{F,F}$ = 145.7 Hz, $^3J_{F,H}$ = 5.2 Hz, 4F), 85.0 (m, 1F). ^{1}H NMR ($CDCl_3$, 300 MHz): δ 2.8-2.9 (m, 2H), 3.1-3.2 (m, 2H), 3.43 (m, 1H), 3.6-3.7 (m, 2H), 4.36 (dd, $^2J_{H,H}$ = 14.5 Hz, $^3J_{H,H}$ = 5.1 Hz, 1H), 4.46 (dd, $^2J_{H,H}$ = 14.5 Hz, $^3J_{H,H}$ = 5.1 Hz, 1H), 5.00 (m, 1H), 6.07 (br s, 1H), 7.2-7.3 (m, 10H). ^{13}C NMR ($CDCl_3$, 75 MHz): δ 43.9, 48.7 (q_t, $^3J_{F,C}$ = 3.6 Hz), 56.5 (m), 56.6, 59.1, 84.6 (q_t, $^2J_{F,C}$ = 11.0 Hz), 126.7, 127.4 (2C), 127.7 (2C), 128.1, 128.5 (2C), 128.8 (2C), 137.6, 137.7, 171.0. ATR-FTIR (cm^{-1}): 3269, 2796, 1639, 1557, 1431. HRMS (ESI$^+$): *m/z* calcd for $C_{19}H_{22}F_5N_2OS$ $[M+H]^+$ 421.1373, found 421.1366.

N-[(1R)-1-Phenylethyl]-1-benzyl-4-pentafluorosulfanylpyrrolidinyl-3-carboxamide (5g)

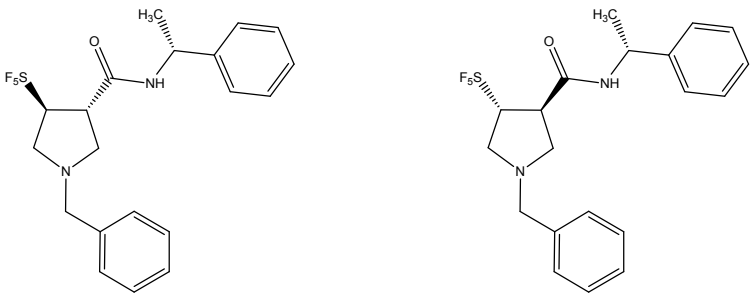

The title compound was prepared according to the general procedure as described above. The resulting crude product was purified by silica gel column chromatography

(cyclohexane/AcOEt: 82/18) to afford two diastereomers in 44% and 40% yield respectively, as white solids.

Diastereomer n°1:
M.p. 120-121 °C. R*f* (cyclohexane/AcOEt: 82/18) = 0.18. ^{19}F NMR ($CDCl_3/CFCl_3$, 282 MHz): δ 59.3 (dd, $^2J_{F,F}$ = 143.9 Hz, $^3J_{F,H}$ = 5.2 Hz, 4F), 85.1 (m, 1F). ^{1}H NMR ($CDCl_3$, 300 MHz): δ 1.47 (d, $^3J_{H,H}$ = 6.5 Hz, 3H), 2.7-2.8 (m, 2H), 3.13 (m, 2H), 3.39 (m, 1H), 3.5-3.7 (m, 2H), 4.93 (m, 1H), 5.10 (m, 1H), 6.07 (d, $^3J_{H,H}$ = 7.1 Hz, 1H), 7.2-7.5 (m, 10H). ^{13}C NMR ($CDCl_3$, 75 MHz): δ 21.6, 48.4 (q_t, $^3J_{F,C}$ = 3.3 Hz), 49.1, 56.3 (m), 56.4, 59.0, 84.6 (q_t, $^2J_{F,C}$ = 11.0 Hz), 126.0 (2C), 127.4, 127.5, 128.43 (2C), 128.45 (2C), 128.7 (2C), 137.6, 142.7, 170.1. ATR-FTIR (cm^{-1}): 3305, 2806, 1641, 1545, 1453. HRMS (ESI$^+$): *m/z* calcd for $[M+H]^+$ $C_{20}H_{24}F_5N_2OS$ 435.1530, found 435.1524.

Diastereomer n°2:
M.p. 116-118 °C. R*f* (cyclohexane/AcOEt: 82/18) = 0.07. ^{19}F NMR ($CDCl_3/CFCl_3$, 282 MHz): δ 59.3 (dd, $^2J_{F,F}$ = 145.7 Hz, $^3J_{F,H}$ = 5.2 Hz, 4F), 85.2 (m, 1F). ^{1}H NMR ($CDCl_3$, 300 MHz): δ 1.52 (d, $^3J_{H,H}$ = 6.8 Hz, 3H), 2.8-2.9 (m, 2H), 3.1-3.3 (m, 2H), 3.44 (m, 1H), 3.63 (d, $^2J_{H,H}$ = 12.7 Hz, 1H), 3.75 (d, $^2J_{H,H}$ = 12.7 Hz, 1H), 4.95 (m, 1H), 5.14 (m, 1H), 6.17 (br s, 1H), 7.3-7.5 (m, 10H). ^{13}C NMR ($CDCl_3$, 75 MHz): δ 21.6, 48.3 (q_t, $^3J_{F,C}$ = 3.3 Hz), 49.0, 56.5 (m), 56.6, 59.0, 84.6 (q_t, $^2J_{F,C}$ = 10.7 Hz), 125.9 (2C), 127.3, 127.4, 128.43 (2C), 128.47 (2C), 128.6 (2C), 137.6, 142.7, 170.3. ATR-FTIR (cm^{-1}): 3326, 2804, 1650, 1549, 1451. HRMS (ESI$^+$): *m/z* calcd for $C_{20}H_{24}F_5N_2OS$ $[M+H]^+$ 435.1530, found 435.1541.

(±)-N-Morpholino-1-benzyl-4-pentafluorosulfanylpyrrolidinyl-3-carboxamide (5h)

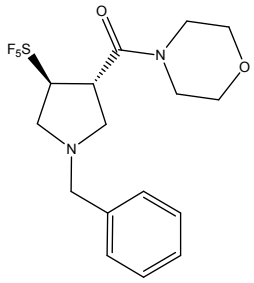

The title compound was prepared according to the general procedure as described above. The resulting crude product was purified by silica gel column chromatography (PE/AcOEt: 7/3) to afford **5h** in 73% yield as a white solid. M.p. 96 °C. R*f* (cyclohexane/AcOEt: 7/3) = 0.25. ^{19}F NMR ($CDCl_3/CFCl_3$, 282 MHz): δ 59.0 (dd, $^2J_{F,F}$ = 145.7 Hz, $^3J_{F,H}$ = 5.2 Hz, 4F), 85.5 (m, 1F). ^{1}H NMR ($CDCl_3$, 300 MHz): δ 2.58 (m, 1H), 2.98 (m, 1H), 3.1-3.3 (m, 2H), 3.4-39 (m, 11H), 5.33 (m, 1H), 7.3-7.4 (m, 5H). ^{13}C NMR ($CDCl_3$, 75 MHz): δ 42.7, 44.0 (q_t, $^3J_{F,C}$ = 3.6 Hz), 46.0, 56.0 (q_t, $^3J_{F,C}$ = 5.0 Hz), 56.1, 59.0, 66.5, 66.7, 84.1 (q_t, $^2J_{F,C}$ = 10.5 Hz), 127.3, 128.36 (2C), 128.43 (2C), 137.4, 170.0. ATR-FTIR (cm^{-1}): 2925, 2852, 1644, 1437, 1230. HRMS (ESI$^+$): *m/z* calcd for $[M+H]^+$ $C_{16}H_{22}F_5N_2O_2S$ 401.1322, found 401.1310.

(±)-N-Benzyl-1-benzyl-3-methyl-4-pentafluorosulfanylpyrrolidinyl-3-carboxamide (5i)

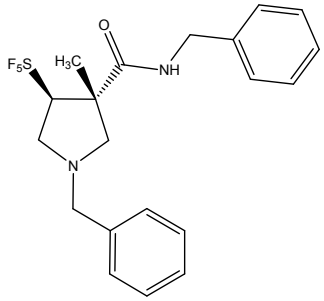

The title compound was prepared according to the general procedure as described above. The resulting crude product was purified by silica gel column chromatography (EP/AcOEt: 85/15) to afford **5i** in 36% yield as a colorless liquid. R*f* (EP/AcOEt: 80/20) = 0.24. ^{19}F NMR ($CDCl_3/CFCl_3$, 282 MHz): δ 65.6 (dd, $^2J_{F,F}$ = 143.9 Hz, $^3J_{F,H}$ = 3.5 Hz, 4F), 85.4 (m, 1F). ^{1}H NMR ($CDCl_3$, 300 MHz): δ 1.68 (s, 3H), 2.75 (d, $^2J_{H,H}$ = 8.8 Hz, 1H), 2.98 (d, $^2J_{H,H}$ = 8.8 Hz, 1H), 3.22 (m, 1H), 3.51 (m, 1H), 3.75 (s, 2H), 4.45 (dd, $^2J_{H,H}$ = 14.6 Hz, $^3J_{H,H}$ = 5.0 Hz, 1H), 4.60 (dd, $^2J_{H,H}$ = 14.6 Hz, $^3J_{H,H}$ = 5.0 Hz, 1H), 5.42 (m, 1H), 6.27 (br s, 1H), 7.3-7.4 (m, 10H). ^{13}C NMR ($CDCl_3$, 75 MHz): δ 18.9 (m), 44.1, 53.3 (q_t, $^3J_{F,C}$ = 5.0 Hz), 52.9, 59.8, 65.1, 86.7 (q_t, $^2J_{F,C}$ = 9.9 Hz), 127.3, 127.7 (2C), 128.1, 128.3 (2C), 128.4 (2C), 128.8 (2C), 137.8, 138.1, 172.3. ATR-FTIR (cm^{-1}): 3346, 3027, 1642, 1532, 1453. HRMS (ESI$^+$): *m/z* calcd for $[M+H]^+$ $C_{20}H_{24}F_5N_2OS$ 435.1530, found 435.1519.

(±)-N-(*p*-Methoxybenzyl)-3-(benzyloxycarbonyl)-4-pentafluorosulfanylpyrrolidine (5j)

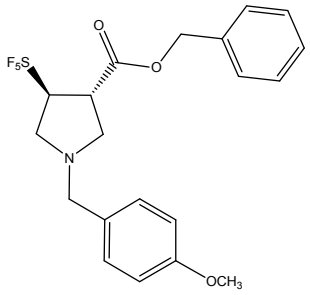

The title compound was prepared according to the general procedure as described above. The resulting crude product was purified by silica gel column chromatography (PE/AcOEt: 92/8) to afford **5j** in 66% yield as a colourless oil. R*f* (PE/AcOEt: 94/6) = 0.27. ^{19}F NMR ($CDCl_3/CFCl_3$, 282 MHz): δ 59.2 (dd, $^2J_{F,F}$ = 144.8 Hz, $^3J_{F,H}$ = 6.1 Hz, 4F), 84.7 (m, 1F). ^{1}H NMR ($CDCl_3$, 300 MHz): δ 2.8-3.0 (m, 3H), 3.22 (m, 1H), 3.52 (d, $^2J_{H,H}$ = 12.8 Hz, 1H), 3.60 (d, $^2J_{H,H}$ = 12.8 Hz, 1H), 3.6-3.7 (m, 1H), 3.81 (s, 3H), 5.02 (m, 1H), 5.19 (s, 2H), 6.86 (d, $^3J_{H,H}$ = 8.6 Hz, 2H), 7.19 (d, $^3J_{H,H}$ = 8.6 Hz, 2H), 7.3-7.4 (m, 5H). ^{13}C NMR ($CDCl_3$, 75 MHz): δ 46.7 (q_t, $^3J_{F,C}$ = 3.3 Hz), 55.3, 55.8, 56.4 (q_t, $^3J_{F,C}$ = 4.7 Hz), 58.4, 67.4, 83.3 (q_t, $^2J_{F,C}$ = 11.1 Hz), 113.8 (2C), 128.1 (2C), 128.4, 128.6 (2C), 129.4, 129.7 (2C), 135.3, 159.0, 171.7. ATR-FTIR (cm^{-1}): 2835, 1743, 1615, 1515. HRMS (ESI$^+$): *m/z* calcd for $[M+H]^+$ $C_{20}H_{23}F_5NO_3S$ 452.1319, found 452.1320.

(±)-N-(*p*-Methoxybenzyl)-3-(dodecyloxycarbonyl)-4-pentafluorosulfanylpyrrolidine (5k)

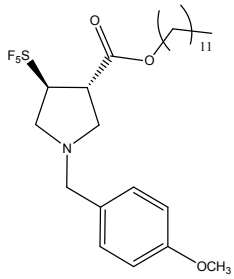

The title compound was prepared according to the general procedure as described above. The resulting crude product was purified by silica gel column chromatography (PE/AcOEt: 94/6) to afford **5k** in 46% yield as a colourless oil. R*f* (PE/AcOEt: 90/10) = 0.44. ^{19}F NMR ($CDCl_3/CFCl_3$, 282 MHz): δ 59.1 (dd, $^2J_{F,F}$ = 145.7 Hz, $^3J_{F,H}$ = 5.2 Hz, 4F), 84.9 (m, 1F). ^{1}H NMR ($CDCl_3$, 300 MHz): δ 0.89 (t, $^3J_{H,H}$ = 6.6 Hz, 3H), 1.2-1.4 (m, 18H), 1.63 (m, 2H), 2.87 (d, $^3J_{H,H}$ = 7.0 Hz, 2H), 2.95 (dd, $^2J_{H,H}$ = 10.2 Hz, $^3J_{H,H}$ = 8.3 Hz, 1H), 3.19 (m, 1H), 3.5-3.6 (m, 3H), 3.81 (s, 3H), 4.15 (t, $^3J_{H,H}$ = 6.7 Hz, 2H), 4.98 (m, 1H), 6.87 (d, $^3J_{H,H}$ = 8.6 Hz, 2H), 7.21 (d, $^3J_{H,H}$ = 8.6 Hz, 2H). ^{13}C NMR ($CDCl_3$, 75 MHz): δ 14.1, 22.7, 25.7, 28.5, 29.2, 29.3, 29.46, 29.54, 29.6 (2C), 31.9, 46.8 (q_t, $^3J_{F,C}$ = 3.6 Hz), 55.2, 55.9, 56.4 (q_t, $^3J_{F,C}$ = 4.4 Hz), 58.5, 65.8, 83.5 (q_t, $^2J_{F,C}$ = 11.6 Hz), 113.8 (2C), 129.6, 129.7 (2C), 159, 171.9. ATR-FTIR (cm^{-1}): 2924, 2854, 1739, 1514, 1462, 1248, 1180.

(±)-(1-Benzyl-4-pentafluorosulfanylpyrrolidin-3-yl)methyl acetate (5l)

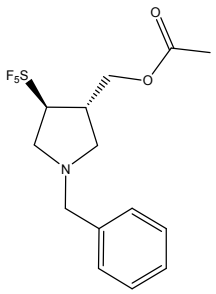

The title compound was prepared according to the general procedure as described above. The resulting crude product was purified by silica gel column chromatography (cyclohexane/AcOEt: 85/15) to afford **5l** in 61% yield as a colourless oil (contaminated by ~5% of starting product). R*f* (cyclohexane/AcOEt: 92/8) = 0.18. ^{19}F NMR ($CDCl_3/CFCl_3$, 282 MHz): δ 59.2 (dd, $^2J_{F,F}$ = 144.8 Hz, $^3J_{F,H}$ = 6.1 Hz, 4F), 85.6 (m, 1F). ^{1}H NMR ($CDCl_3$, 300 MHz): δ 2.07 (s, 3H), 2.62 (d, $^3J_{H,H}$ = 5.6 Hz, 2H), 2.89 (m, 1H), 3.1-3.2 (m, 2H), 3.57 (d, $^2J_{H,H}$ = 12.8 Hz, 1H), 3.65 (d, $^2J_{H,H}$ = 12.8 Hz, 1H), 4.1-4.2 (m, 3H), 7.3-7.5 (m, 5H). ^{13}C NMR ($CDCl_3$, 75 MHz): δ 20.7, 41.1 (q_t, $^3J_{F,C}$ = 3.0 Hz), 55.6, 57.1 (q_t, $^3J_{F,C}$ = 5.0 Hz), 59.3, 65.2, 84.8 (q_t, $^2J_{F,C}$ = 10.6 Hz), 127.3, 128.4 (4C), 137.8, 170.8. ATR-FTIR (cm^{-1}): 2809, 1743, 1226, 1043. HRMS (ESI^+): *m/z* calcd for $[M+H]^+$ $C_{14}H_{19}F_5NO_2S$ 360.1057, found 360.1053.

3. General Procedure for the Synthesis of Pyrrolidines 8-10 and 8'-10'

PPh_3 (0.2 equiv, 0.08 mmol) and AgOAc (0.2 equiv, 0.08 mmol) were dissolved in dry CH_2Cl_2 (3.7 mL) under argon, and stirred at room temperature for 1 h. Then, dipole precursor **6** or **7** (3 equiv, 1.23 mmol), Et_3N (0.25 equiv, 0.10 mmol) and ester **2a** or amide **3e** (1 equiv, 0.41 mmol) were added sequentially. After stirring at room temperature or at reflux (see Table 1) the solvent was removed under reduced pressure. The crude product was purified by silica gel column chromatography leading to pyrrolidines.

3.1. The reaction of ester **2a** with imino ester **6** was carried out according to the general procedure as described above and led to a 1:1 mixture of regioisomers **8** and **8'**. The resulting crude product was purified by silica gel column chromatography (EP/AcOEt: 84/16) to afford **8** and **8'** in 37% and 36% yield, respectively.

(±)-3-Benzyl-2-methyl-4-pentafluorosulfanyl-5-phenylpyrrolidine-2,3-dicarboxylate (8)

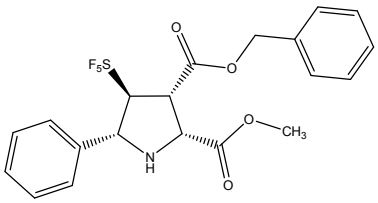

White solid. M.p. 118-120 °C. R*f* (EP/AcOEt: 80/20) = 0.18. ^{19}F NMR ($CDCl_3/CFCl_3$, 282 MHz): δ 63.1 (dm, $^2J_{F,F}$ = 145.7 Hz, 4F), 84.7 (m, 1F). ^1H NMR ($CDCl_3$, 300 MHz): δ 2.63 (br s, 1H), 3.51 (s, 3H), 4.1-4.2 (m, 1H), 4.2-4.3 (m, 1H), 4.60 (d, $^3J_{H,H}$ = 7.6 Hz, 1H), 5.02 (m, 1H), 5.19 (s, 2H), 7.3-7.7 (m, 10H). ^{13}C NMR ($CDCl_3$, 75 MHz): δ 52.3 (m), 52.4, 62.5, 66.3 (m), 68.0, 91.9 (q_t, $^2J_{F,C}$ = 7.4 Hz), 127.4 (2C), 128.6 (5C), 128.7, 129.0 (2C), 134.7, 137.6, 170.0, 170.9. ATR-FTIR (cm^{-1}): 2966, 1746, 1727, 1456, 1338, 1277, 1222, 1201. HRMS (ESI^+): *m/z* calcd for $[M+H]^+$ $C_{20}H_{21}F_5NO_4S$ 466.1111, found 466.1129.

(±)-4-Benzyl-2-methyl-3-pentafluorosulfanyl-5-phenylpyrrolidine-2,4-dicarboxylate (8')

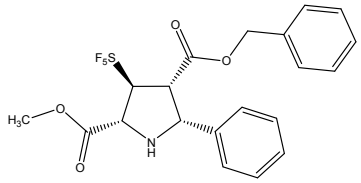

White solid. M.p. 98-99 °C. R*f* (EP/AcOEt: 80/20) = 0.25. ^{19}F NMR ($CDCl_3/CFCl_3$, 282 MHz): δ 61.4 (dd, $^2J_{F,F}$ = 145.7 Hz, $^3J_{F,H}$ = 5.2 Hz, 4F), 83.9 (m, 1F). ^1H NMR ($CDCl_3$, 300 MHz): δ 2.66 (br s, 1H), 3.88 (s, 3H), 3.99 (m, 1H), 4.3-4.4 (m, 2H), 4.7-4.8 (m, 2H), 5.3-5.5 (m, 1H), 6.9-7.0 (m, 2H), 7.3-7.6 (m, 8H). ^{13}C NMR ($CDCl_3$, 75 MHz): δ 53.0, 53.4, 63.4 (q_t, $^3J_{F,C}$ = 3.9 Hz), 64.6, 67.4, 86.9 (q_t, $^2J_{F,C}$ = 10.9 Hz), 127.2 (2C), 128.33 (3C), 128.38 (2C), 128.44 (2C), 128.48, 134.6, 136.8, 170.1, 170.2. ATR-FTIR (cm^{-1}): 2960, 1734, 1716, 1440,

1392, 1261, 1240, 1177. HRMS (ESI$^+$): *m/z* calcd for $[M+H]^+$ $C_{20}H_{21}F_5NO_4S$ 466.1111, found 466.1118.

3.2. The reaction of ester **2a** with imino ester **7** was carried out according to the general procedure as described above and led to a 2:1 mixture of regioisomers **9** and **9'**. The resulting crude product was purified by silica gel column chromatography (EP/AcOEt: 84/16) to afford the mixture of **9** and **9'** in 35% overall yield.

(±)-3-Benzyl-2-methyl-4-pentafluorosulfanyl-5-(*p*-methoxyphenyl)pyrrolidine-2,3-dicarboxylate (9)

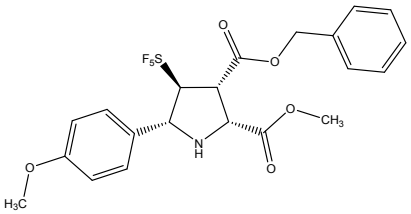

White solid. M.p. 118-119 °C . R*f* (EP/AcOEt: 84/16) = 0.14. ^{19}F NMR ($CDCl_3$/$CFCl_3$, 282 MHz): δ 63.0 (dd, $^2J_{F,F}$ = 145.7 Hz, $^3J_{F,H}$ = 5.2 Hz, 4F), 84.9 (m, 1F). ^{1}H NMR ($CDCl_3$, 300 MHz): δ 3.51 (s, 3H), 3.83 (s, 3H), 4.10-4.14 (m, 1H), 4.20 (d, $^3J_{H,H}$ = 8.2 Hz, 1H), 4.56 (d, $^3J_{H,H}$ = 8.4 Hz, 1H), 4.96 (m, 1H), 5.19 (s, 2H), 6.91 (d, $^3J_{H,H}$ = 7.8 Hz, 2H), 7.3-7.5 (m, 7H). ATR-FTIR (cm^{-1}): 2958, 2841, 1743, 1609, 1520, 1459, 1437. HRMS (ESI$^+$): *m/z* calcd for $[M+H]^+$ $C_{21}H_{23}F_5NO_5S$ 496.1217, found 496.1219.

(±)-4-Benzyl-2-methyl-3-pentafluorosulfanyl-5-(*p*-methoxypheny)pyrrolidine-2,4-dicarboxylate (9')

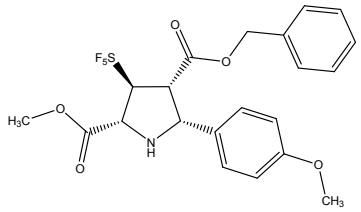

White solid. M.p. 103-104 °C. R*f* (EP/AcOEt: 84/16) = 0.19. ^{19}F NMR ($CDCl_3$/$CFCl_3$, 282 MHz): δ 61.3 (dd, $^2J_{F,F}$ = 145.7 Hz, $^3J_{F,H}$ = 5.2 Hz, 4F), 84.0 (m, 1F). ^{1}H NMR ($CDCl_3$, 300 MHz): δ 3.79 (s, 3H), 3.87 (s, 3H), 3.8-3.9 (m, 1H), 4.36 (d, $^3J_{H,H}$ = 9.0 Hz, 1H), 4.46 (d, $^2J_{H,H}$ = 12.1 Hz, 1H), 4.69 (d, $^3J_{H,H}$ = 9.0 Hz, 1H), 4.80 (d, $^2J_{H,H}$ = 12.1 Hz, 1H), 5.37 (m, 1H), 6.80 (d, $^3J_{H,H}$ = 8.1 Hz, 2H), 6.9-7.1 (m, 3H), 7.21 (d, $^3J_{H,H}$ = 7.7 Hz, 2H), 7.3-7.4 (m, 1H), 7.86 (d, $^3J_{H,H}$ = 7.7 Hz, 2H). ATR-FTIR (cm^{-1}): 2958, 2835, 1750, 1609, 1515. HRMS (ESI$^+$): *m/z* calcd for $[M+H]^+$ $C_{21}H_{23}F_5NO_5S$ 496.1217, found 496.1217.

3.3. The reaction of amide **3e** with imino ester **6** was carried out according to the general procedure as described above and led to a 1:1.5 mixture of regioisomers **10** and **10'**. The

resulting crude product was purified by silica gel column chromatography (EP/AcOEt: 68/32) to afford **10** and **10'** in 18% and 30% yield, respectively.

(±)-2-Methyl-3-morpholinocarbonyl-4-pentafluorosulfanyl-5-phenylpyrrolidine-2-carboxylate (10)

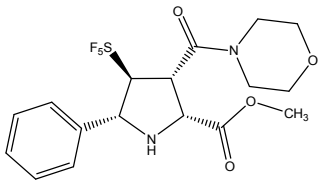

White solid. M.p. 103-105 °C. R*f* (EP/AcOEt: 68/32) = 0.24. ^{19}F NMR ($CDCl_3/CFCl_3$, 282 MHz): δ 63.2 (dd, $^2J_{F,F}$ = 145.7 Hz, $^3J_{F,H}$ = 5.2 Hz, 4F), 85.7 (m, 1F). ^{1}H NMR ($CDCl_3$, 300 MHz): δ 3.00 (br s, 1H), 3.6-3.9 (m, 11H), 4.22 (m, 1H), 4.36 (m, 1H), 4.57 (d, $^3J_{H,H}$ = 8.3 Hz, 1H), 5.06 (m, 1H), 7.3-7.5 (m, 3H), 7.5-7.6 (d, $^3J_{H,H}$ = 6.8 Hz, 2H). ^{13}C NMR ($CDCl_3$, 75 MHz): δ 42.6, 46.9, 52.7, 64.0, 66.4, 66.7, 66.8 (m), 70.5 (m), 94.0 (q_t, $^2J_{F,C}$ = 6.3 Hz), 127.5 (2C), 128.7, 129.0 (2C), 137.5, 169.7, 170.8. ATR-FTIR (cm^{-1}): 3303, 2919, 2858, 1738, 1632, 1459. HRMS (ESI$^+$): *m/z* calcd for $[M+H]^+$ $C_{17}H_{21}F_5N_2O_4S$ 445.1220, found 445.1225.

(±)-2-Methyl-4-morpholinocarbonyl-3-pentafluorosulfanyl-5-phenylpyrrolidine-2-carboxylate (10')

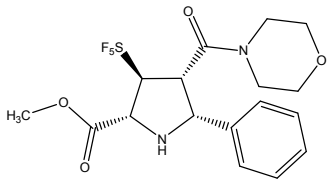

White solid. M.p. 93-94 °C . R*f* (EP/AcOEt: 68/32) = 0.32. ^{19}F NMR ($CDCl_3/CFCl_3$, 282 MHz): δ 61.4 (dd, $^2J_{F,F}$ = 145.7 Hz, $^3J_{F,H}$ = 6.9 Hz, 4F), 85.3 (m, 1F). ^{1}H NMR ($CDCl_3$, 300 MHz): δ 2.6-2.7 (m, 1H), 2.8-2.9 (m, 1H), 3.0-3.5 (m, 6H), 3.88 (s, 3H), 4.10 (dd, $^3J_{H,H}$ = 7.9 Hz, $^3J_{H,H}$ = 4.5 Hz, 1H), 4.40 (d, $^3J_{H,H}$ = 7.8 Hz, 1H), 4.54 (d, $^3J_{H,H}$ = 7.9 Hz, 1H), 5.53 (m, 1H), 7.3-7.4 (m, 5H). ^{13}C NMR ($CDCl_3$, 75 MHz): δ 42.0, 45.9, 49.4 (m), 53.0, 53.4, 64.1 (q_t, $^3J_{F,C}$ = 4.4 Hz), 65.7, 66.1, 89.5 (q_t, $^2J_{F,C}$ = 8.8 Hz), 127.6 (2C), 128.7 (2C), 129.0, 136.0, 163.4, 170.0. ATR-FTIR (cm^{-1}): 3291, 2927, 2857, 1748, 1650, 1441.

4. Theoretical analysis

4.1. Computational details

All density functional theory (DFT) calculations were performed with the Gaussian09 software,[1] using the dispersion-corrected range-separated hybrid ωB97X-D exchange-correlation functional,[2] the 6-31++G(d,p) basis set for all non-metallic atoms and the LANL2DZ one in conjunction with the associated pseudopotential[3] for silver. All geometries were fully optimized in the singlet spin state, solvent (dichloromethane) effects being implicitly accounted for by the latest IEF polarizable continuum model (IEFPCM).[4] The nature of stationary points was determined through (harmonic) vibrational analyses. Transition states (TS) were notably identified by their unique imaginary frequency and characterized by performing intrinsic reaction coordinate (IRC)[5] calculations to confirm that reactants and products were correctly connected. All Bader's Atom-in-molecules theory[6] calculations were carried out with the Keith's AIMAll software.[7]

The investigated model systems are depicted below in Scheme S1.

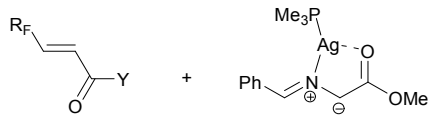

11: Y = OMe, $R_F = CF_3$
12: Y = OMe, $R_F = SF_5$
13: Y = NMe_2, $R_F = SF_5$

Scheme S1. Studied model systems **11-13**.

The six studied relative orientations of the reagents are represented in the following Figure S1. Note that in the corresponding preceding non-covalent adducts, the C…C bond distances are about 3 Å.

As for charge transfers upon the formation of the precomplexes, we evaluated the total charge on the acrylic ester and amide moiety for the **Adduct1a** and **Adduct2b** approaches using Bader's atomic charges. They were found slightly negative but rather small in absolute value (in *e*): -0.14 and -0.09 (CF_3-compound), -0.14 and -0.13 (SF_5-species), -0.09 and -0.08 (amide), respectively.

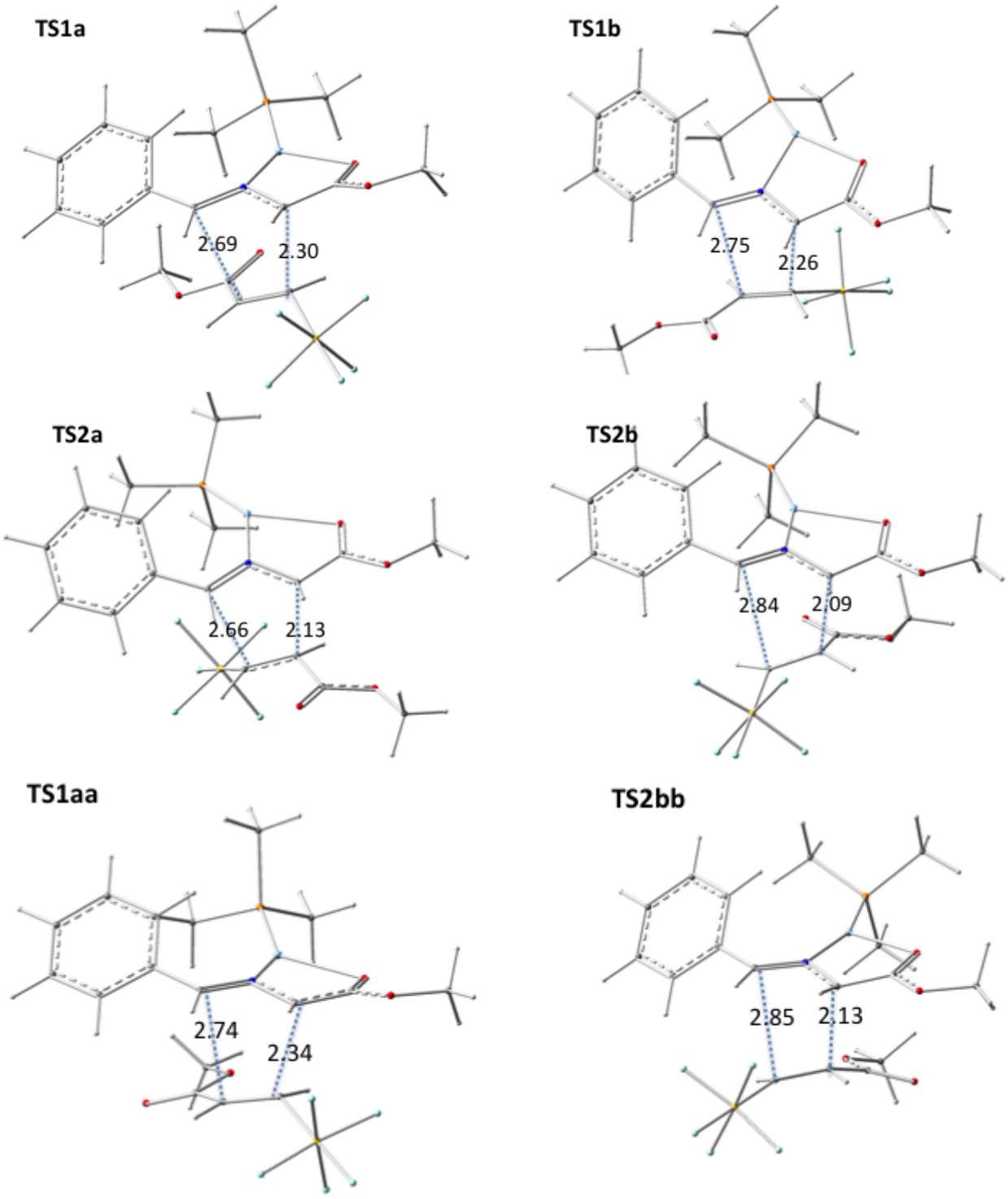

Figure S1. The six considered transition states involving the SF_5-ester compound. Distances between coupling carbon atoms in Å.

Table S1. Possible isomerizations for the ester/amide reactant. All energies in kcal/mol.

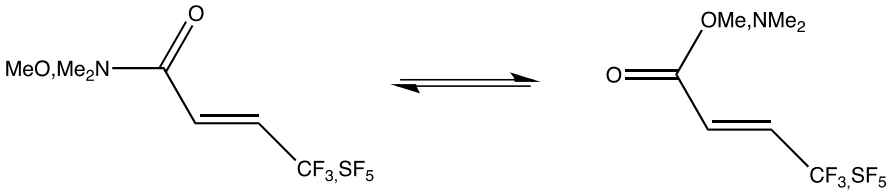

Compound	$\Delta G^{\circ}_{activation}$	$\Delta G^{\circ}_{reaction}$
Ester-CF_3 (**11**)	5.2	0.8
Ester-SF_5 (**12**)	3.7	-0.1
Amide-SF_5 (**13**)	5.2	0.1

In order to characterize nucleophilic/electrophilic behaviours, the first-state specific dual descriptor has been defined by:[8]

$$\Delta f_1(\vec{r}) = \rho^{ES1}(\vec{r}) - \rho^{GS}(\vec{r}), \qquad \text{(S1)}$$

where ρ^{ES1} denotes the electron density of the first excited state (here obtained using the TDDFT formalism with 10 states). It takes positive values in electrophilic zones and is negative in nucleophilic regions. Contrarily to the more usual frontier molecular orbital model, it takes the effect of all electrons into account and also include polarization effects as discussed more in details in ref. 8.

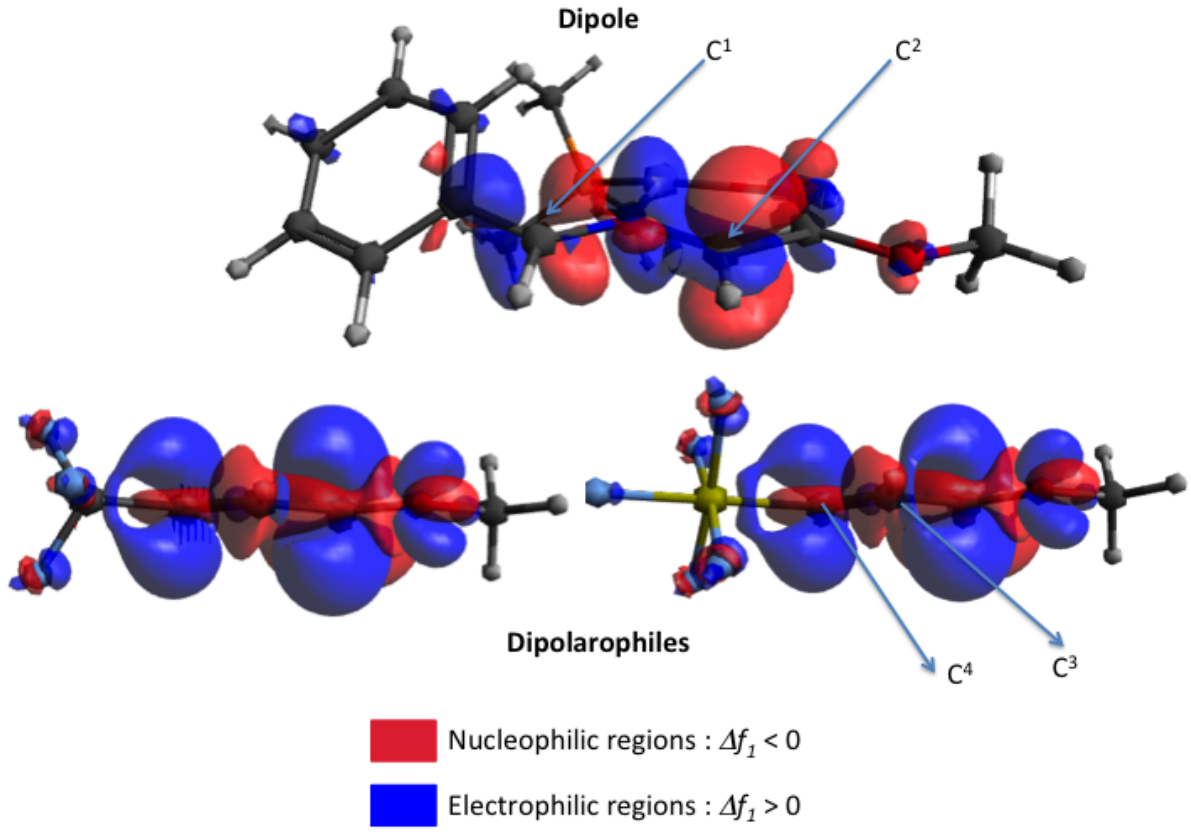

Figure S2. Views of Δf_1 isosurfaces (isovalues = 0.002 a.u.), generated with the Avogadro software (http://avogadro.openmolecules.net/) for the reactants (top: dipole, bottom left: CF_3-ester, bottom right: SF_5-ester). H atoms in light grey, C in dark grey, N in bright blue, O in red, P in orange, F in pale blue, S in yellow, Ag in grey.

Graph S1 shows the energetic profile for the cycle formation with the CF_3-ester compound (**11**) in the "2b" type orientation.

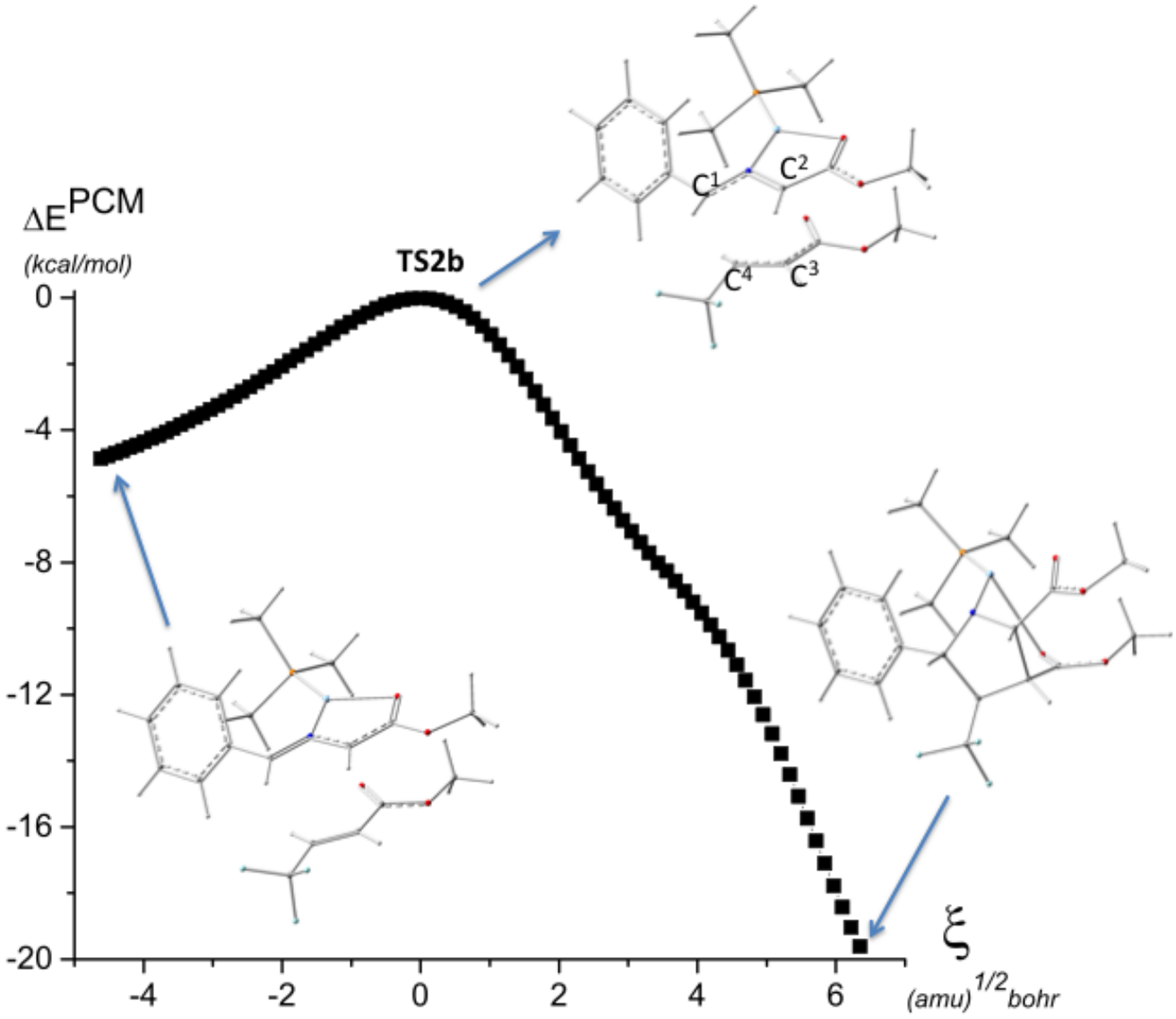

Graph S1. Minimum energy path corresponding to transition state **TS2b** for the cyclisation involving the CF_3-ester compound (**11**). H atoms in white, C in dark grey, N in bright blue, O in red, P in orange, F in pale blue, Ag in light grey.

According to Toro-Labbé, the reaction force along a reaction path is defined by (where ξ represents the reaction coordinate):[9]

$$F(\xi) = -\frac{dE^{SCF}}{d\xi}. \qquad \text{(S2)}$$

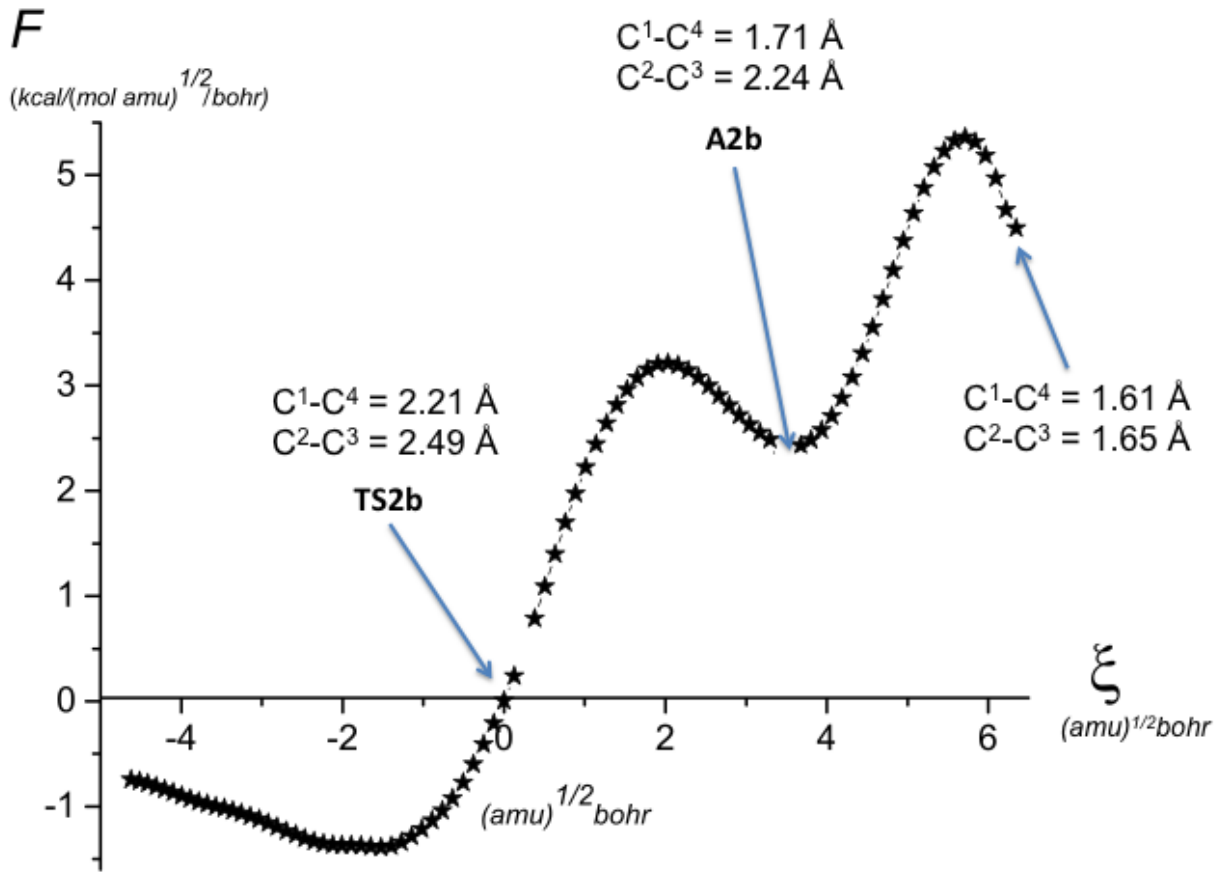

Graph S2. Reaction force profile with respect to the intrinsic reaction coordinate ξ and selected C-C distances, corresponding to transition state **TS2b** for the cyclisation involving the CF_3-ester compound (**11)**.

As can be inferred from Graphs S1-S2, the formation occurs in one concerted step, but a local minimum appears in the reaction force profile at the point named **A2b**: this is the signature of a strong asynchronicity[9] (note that if the mechanism was in two steps, the intermediate would correspond to a minimum *F* value equal to 0). We found that from **Adduct2b** to **A2b**, the C^1-C^4 bond almost fully forms while C^2-C^3 only slightly varies. Conversely, from **A2b** to the product, C^2-C^3 ends its creation.

We now explore the PES related to another regiochemistry, namely that corresponding to **TS1a** (see Graph S3), again for the CF_3-ester reactant.

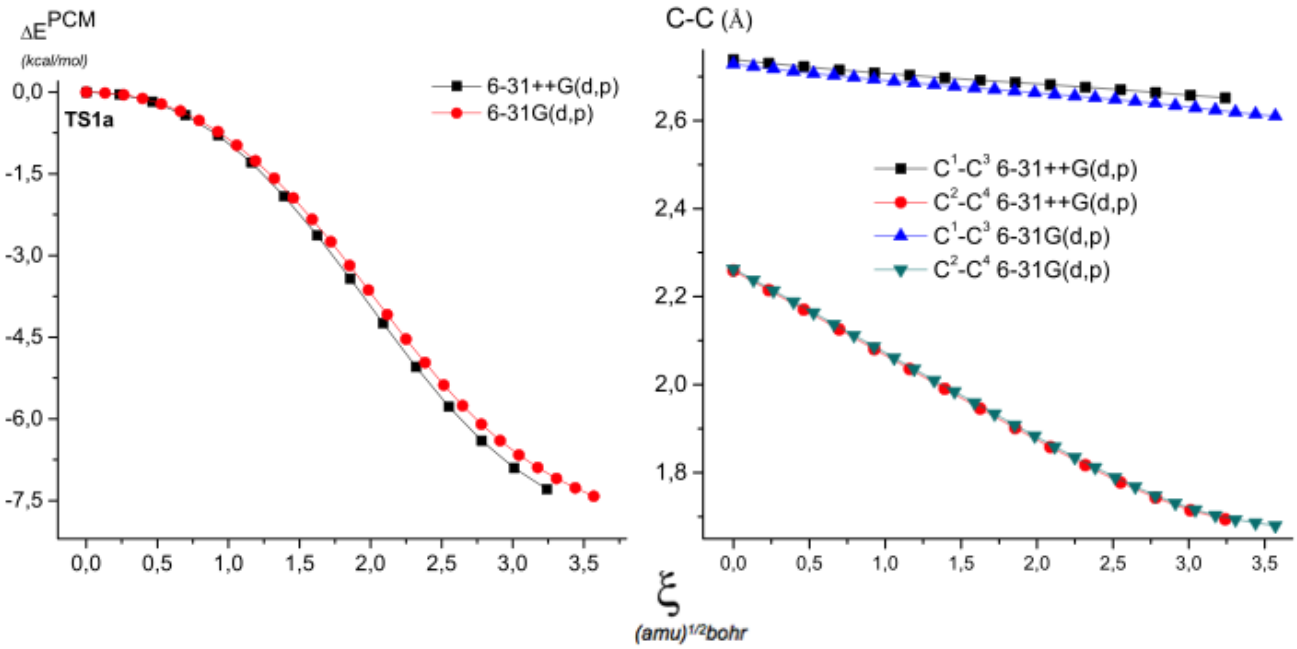

Graph S3. Forward direction for the minimum energy path corresponding to **TS1a** transition state for the cyclisation involving the CF_3-ester compound (two different basis sets are compared for non-metallic atoms). Left: energy variation; right: selected distances.

It follows from Graph S3 that the C^1-C^3 distance begins to decrease, as also observed for **TS2b**. However, it was unfortunately not possible (even changing algorithm, stepsize) to go further than ξ=3.5 $(amu)^{1/2}$ bohr and to determine from the IRC calculation whether the cycle is formed or not during this step. The last converged geometry was then recovered and used as the geometrical guess for full geometry optimization. Surprisingly, the optimization procedure results in getting minimum **Int1a** (represented in Figure S3) where C^1-C^3 = 2.89 Å, in contrast with the trend observed for the C^1-C^3 variation. Some doubts still remained since the optimization algorithm is not contrained to follow the minimum energy path.

We then considered using molecular dynamics at very small temperature, since trajectories must tend towards the IRC path in the limit $T \to 0\,K$. Due to numerical and computational reasons, we had to switch to the 6-31G(d,p) basis set (for atoms other than Ag). As shown in Graph S3, its PES is expected to be close to the 6-31++G(d,p) one. Thus, starting from the last point in the IRC path obtained at the B3LYP/6-31G(d,p) theory level (the TS having been reoptimized), we ran a Born-Oppenheimer trajectory (the SCF energy is converged at each time step) in the NVT ensemble at T = 2 K (controlled by velocity rescaling, corresponding to a nuclear kinetic energy of 485 μE_h), with a propagation time step equal to 0.50 fs.

The following energy curve (Graph S4) was obtained by taking snapshots every 15 fs: importantly, the SCF energy decreases during the simulation and it is thus reasonable to assume that the trajectory remains quite close to the minimum energy path. Importantly, after

150 fs of simulation, the C^1-C^3 distance begins to considerably increase, in full agreement with the existence of **Int1a**.

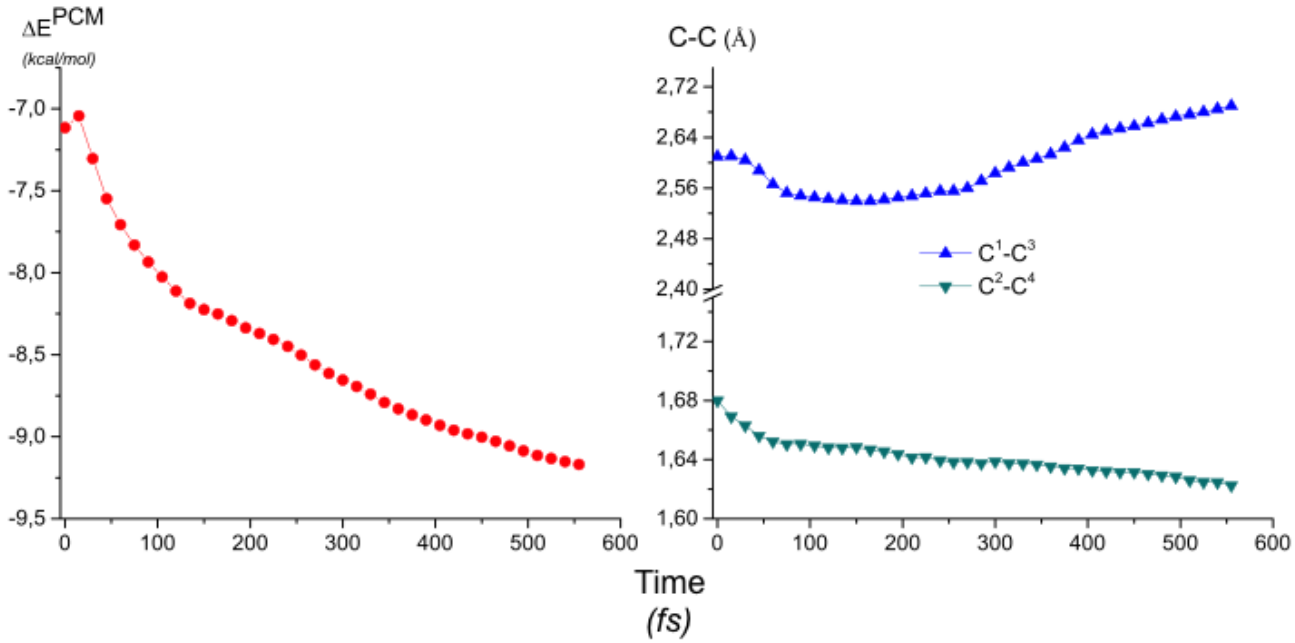

Graph S4. Quantum molecular dynamics results for the CF_3-ester compound. Left: SCF energy variation; right: selected distances.

In summary, from **Adduct1a** two unconcerted steps are needed to afford the product: the first leads to a local minimum (**Int1a)** on the PES that evolves through a second TS (**TS1a2**, Figure S3) to the product, a step being not rate determining (ΔG^0_{act} = 3.7 kcal/mol, **TS1a2** being 7 kcal/mol more stable than **TS1a** in the CF_3 case). In **Int1a**, one bond is fully formed, while C^1-C^3 is close to that found in adduct, suggesting it remains almost constant. However, this is more intricate. Indeed, silver is not spectator, since it flips during the first step (as shown by the $\angle C_1NC_2Ag$ dihedral angle), preferentially interacting with O^5 in **TS1a** and with O^6 in **Int1a**. The geometrical reorganization induced by this flip makes the C^1-C^3 distance variation complex to analyse.

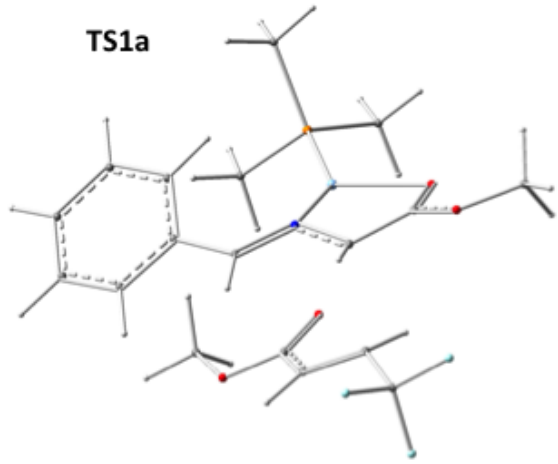

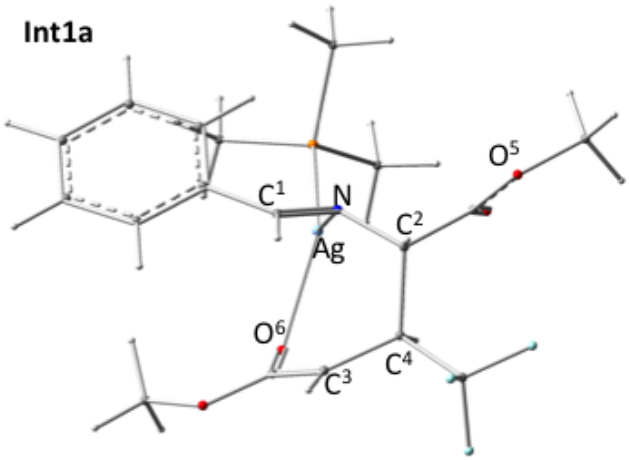

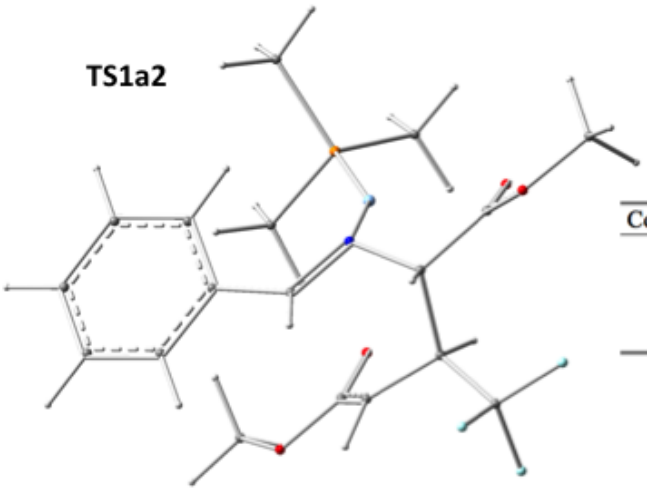

Compound	C^1-C^3	C^2-C^4	Ag-N	Ag-O^5	Ag-O^6	C^1NC^2Ag
TS1a	2.738	2.259	2.371	2.488	2.593	153
Int1a	2.886	1.596	2.478	3.192	2.283	137
TS1a2	2.287	1.626	2.277	2.757	2.596	134

Figure S3. Views of **TS1a**, **Int1a**, and **TS1a2** for the reaction involving the CF_3-ester (**11**). H atoms in white, C in dark grey, N in bright blue, O in red, P in orange, F in pale blue, Ag in light grey. Selected distances (in Å) and dihedral angles (in °).

The competition between paths 1 and 2 can now be discussed in terms of the relative energies collected in Table S2.

Table S2. Relative energies (with respect to the reactants) for the first transition states and products. All values in kcal/mol. For each regiochemistry ("path 1" and "path 2"), the most favoured orientation (in terms of the considered energy type) is written in coloured bold fonts (red and blue, respectively).

Compound	Orientation	ΔE_{TS}^{PCM}	ΔG_{TS}^{0}	ΔG_{prod}^{0}
CF_3-ester (**11**)	1a	**-6.6**	**10.7**	-8.8
	1aa	-3.3	13.7	-7.4
	1b	-2.1	14.3	**-9.3**
	2a	2.1	18.7	-8.2
	2b	**-1.3**	**16.0**	-11.8
	2bb	0.6	17.9	**-12.3**
SF_5-ester (**12**)	1a	**-5.7**	**11.8**	-11.9
	1aa	-2.4	14.2	**-13.9**
	1b	-0.5	16.2	-10.1
	2a	-0.3	15.0	-6.5
	2b	**-3.4**	**11.7**	**-13.4**
	2bb	-2.2	14.1	-12.6
SF_5-amide (**13**)	1a	**-3.8**	**14.1**	-12.1
	1aa	3.9	22.9	**-13.9**
	1b	1.5	17.9	-8.8
	2a	0.7	17.5	-6.4
	2b	**-2.8**	**13.4**	**-13.2**
	2bb	-1.4	13.6	-10.3

As deduced from Table S2, **Product2b(b)** are considerably more stable (in terms of ΔG^0) than the others in the CF_3-ester series. The conclusions are different for the SF_5-ester and amide where the most favourable thermodynamical products are **Product1a** and **Product2b**. These are not the experimentally obtained ones (only products 1 for CF_3-esters, mixtures of types 1, 2 with the SF_5 derivatives). From the Gibbs activation barrier point of view, the pathway 1a is privileged for CF_3-ester, while 1a and 2b are ΔG_{act}^{0}-confounded for SF_5-ester, and 2b is only slightly favoured with respect to 1a for SF_5-amide, in relevant agreement with the experimental regiochemistries

We now aim at identifying the factors governing the regiochemistry. To this aim, a detailed energetic decomposition (eq. S6) was performed for the most favoured types 1 and 2 approaches (which correspond to the six bolded orientations in Table S2). This could also be visualized by a graphical representation, as that provided in Figure S4.

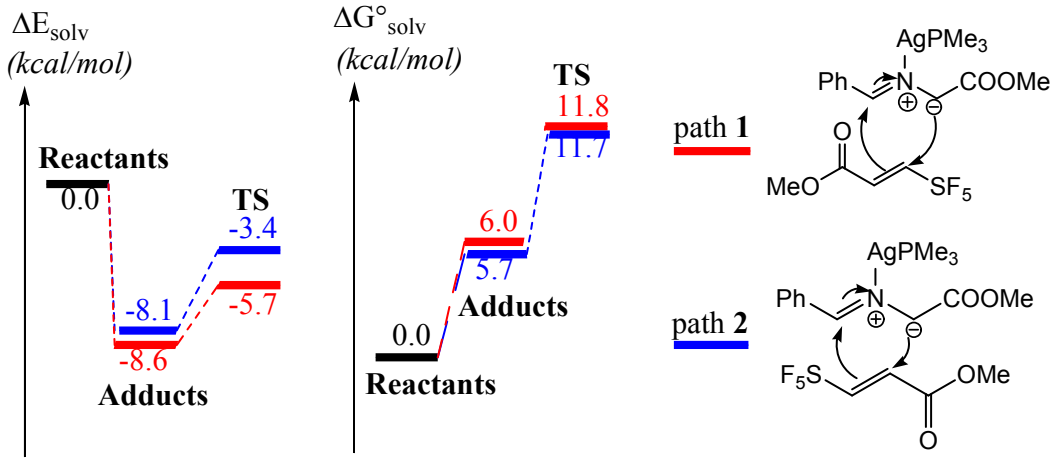

Figure S4. Regiochemistry according to ΔE_{solv} and $\Delta G°$ viewpoints for the SF_5-ester compound. Note that appropriate relaxed energy scans on C-C distances insured that no TS were present between the reactants and the adducts.

To better understand this regiochemistry, the overall activation standard Gibbs energy can be written according to:

$$\Delta G^0_{act} = \Delta G^0_{TS} - \Delta G^0_{\text{reactants}} = \underbrace{\Delta G^0_{adduct} - \Delta G^0_{\text{reactants}}}_{\Delta G^0_{actAdduct}} + \underbrace{\Delta G^0_{TS} - \Delta G^0_{adduct}}_{\Delta G^0_{actTS}} \quad . \tag{S3}$$

Each of these two main contributions could be divided into:

$$\Delta G^0_{actAdduct} = \underbrace{E_{adduct} - E_{\text{reactants}}}_{\Delta G^{elec}_{Adduct}} + \underbrace{\left(\Delta H_{TS1} - \Delta H_{\text{reactants}} + E^{PCM}_{\text{reactants}} - E^{PCM}_{TS1}\right)}_{\Delta G^{TnonS}_{adduct}} + \underbrace{T\left(S^{vib}_{\text{reactants}} - S^{vib}_{adduct}\right)}_{\Delta G^{Svib}_{TS}} + \underbrace{T\left(S^{trans}_{\text{reactants}} + S^{rot}_{\text{reactants}} - S^{trans}_{adduct} - S^{rot}_{adduct}\right)}_{\Delta G^{SnonVib}_{adduct}} . \tag{S4}$$

$$\Delta G^0_{actTS} = \underbrace{E_{TS} - E_{\text{adduct}}}_{\Delta G^{elec}_{TS}} + \underbrace{\left(\Delta H_{TS1} - \Delta H_{adduct} + E^{PCM}_{\text{adduct}} - E^{PCM}_{TS}\right)}_{\Delta G^{TnonS}_{TS}} + \underbrace{T\left(S^{vib}_{adduct} - S^{vib}_{TS}\right)}_{\Delta G^{Svib}_{TS}} + \underbrace{T\left(S^{trans}_{adduct} + S^{rot}_{adduct} - S^{trans}_{TS} - S^{rot}_{TS}\right)}_{\Delta G^{SnonVib}_{TS}} . \tag{S5}$$

so that :

$$\Delta G^{0}_{act} = \Delta G^{elec}_{Adduct} + \Delta G^{elec}_{TS} + \Delta G^{TnonS}_{Adduct} + \Delta G^{TnonS}_{TS} + \Delta G^{Svib}_{Adduct} + \Delta G^{Svib}_{TS} + \Delta G^{SnonVib}_{adduct} + \Delta G^{SnonVib}_{TS}, \quad \text{(S6)}$$

where ΔG^{elec}_{act} represents the pure electronic component, ΔG^{nonT}_{act} collects all temperature effects (and ZPE) that are not entropic, and $\Delta G^{S(non)vib}_{act}$ gathers the (non: i.e. translational and rotational) vibrational entropy contributions. The values are gathered in Table S3.

Table S3. Energetic decomposition of the overall activation standard Gibbs energy. All values in kcal/mol.

		ΔG^{elec}_{adduct}	ΔG^{elec}_{TS}	$\Delta G^{TnonS}_{adduct}$	ΔG^{TnonS}_{TS}	$\Delta G^{SnonVib}_{adduct}$	$\Delta G^{SnonVib}_{TS}$	ΔG^{Svib}_{adduct}	ΔG^{Svib}_{TS}	ΔG°_{act}
CF_3-	1a	-8.9	2.3	1.4	-0.2	20.3	0.0	-7.3	3.1	10.7
ester	2b	-8.0	6.8	1.7	-0.7	20.3	0.1	-7.2	3.0	16.0
SF_5-	1a	-8.6	2.9	2.4	-0.6	20.7	0.0	-8.5	2.6	10.9
ester	2b	-8.1	4.7	2.2	-0.5	20.7	0.0	-9.1	0.9	10.8
SF_5-	1a	-9.0	5.2	1.6	-0.3	20.8	0.0	-6.4	2.1	14.1
amide	2b	-10.3	7.5	1.8	-0.6	22.1	0.0	-5.7	0.0	14.7

We now try to determine which contributions can account for regiochemistry. Obviously, neither $\Delta G^{SnonVib}_{TS}$, ΔG^{TnonS}_{TS}, $\Delta G^{TnonS}_{adduct}$, nor $\Delta G^{SnonVib}_{adduct}$, since the two first are too small while the two last ones cannot discriminate between 1a and 2b orientations for a given compound. There thus remain four contributions that play a role in differentiating the two pathways: ΔG^{elec}_{adduct}, ΔG^{elec}_{TS}, ΔG^{Svib}_{adduct}, and ΔG^{Svib}_{TS}.

The first pure electronic contribution (linked to the formation of adducts from the reactants) can be inspected within the conceptual DFT framework. When aiming to compare the intrinsic properties of molecules with a different number of electrons, one has to shift to the grand-canonical ensemble,[10] thus considering (in first approximation) $S^2\Delta f_1$ instead of Δf_1. The softness S was here evaluated using finite difference linearization.[11] This local information is then translated into the language of reactive sites using Yang-Mortier condensation.[12] For this purpose, Bader's atomic charges were employed. We seek to predict energetic stabilization of adducts using only descriptors calculated on the isolated molecules. These intermediates are obtained by the formation of the generic C_A-C_B and C_C-C_D bonds, where C_A and C_B (resp. C_C and C_D) belong to molecule 1 (resp. 2). In the spirit of ref. 13, one can introduce the preference dual descriptor defined by:

$$\mathrm{Pref}\Delta f_1 = S^2_{mol1} S^2_{mol2} \left[\Delta f_1(C_A)\Delta f_1(C_B) + \Delta f_1(C_C)\Delta f_1(C_D) \right]. \quad \text{(S7)}$$

The following hierarchy is then obtained (in atomic units): -3.26 (SF_5-amide adduct regiochemistry type 2) < -2.34 (SF_5-amide type 1) < -1.81 (CF_3-ester type 1) < -1.55 (SF_5-ester type 1) < -1.28 (SF_5ester type 2) < -0.80 (CF_3-ester type 2). This is exactly the same order as that obtained when looking at the ΔG_{adduct}^{elec} contribution for the most stable adducts of types 1 and 2 (in kcal/mol): -10.34 (SF_5-amide adduct regiochemistry type 2) < -8.98 (SF_5-amide type 1) < -8.90 (CF_3-ester type 1) < -8.64 (SF_5-ester type 1) < -8.10 (SF_5-ester type 2) < -8/02 (CF_3-ester type 2). Besides this correct classification, $\mathrm{Pref}\Delta f_1$ also affords an accurate numerical prediction through linear regression ($R^2 = 0.94$), as represented in Graph S5.

It can also be noticed that the fact that all $\mathrm{Pref}\Delta f_1$ values are negative is consistent with the observation that the formation of adducts is electronically favoured. Interestingly, this is no longer the case when $S^2\Delta f_1$ are substituted by atomic charges ("charge control" instead of "orbital control"), the preference values becoming for instance positive with the CF_3-ester.

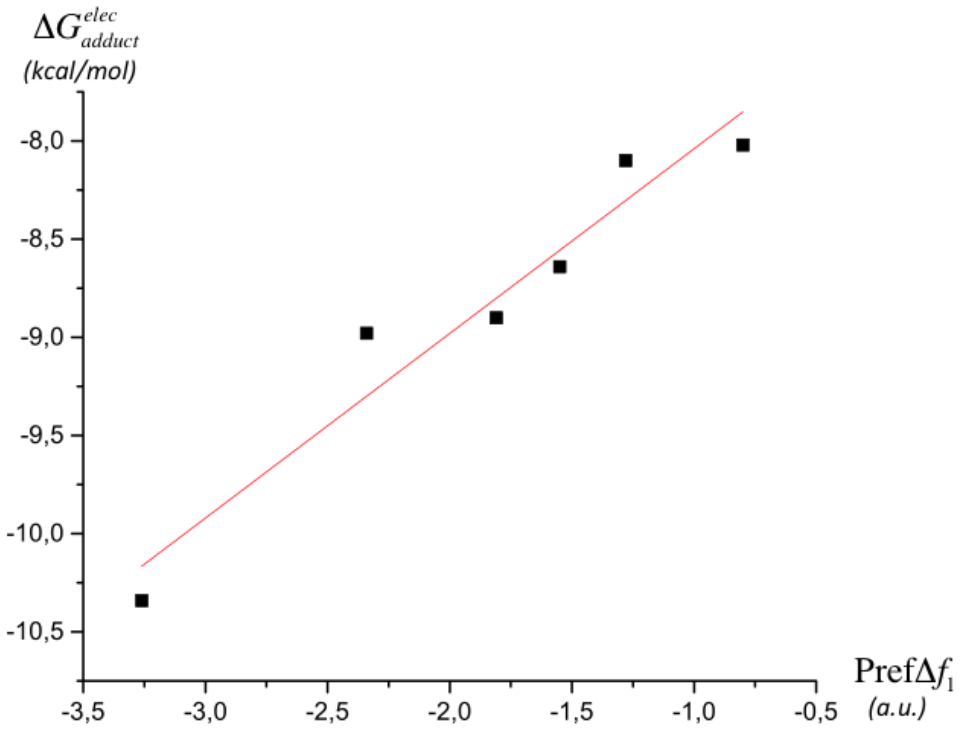

Graph S5. Use of the preference dual descriptor for the prediction of the electronic energy stability of the most stable adducts. In red, corresponding linear regression.

We now deal with the ΔG_{TS}^{elec} contribution. One may wonder if it can be rationalized in terms of the interactions present in the adducts. To this aim, we invoke Bader's Atoms-in-molecules theory. The interactions between the two partners within the adducts are mirrored,

from a topological viewpoint, by the existence of two bond paths between C_A and C_B, and C_C and C_D, as well as the presence of a ring critical point (defining the $C_AC_BC_CC_DN$ cycle). It is thus intuitive to propose the following descriptor:

$$\rho_c = \rho_{BCP}^{C_A-C_B} + \rho_{BCP}^{C_C-C_D} + \rho_{RCP} \,. \tag{S8}$$

The following values are obtained (in atomic units): 0.0237 (SF_5-amide type 2) < 0.0280 (CF_3-ester type 2) < 0.0297 (SF_5-amide type 1) < 0.0306 (SF_5-ester type 2) < 0.0320 (SF_5-ester type 1) < 0.0356 (CF_3-ester type 1). Once more, this order is fully parallel to that for ΔG_{TS}^{elec} (one expects that the higher the interactions in the adducts (i.e. the higher ρ_c), the lower the activation energy): 7.52 (SF_5-amide type 2) > 6.76 (CF_3-ester type 2) > 5.16 (SF_5-amide type 1), 4.67 (SF_5-ester type 2) > 2.90 (SF_5-ester type 1) > 2.34 (CF_3-ester type 1) kcal/mol. These results are plotted in Graph S6 with the corresponding linear regression (R^2 = 0.90).

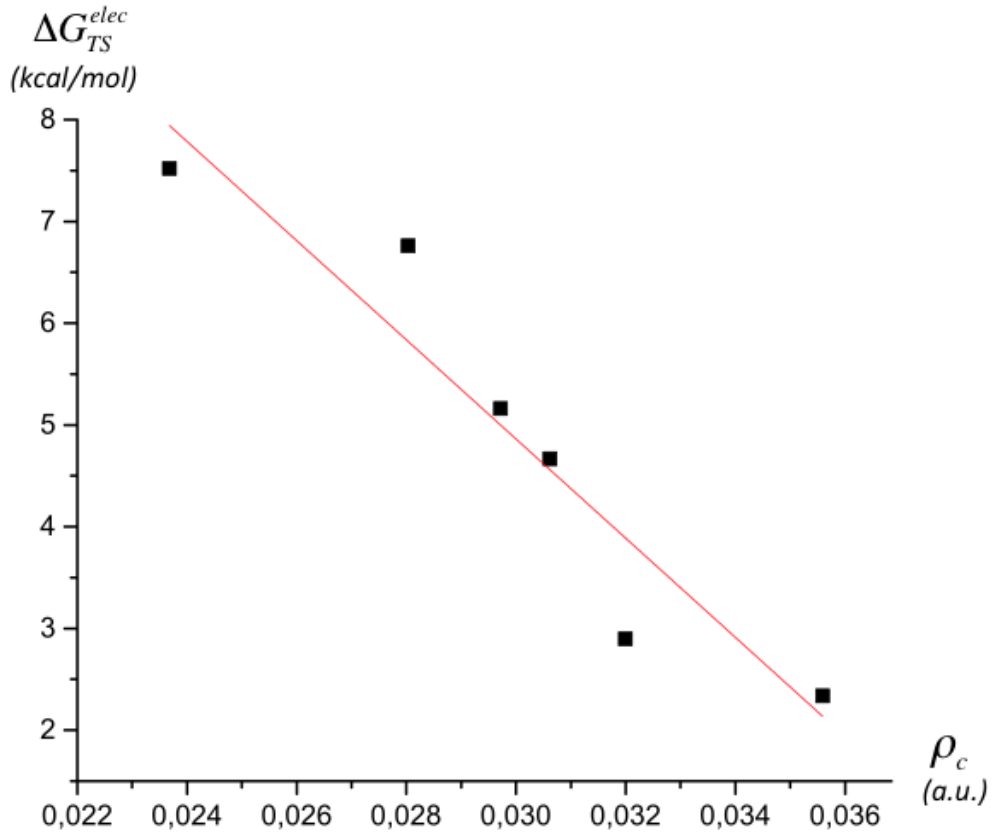

Graph S6. Use of the ρ_c descriptor for the prediction of the SCF energy difference between TSs and adducts. In red, corresponding linear regression.

Finally, we look at the vibrational entropy contributions. As evidenced by Graph S7, a semi-quantitative interpretation is more elusive.

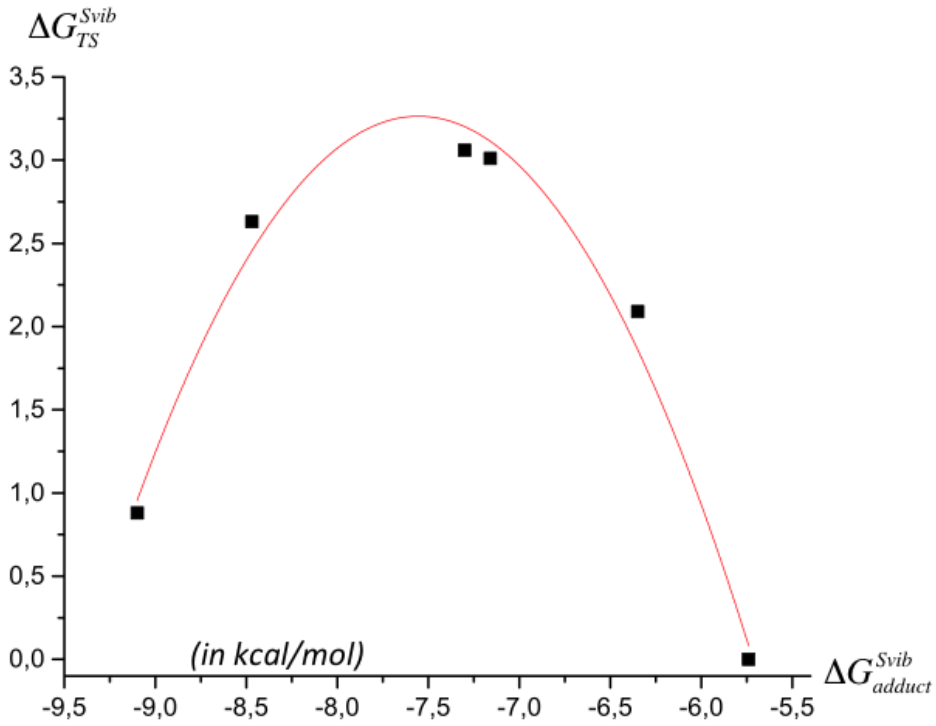

Graph S7. Vibrational entropy contributions. In red, corresponding parabolic regression.

5. X-Ray Crystal Data and Structural Description of 5f and 8

5.1 Crystallographic data for compound 5f

The crystal data are collected in Table S4. The full crystallographic parameters (atomic coordinates, bond length, angles and anisotropic displacements) are deposit to the Cambridge Crystallographic Data Centre (Nr CCDC1024824).[14-17]

Table S4. Crystal data

Chemical Formula	$C_{19}H_{21}F_5N_2OS$
Molecular Weight / $g.mol^{-1}$	420.44
Crystal System	Orthorhombic
Space Group	*P*na2_1 (33)
Z , Z' (asymmetric units per unit cell)	4, 1
a / *Å*	9.2994(9)
b / *Å*	12.5496(1)
c / *Å*	17.0351(2)
V / $Å^3$	1988.1(3)
d_{calc} / $g.cm^{-3}$	1.405
F(000) / e^-	872
Absolute structure parameter	0.10(11)
Absorption coefficient μ (MoKα_1) / mm^{-1}	0.220

Structural description

The asymmetric unit is composed of one molecule of $C_{19}H_{21}F_5N_2OS$ (Figures S5 and S6). The carbon atoms C9 and C 10 exhibit an absolute configuration S and S. Some Hydrogen interactions are established between two consecutive molecules along *a* axis (Figures S7 and S8), Table S5. These interactions lead to the formation of periodic bond chains spreading along *a* direction (Figures S9 and S10).

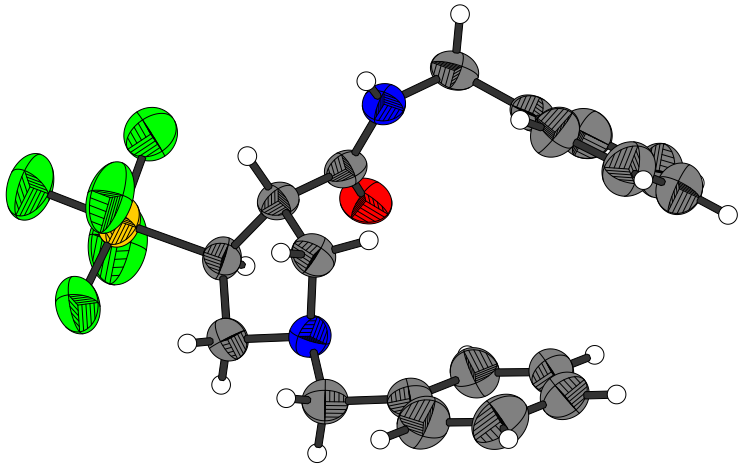

Figure S5. Asymmetric unit in thermal ellipsoidal representation

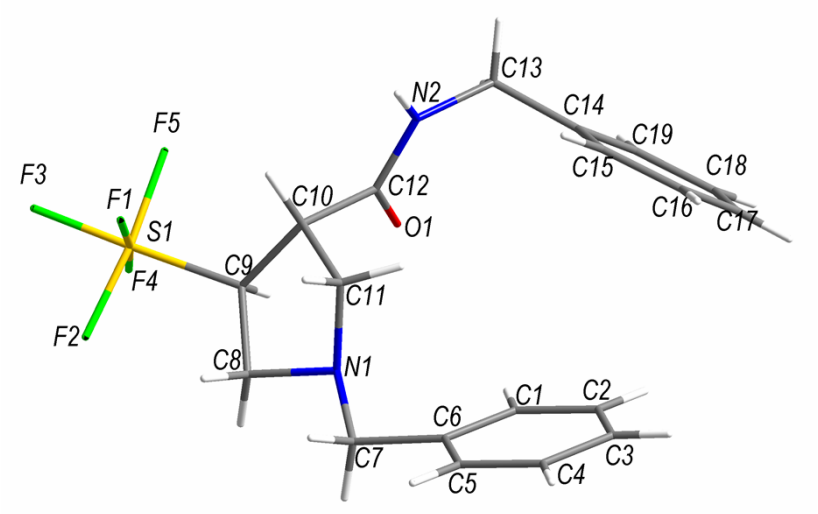

Figure S6. Asymmetric unit with atoms labels

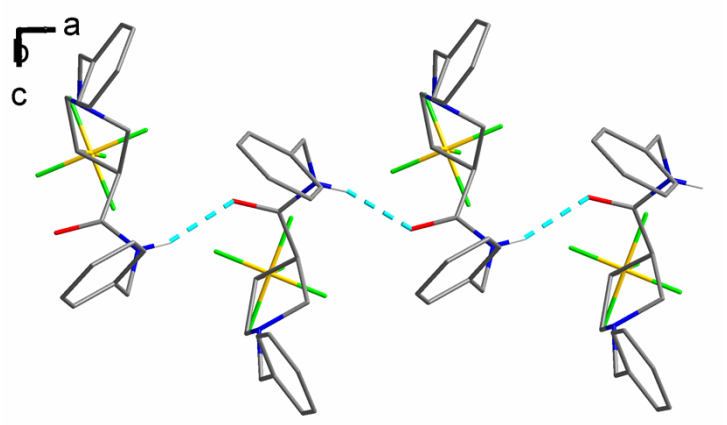

Figure S7. Hydrogen bond between adjacent molecules along a axis (dashed blue lines)

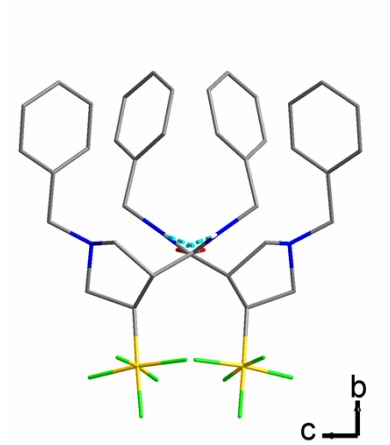

Figure S8. Projection along a of one molecular chain built from the hydrogen bonds

Table S5. Hydrogen bond table

D-H...A	d(D-H)	d(H...A)	d(D...A)	<(DHA)
N(2)-H(2A)...O(1)#1	0.86	2.04	2.866(4)	162.1

Symmetry transformations used to generate equivalent atoms: #1 x-1/2,y,-z+3/2

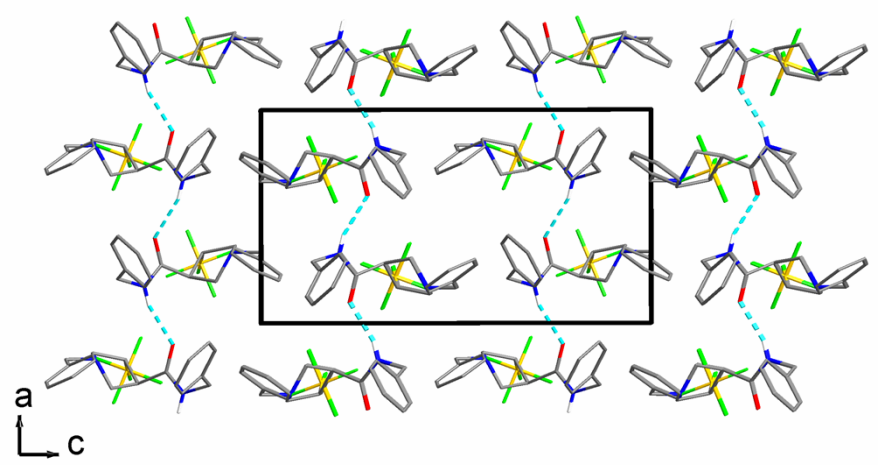

Figure S9. Projection along b axis, the periodic bond chains are stacked along c

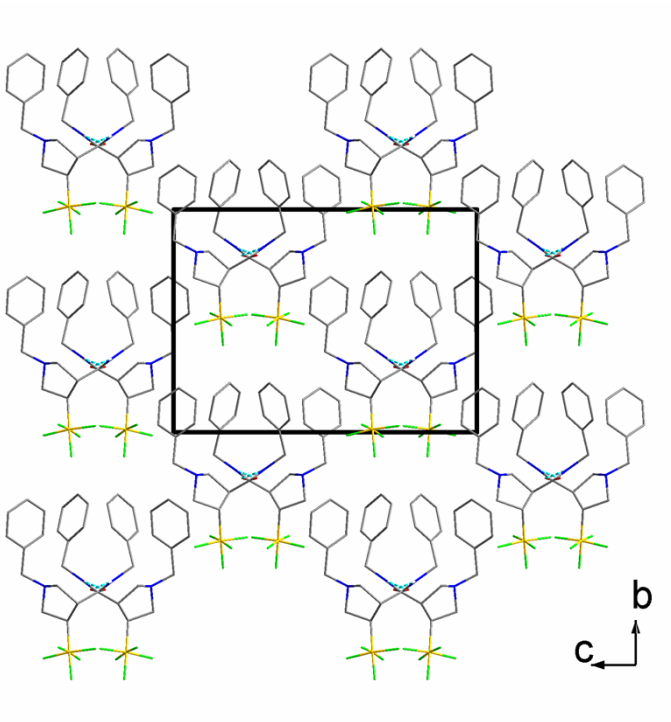

Figure S10. Projection along a axis, the periodic bond chains are organised in conjunction

5.2 Crystallographic data for compound 8

The crystal data are collected in Table S6. The full crystallographic parameters (atomic coordinates, bond length, angles and anisotropic displacements) are deposit to the Cambridge Crystallographic Data Centre (Nr CCDC1024823).[14-17]

Table S6. Crystal data

Chemical Formula	$C_{20}H_{20}F_5NO_4S$
Molecular Weight / $g.mol^{-1}$	465.4
Crystal System	Monoclinic
Space Group	$P2_1$
Z , Z' (asymmetric units per unit cell)	2,1
a / *Å*	5.7359(6)
b / *Å*	14.0228(15)
c / *Å*	12.8595(14)
β / °	97.839(2)
V / $Å^3$	1024.67(19)
d_{calc} / $g.cm^{-3}$	1.509
F(000) / e^-	480
Absolute structure parameter	0.02(7)
Absorption coefficient μ ($MoK\alpha_1$) / mm^{-1}	0.231

Structural description

The asymmetric unit is composed of one molecule of $C_{20}H_{20}F_5NO_4S$ (Figures S11 and S12). Four (F1 to F4) of the five fluorine atoms are statistically disordered. The statistical occupancy is shared between two crystallographic sites for the fluorine atoms F1 to F4. This distribution is 57 /43 %. The packing is represented on Figures S13-S15, the cohesion between molecules is ensured by Van der Waals interactions.

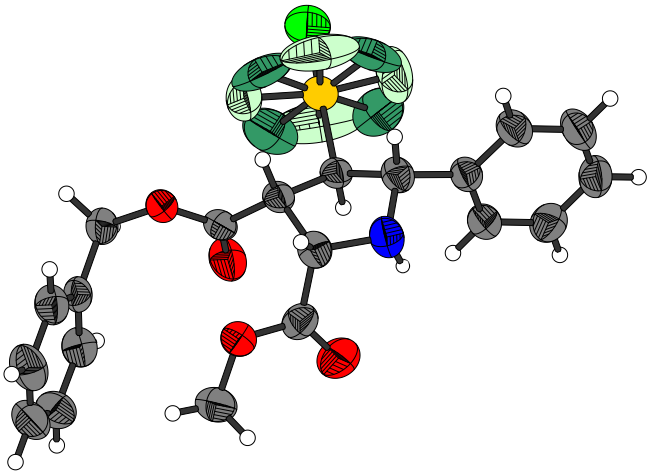

Figure S11. Asymmetric unit in thermal ellipsoidal representation. In light green the fluorine atoms with a statistical occupancy of 43%, in darker green the fluorine atoms with a statistical occupancy of 57%.

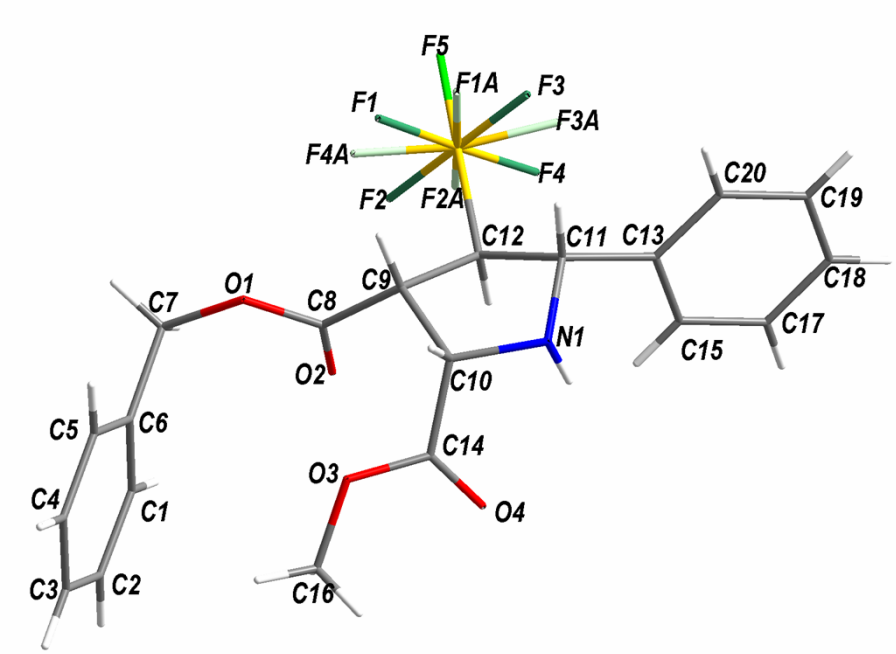

Figure S12. Asymmetric unit with atoms labels. In light green the fluorine atoms with a statistical occupancy of 43%, in darker green the fluorine atoms with a sof of 57%.

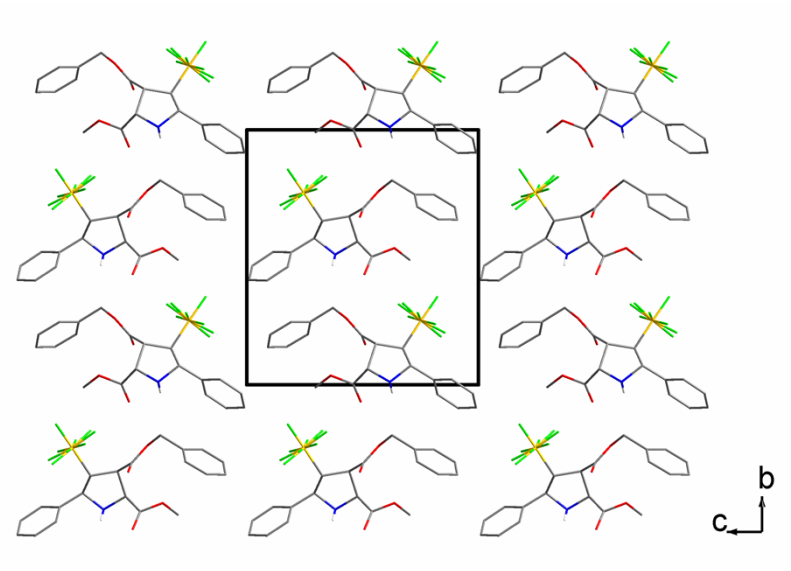

Figure S13. Projection along a axis.

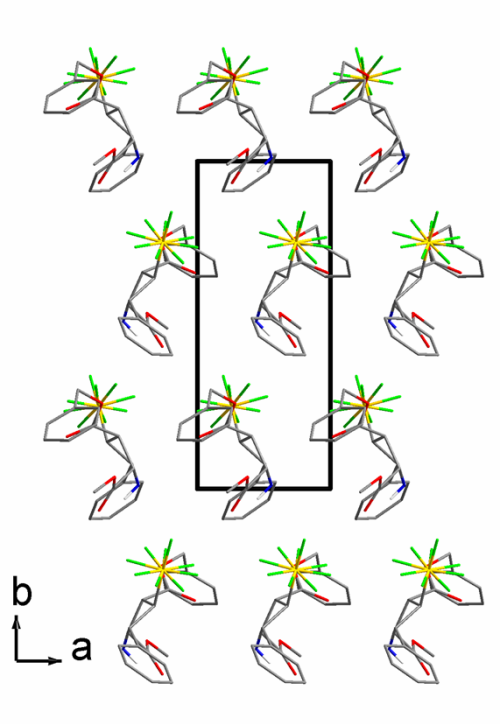

Figure S14. Projection along c axis

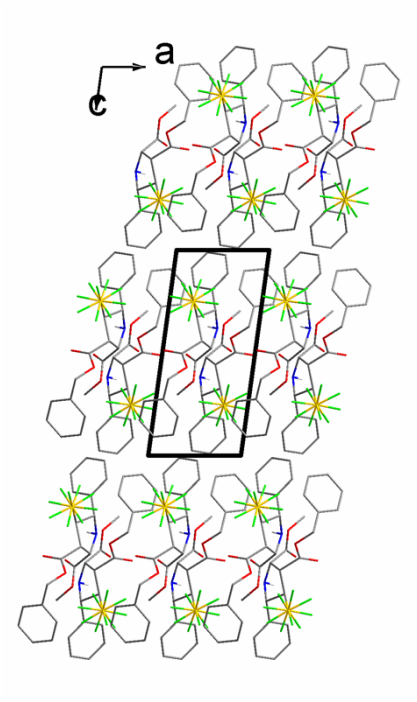

Figure S15. Projection along b axis

6 ^{1}H, ^{19}F and ^{13}C NMR Spectra and NOESY Experiments

^{1}H, ^{19}F and ^{13}C NMR ($CDCl_3$) spectra of **5a**

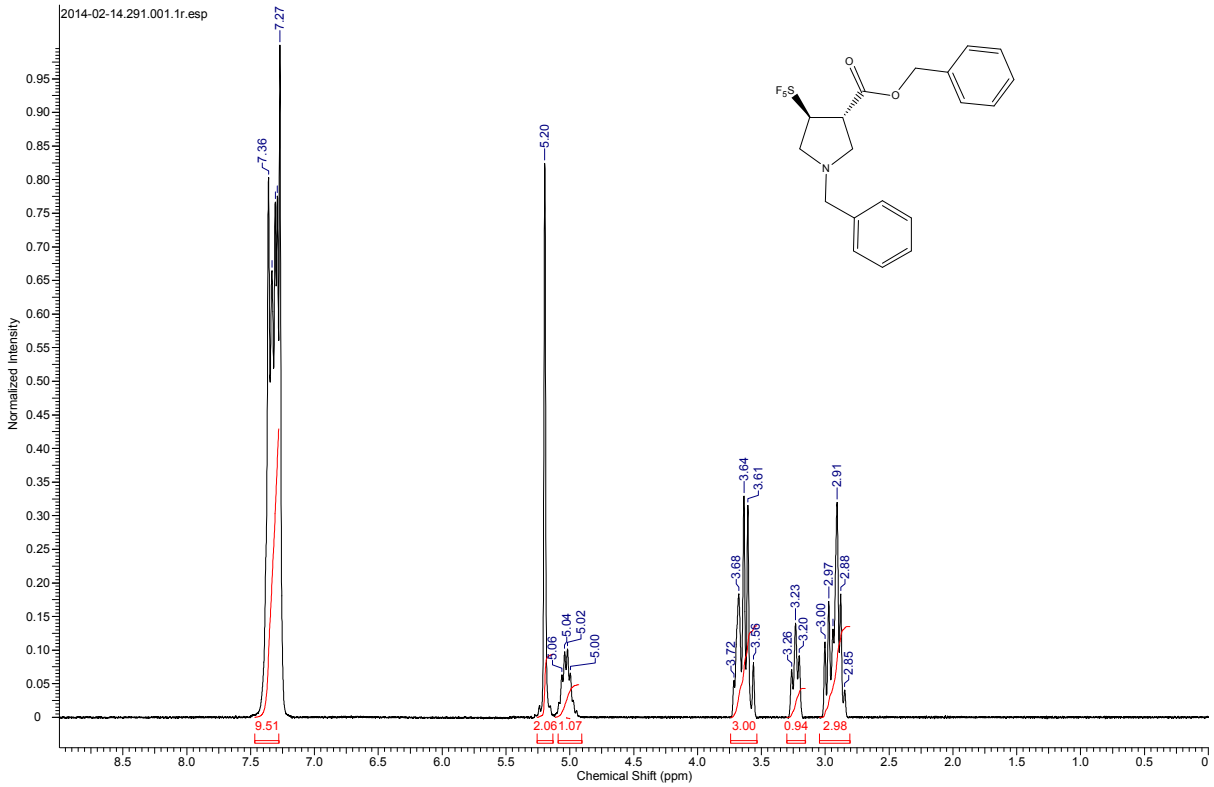

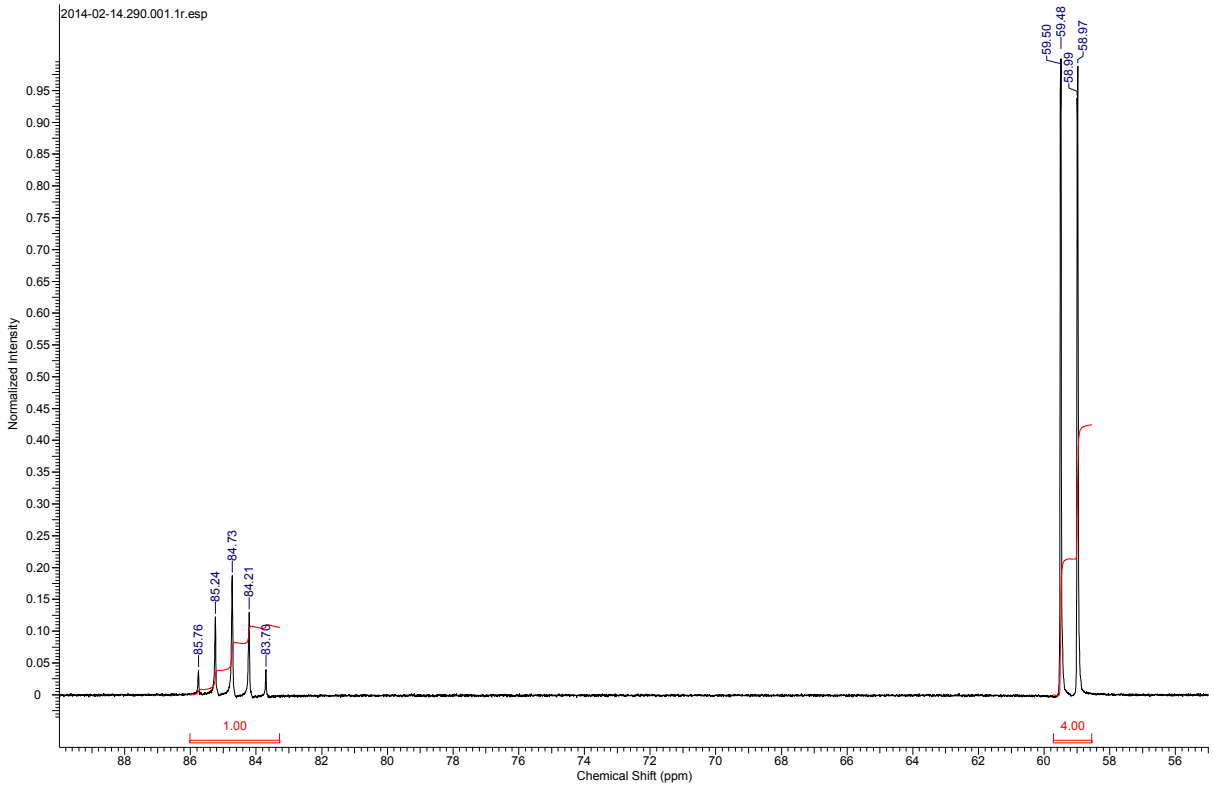

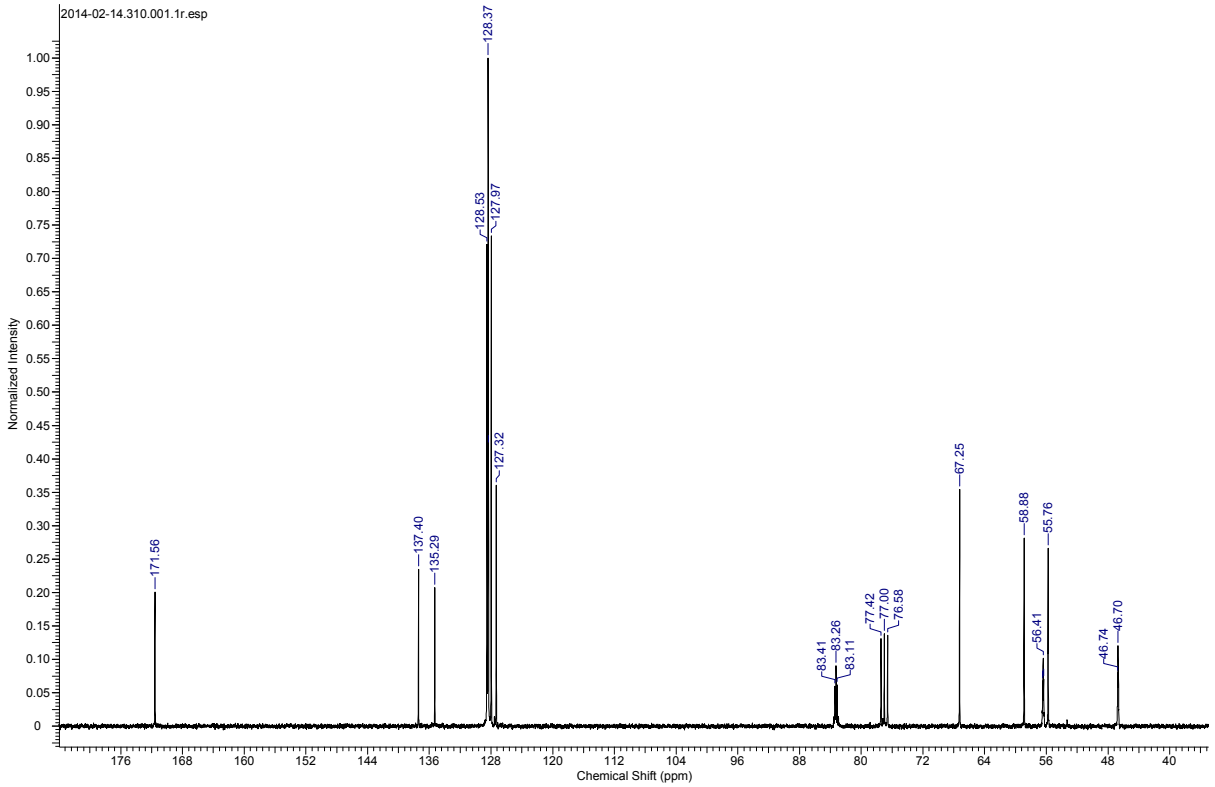

^{1}H, ^{19}F and ^{13}C NMR ($CDCl_3$) spectra of **5b**

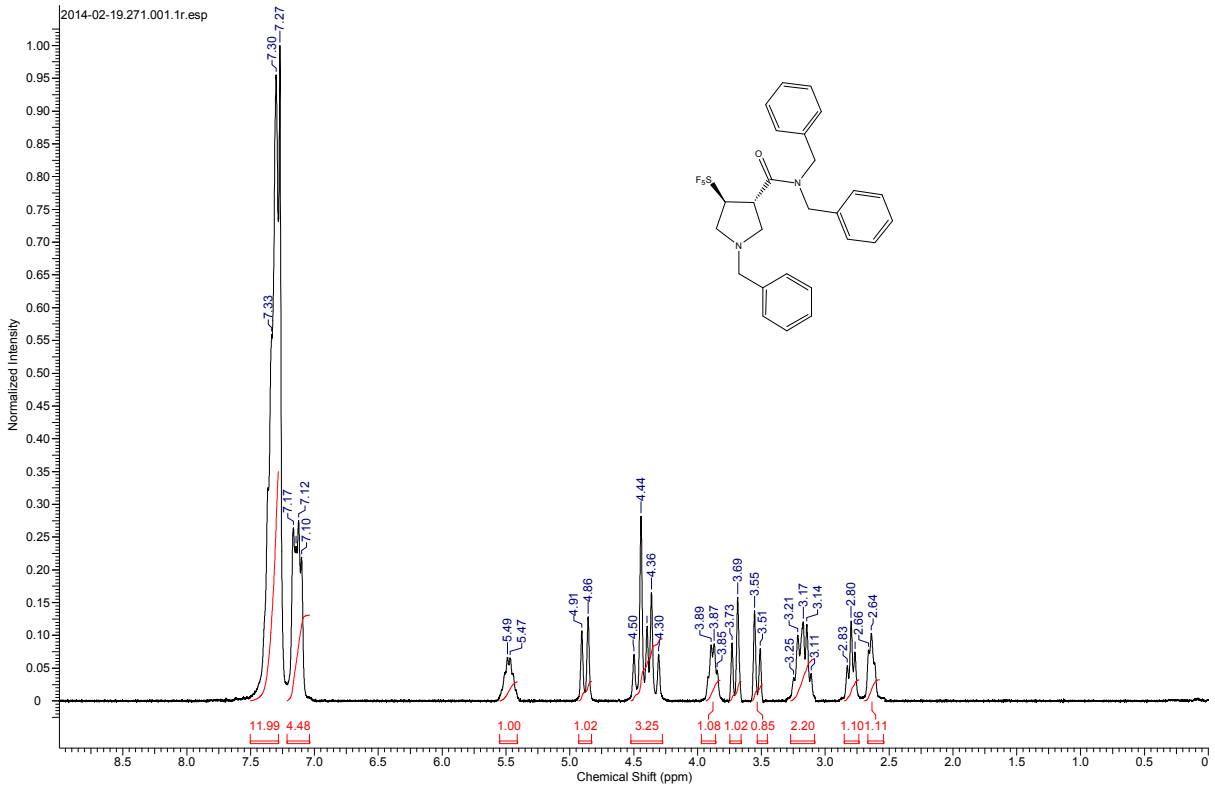

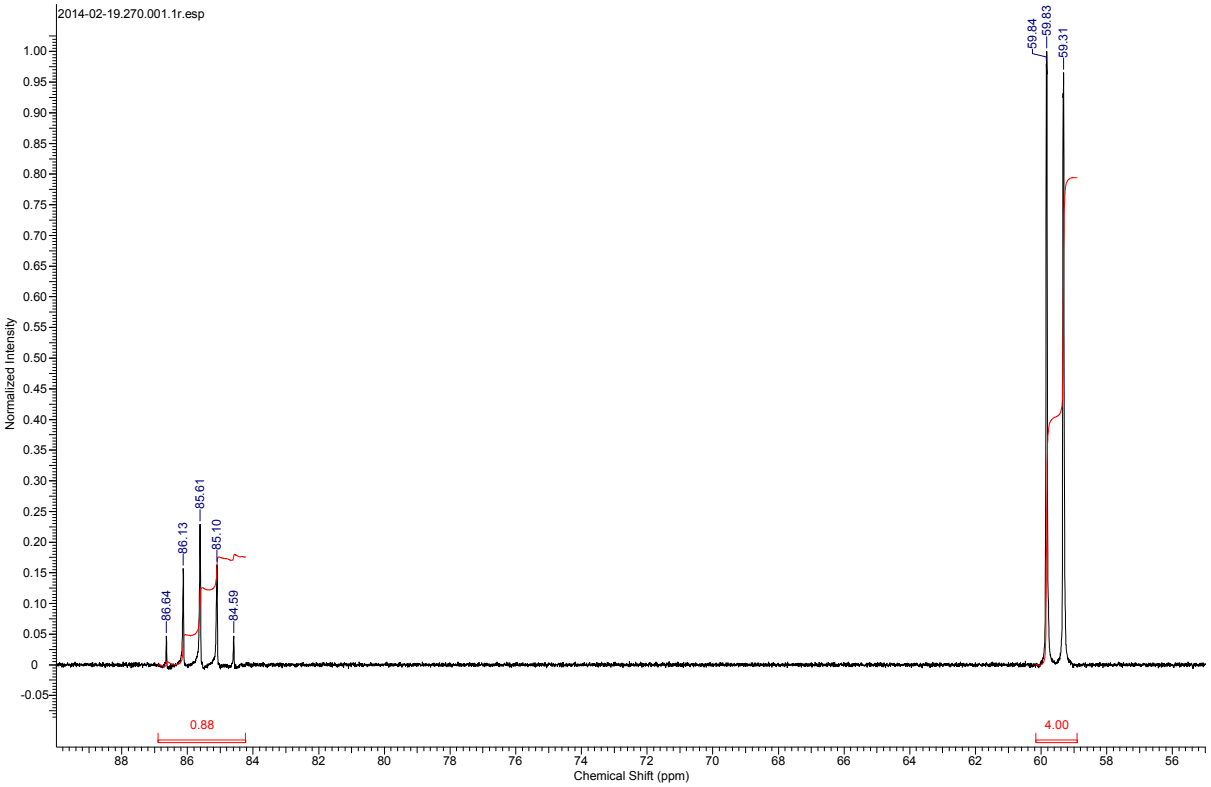
2014-02-19.270.001.1r.esp
Normalized Intensity
Chemical Shift (ppm)
86.64
86.13
85.61
85.10
84.59
59.84
59.83
59.31
0.88
4.00

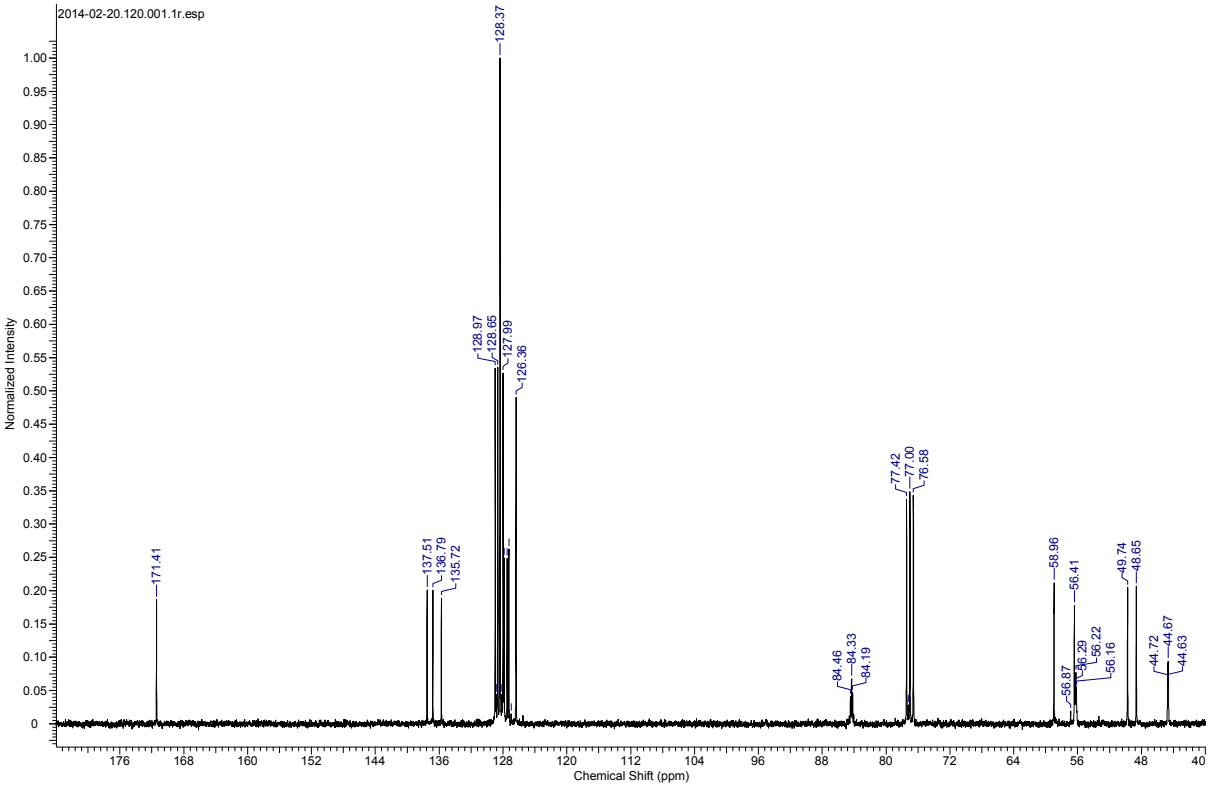
2014-02-20.120.001.1r.esp
Normalized Intensity
Chemical Shift (ppm)
171.41
137.51
136.79
135.72
128.97
128.65
127.99
126.36
128.37
84.46
84.33
84.19
77.42
77.00
76.58
58.96
56.87
56.41
56.29
56.22
56.16
49.74
48.65
44.72
44.67
44.63

^{1}H, ^{19}F and ^{13}C NMR ($CDCl_3$) spectra of **5c**

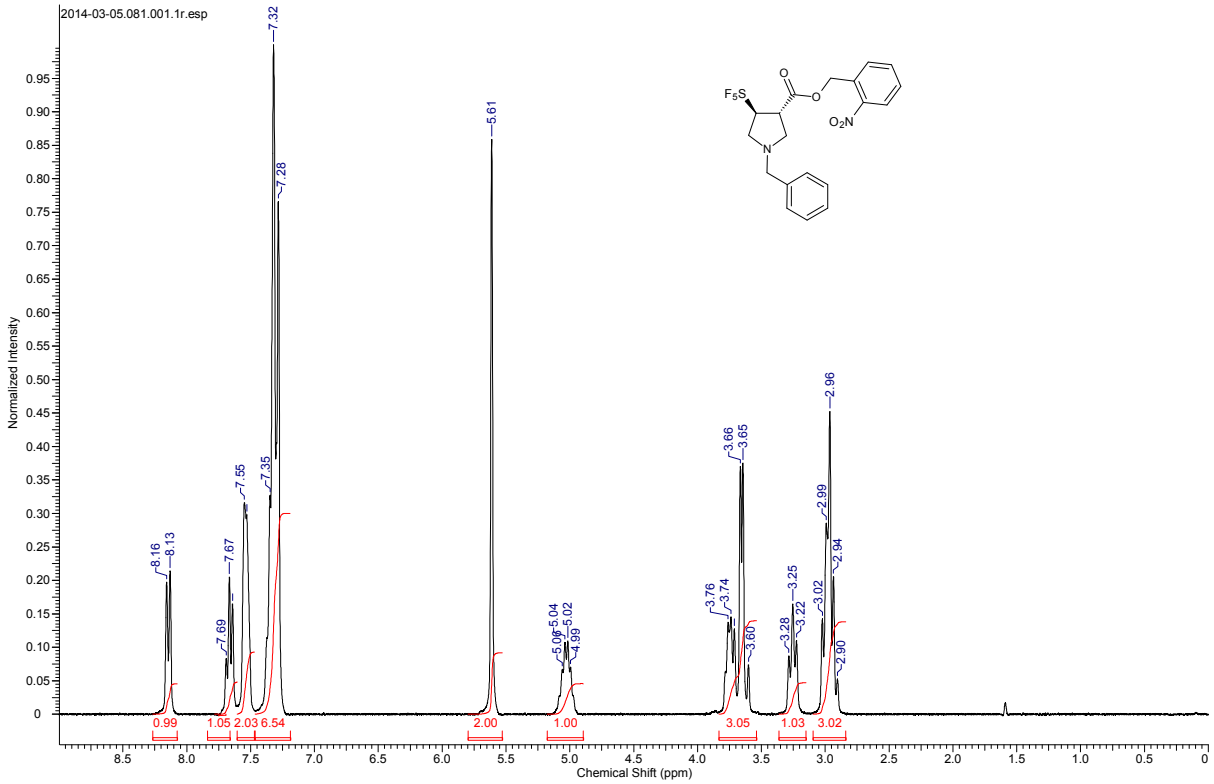

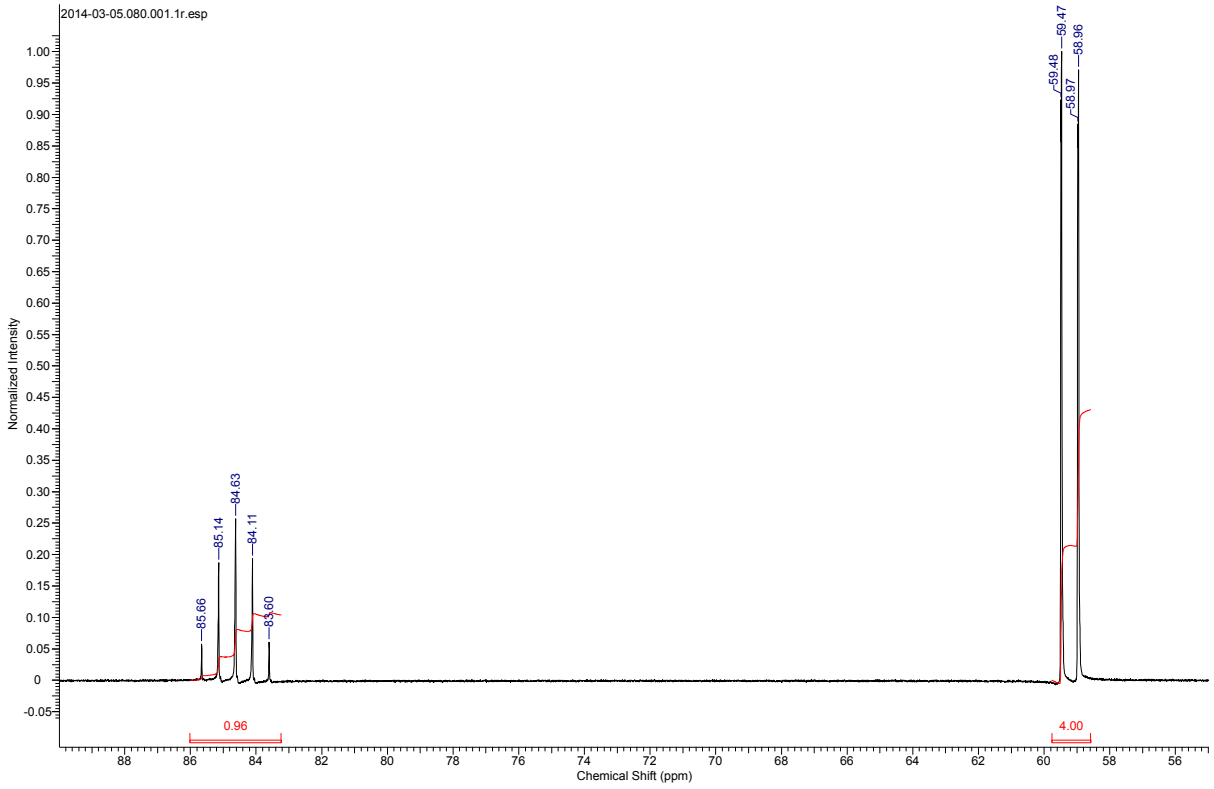

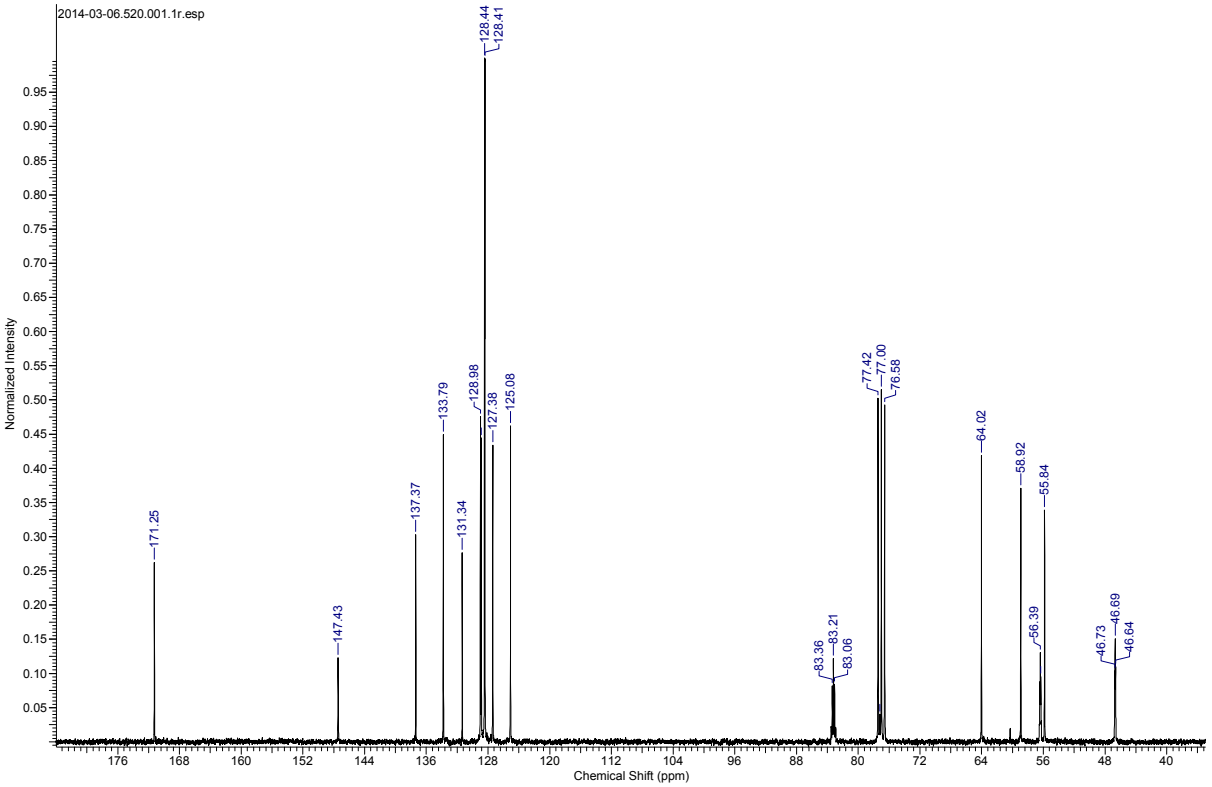
2014-03-06.520.001.1r.esp
Normalized Intensity
Chemical Shift (ppm)
128.44
128.41
171.25
147.43
137.37
133.79
131.34
128.98
127.38
125.08
83.36
83.21
83.06
77.42
77.00
76.58
64.02
58.92
56.39
55.84
46.73
46.69
46.64

^{1}H, ^{19}F and ^{13}C NMR ($CDCl_3$) spectra of **5d**

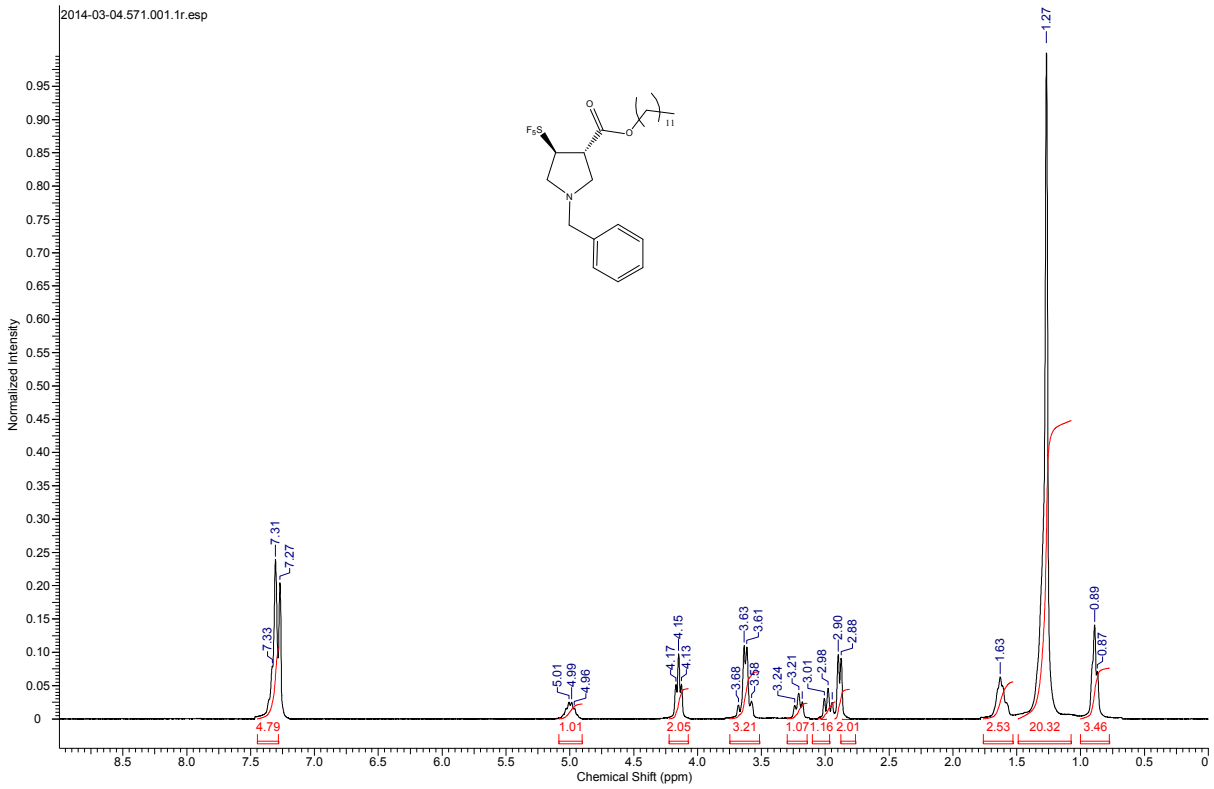

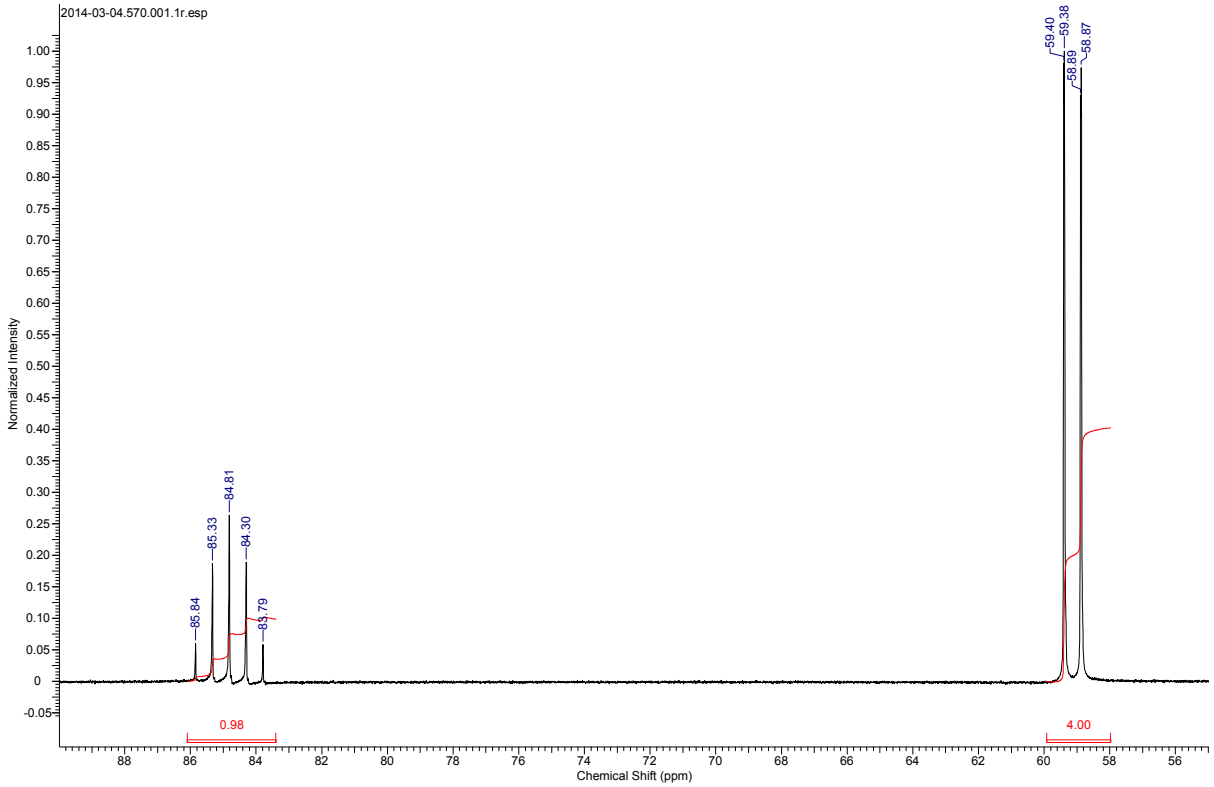

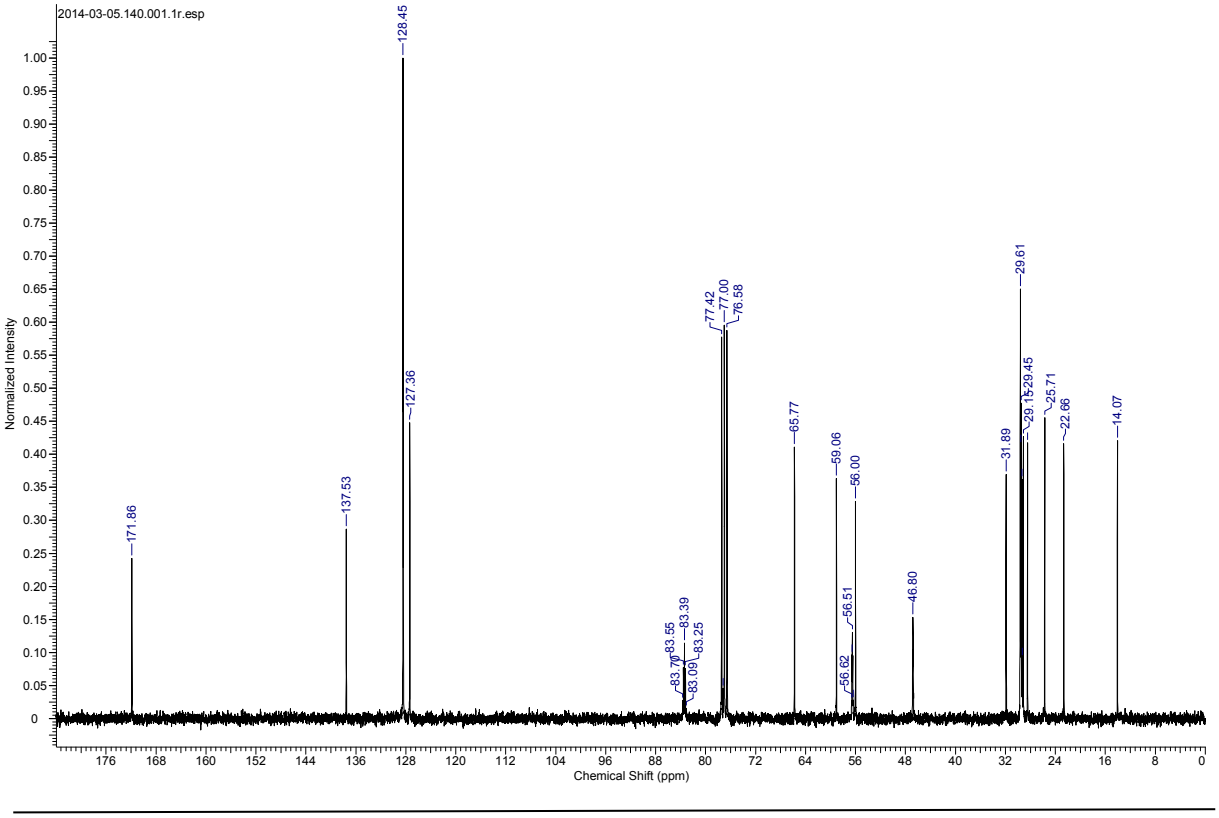
2014-03-05.140.001.1r.esp
Normalized Intensity
Chemical Shift (ppm)
128.45
127.36
137.53
171.86
77.42
77.00
76.58
65.77
59.06
56.00
56.51
56.62
46.80
31.89
29.61
29.45
29.15
25.71
22.66
14.07
83.55
83.39
83.25
83.09

^{1}H, ^{19}F and ^{13}C NMR ($CDCl_3$) spectra of **5e**

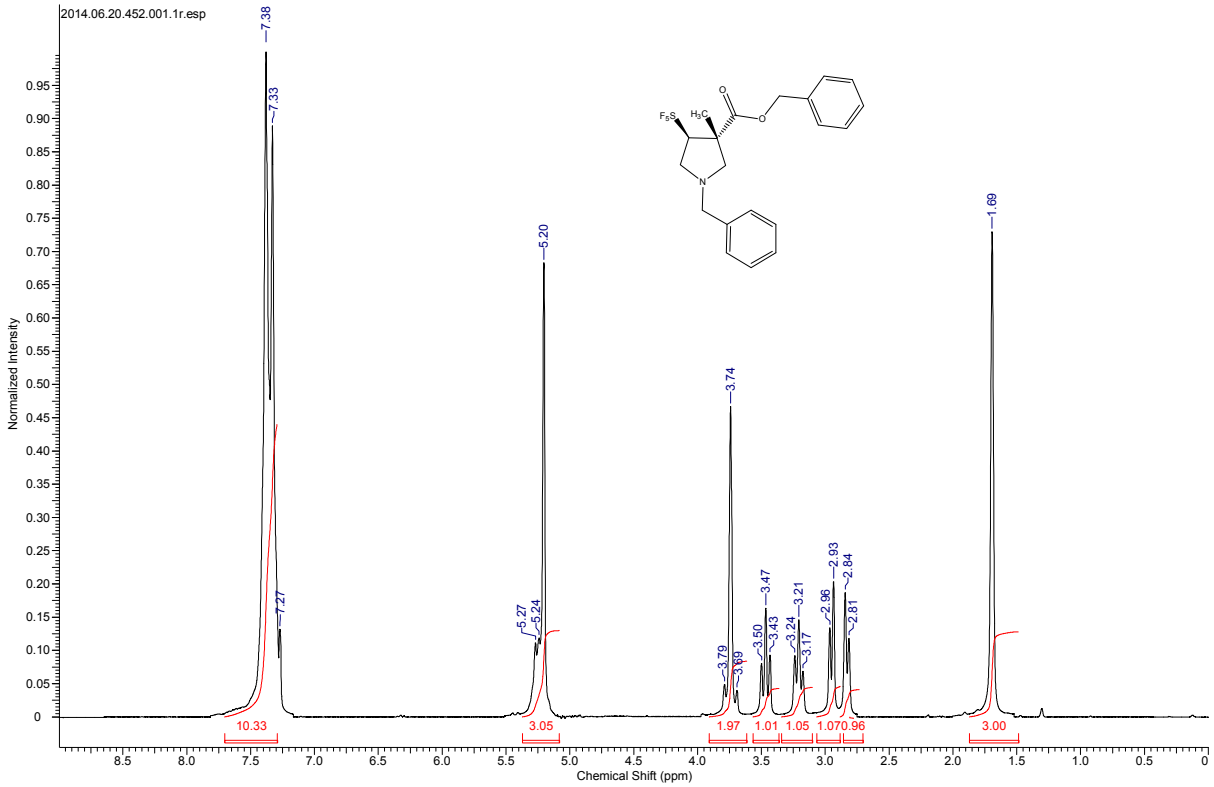

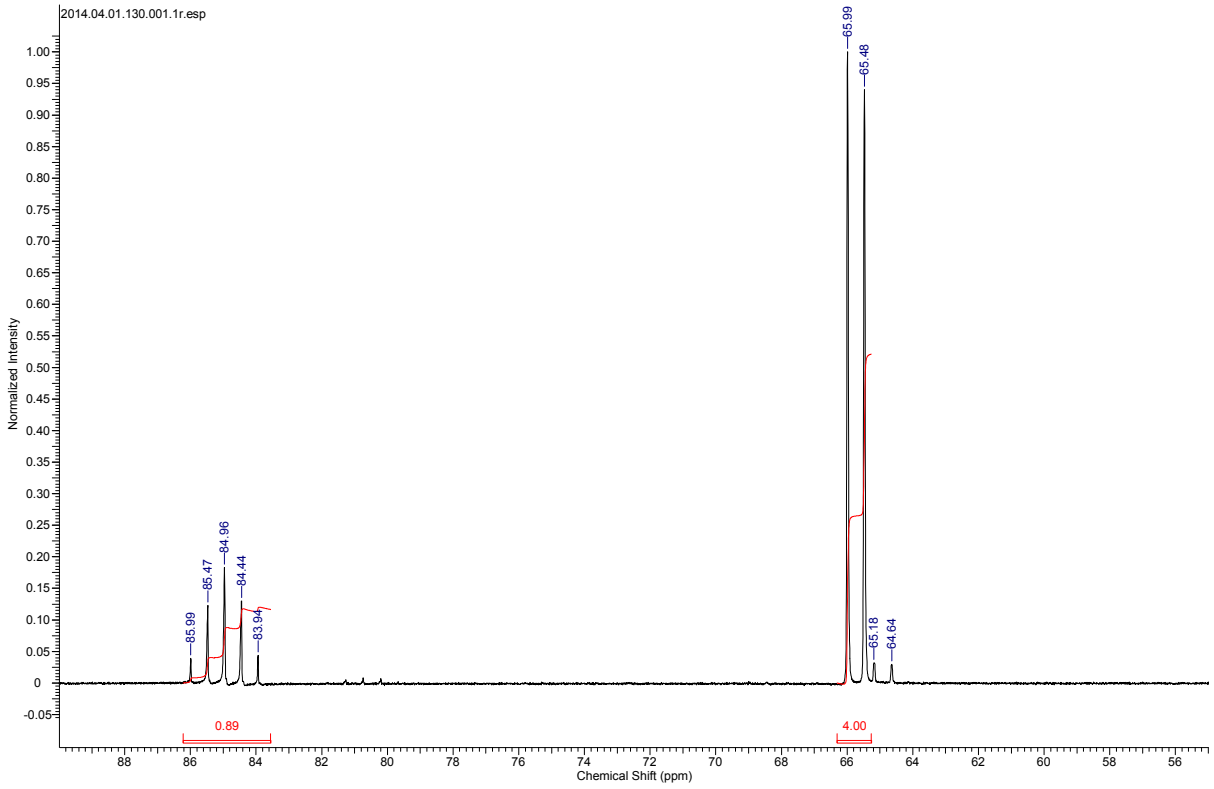

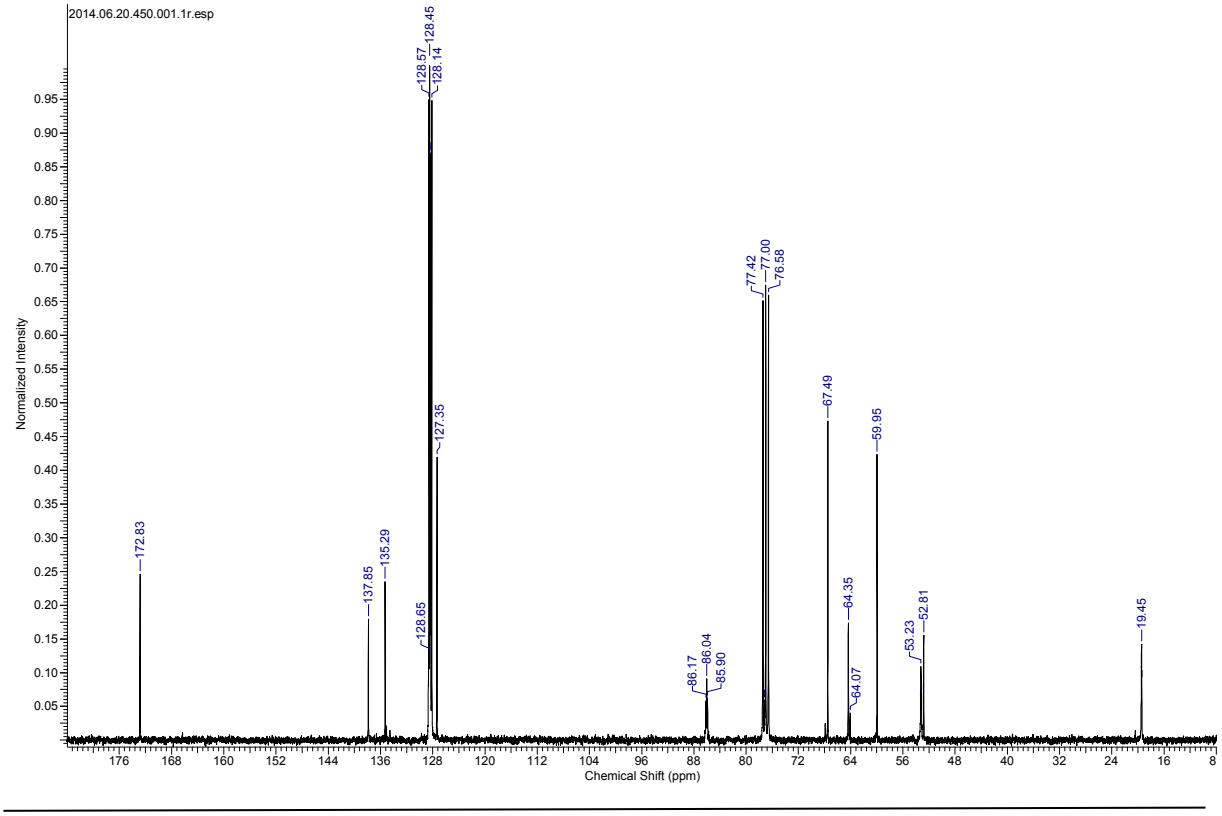
2014.06.20.450.001.1r.esp
Normalized Intensity
Chemical Shift (ppm)
172.83
137.85
135.29
128.65
128.57
128.45
128.14
127.35
86.17
86.04
85.90
77.42
77.00
76.58
67.49
64.35
64.07
59.95
53.23
52.81
19.45

^{1}H, ^{19}F and ^{13}C NMR ($CDCl_3$) spectra of **5f**

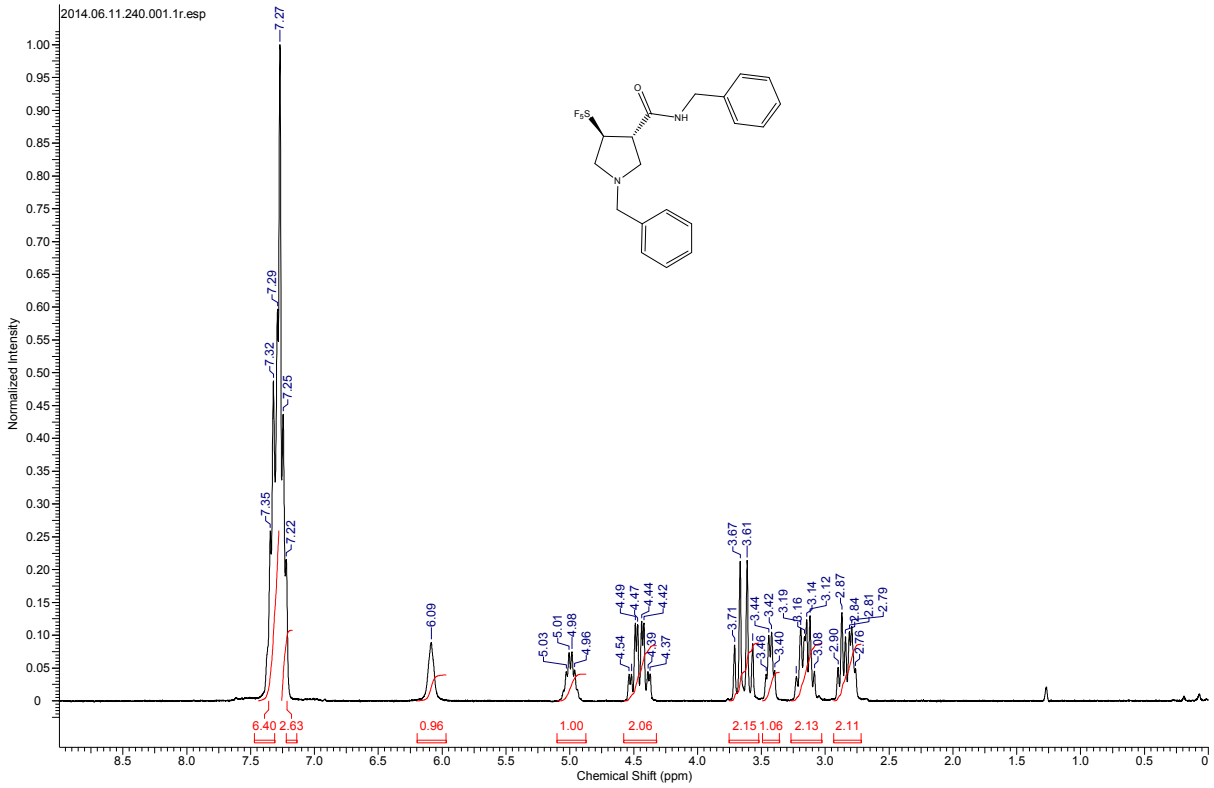

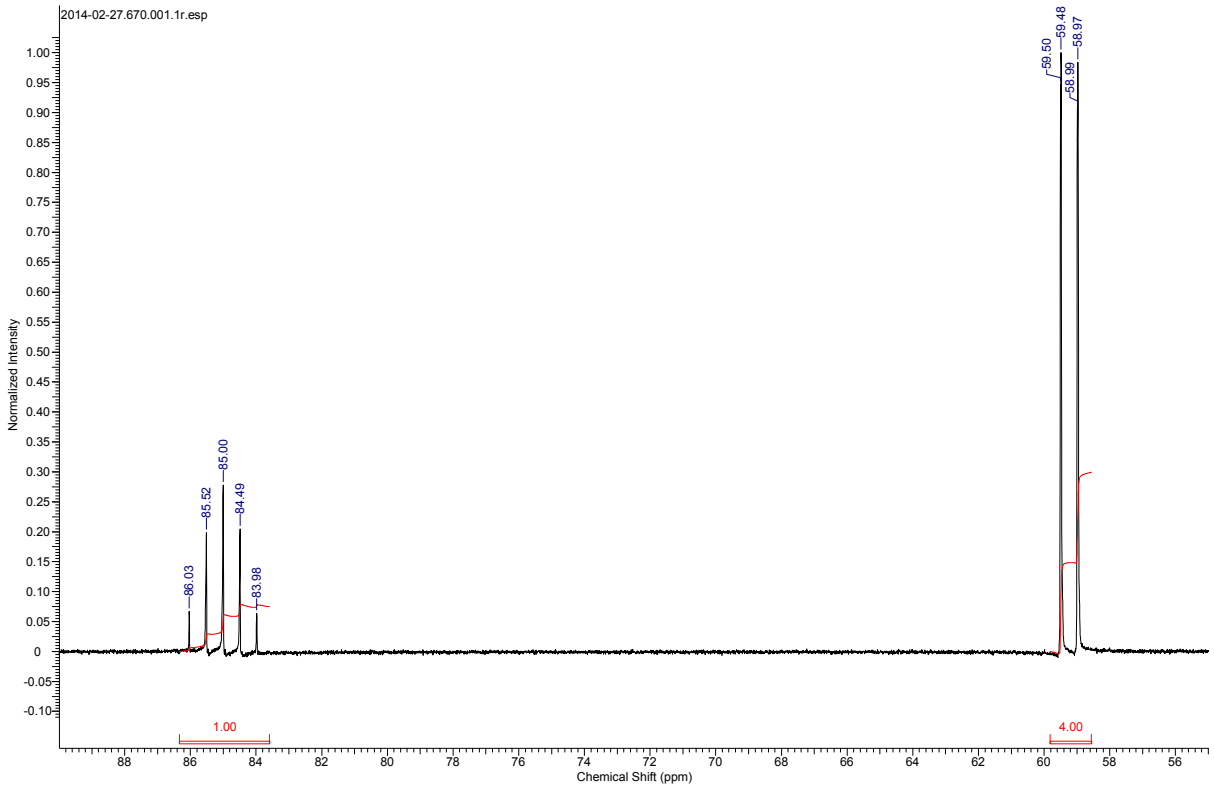

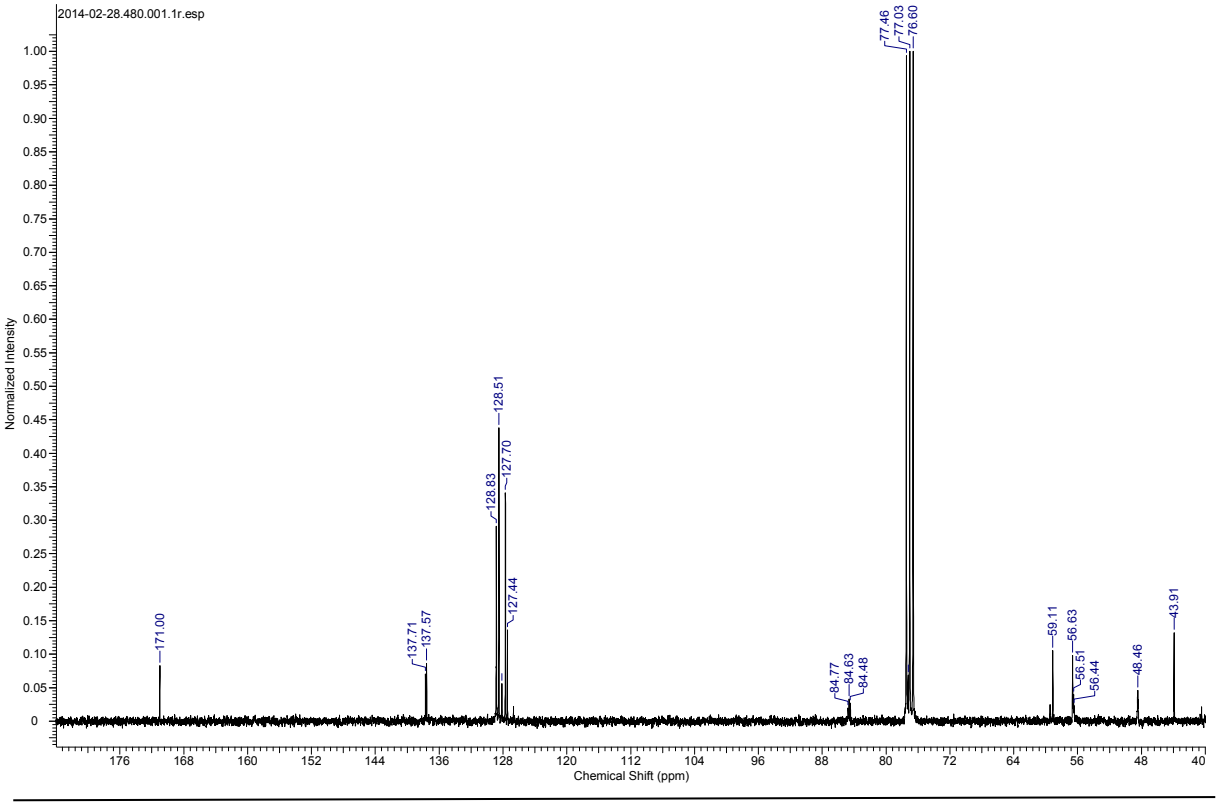
2014-02-28.480.001.1r.esp
Normalized Intensity
Chemical Shift (ppm)
171.00
137.71
137.57
128.83
128.51
127.70
127.44
84.77
84.63
84.48
77.46
77.03
76.60
59.11
56.63
56.51
56.44
48.46
43.91

^{1}H, ^{19}F and ^{13}C NMR ($CDCl_3$) spectra of **5g** (diastereomer n° 1)

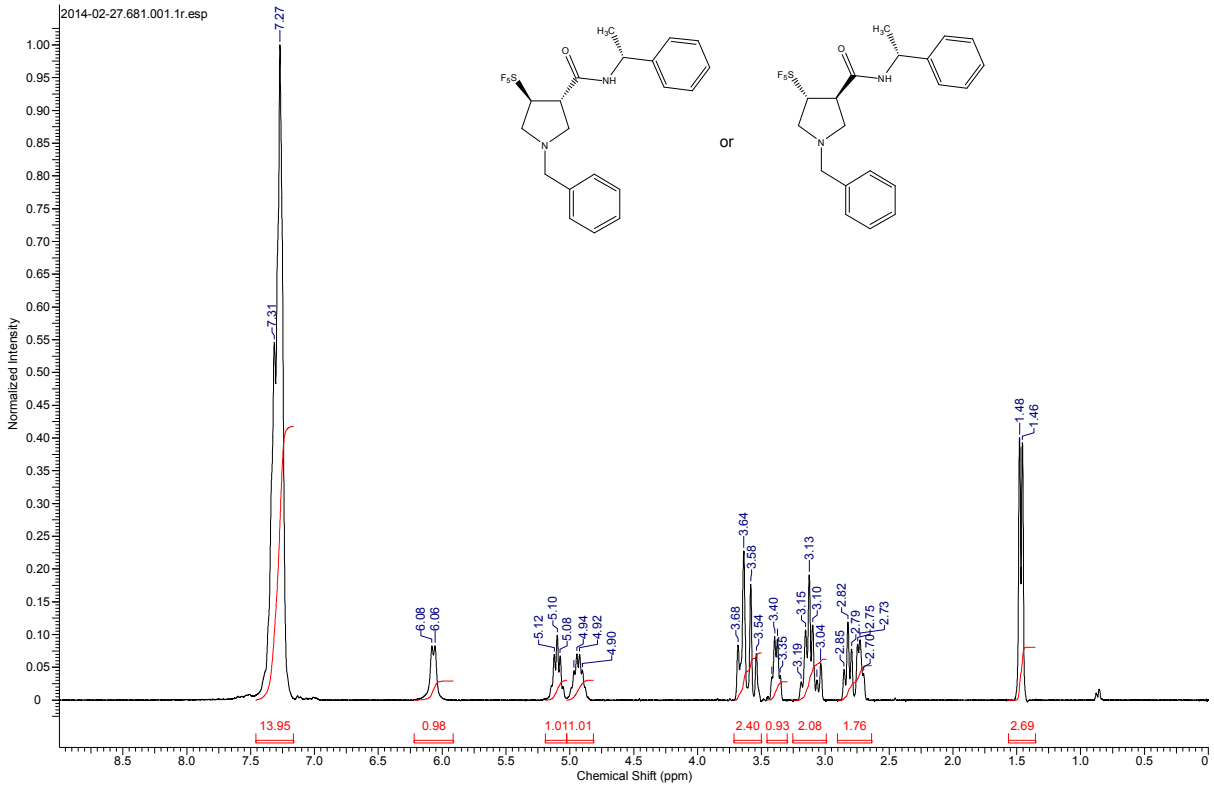

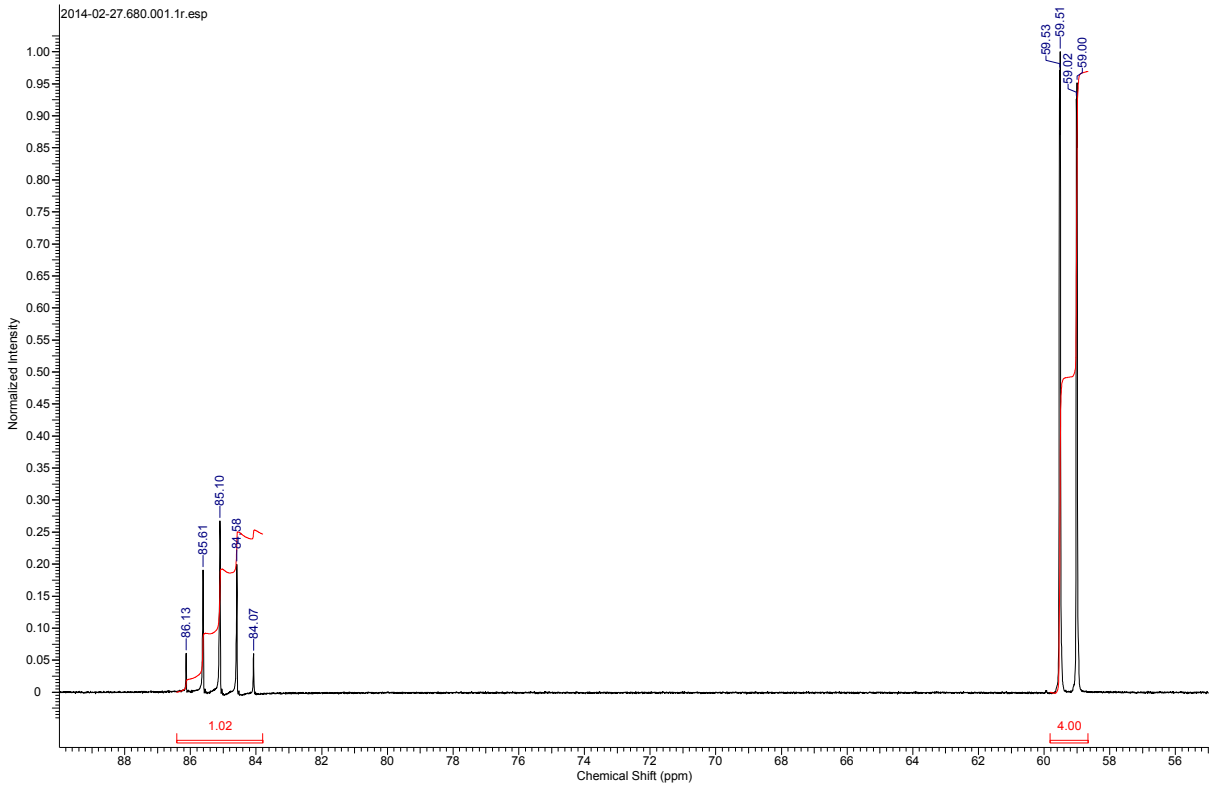

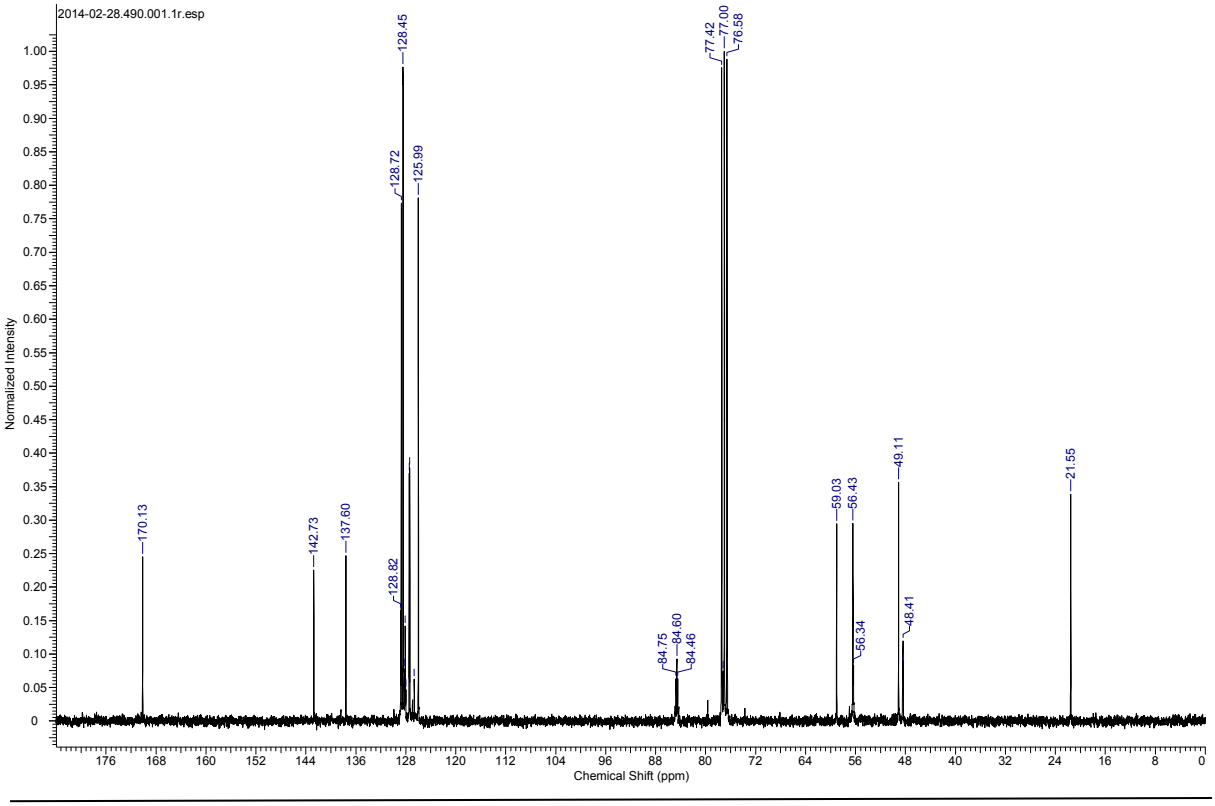
2014-02-28.490.001.1r.esp
Normalized Intensity
Chemical Shift (ppm)
170.13
142.73
137.60
128.82
128.72
128.45
125.99
84.75
84.60
84.46
77.42
77.00
76.58
59.03
56.43
56.34
49.11
48.41
21.55

^{1}H NMR, ^{19}F and ^{13}C ($CDCl_3$) spectra of **5g** (diastereomer n° 2)

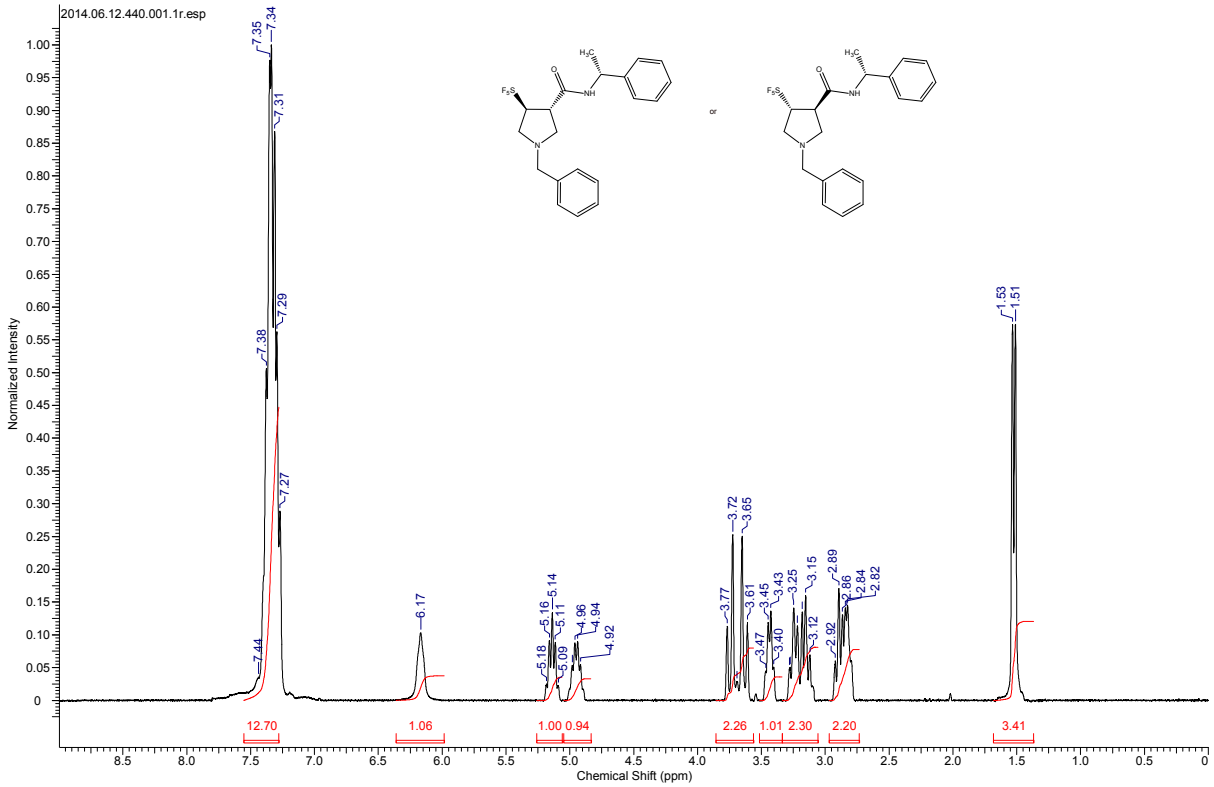

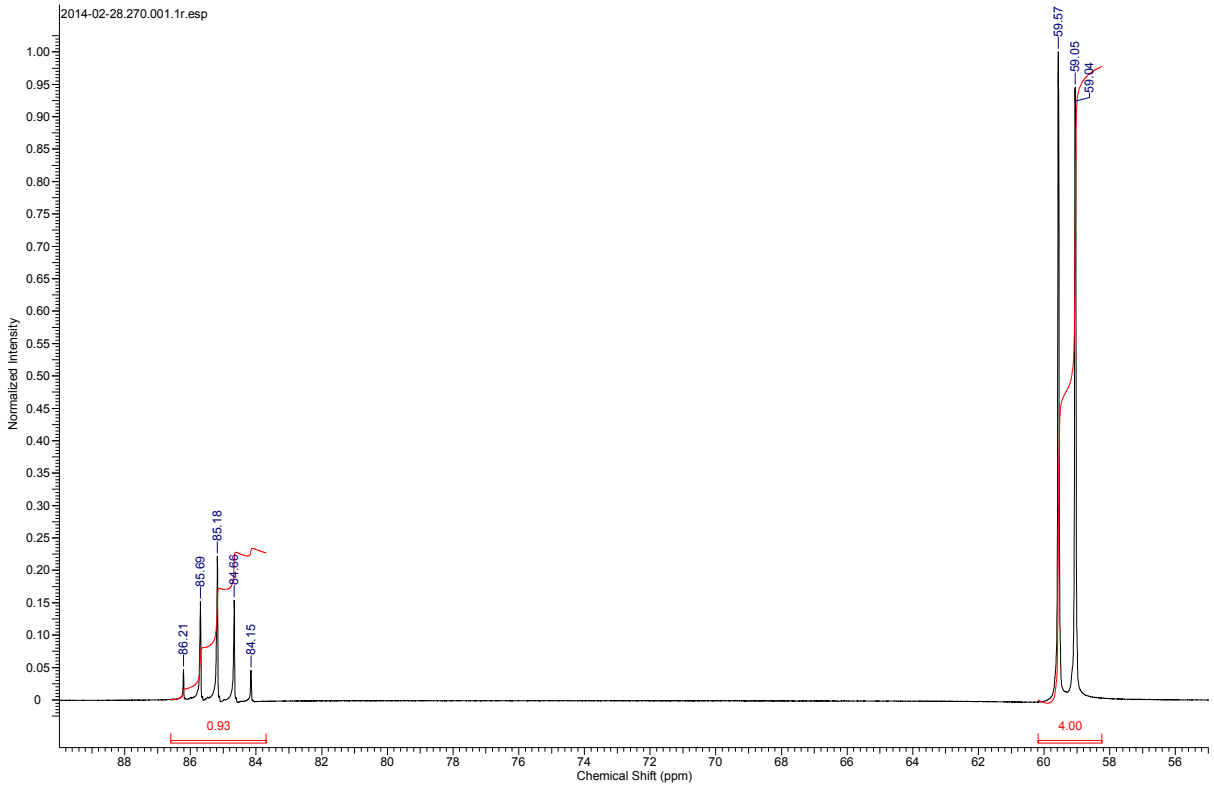

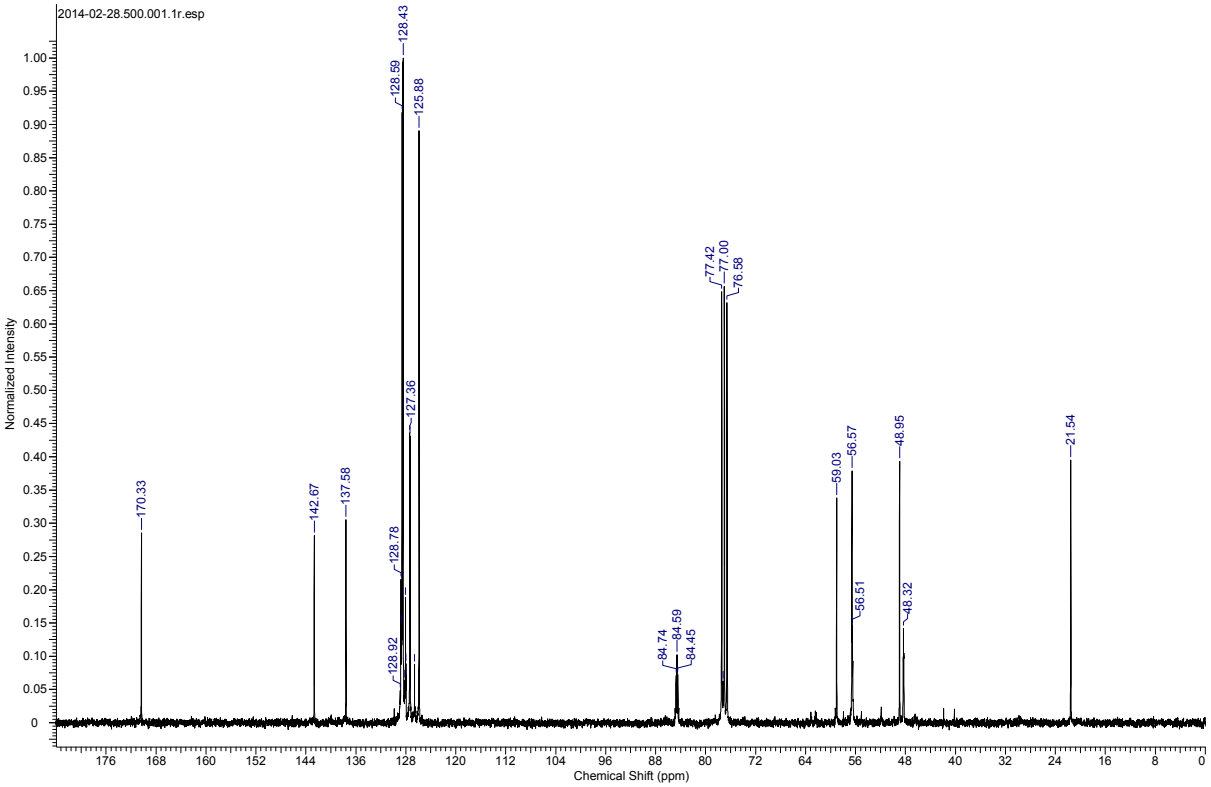
2014-02-28.500.001.1r.esp
Normalized Intensity
Chemical Shift (ppm)
170.33
142.67
137.58
128.92
128.78
128.59
128.43
127.36
125.88
84.74
84.59
84.45
77.42
77.00
76.58
59.03
56.57
56.51
48.95
48.32
21.54

^{1}H, ^{19}F and ^{13}C NMR ($CDCl_3$) spectra of **5h**

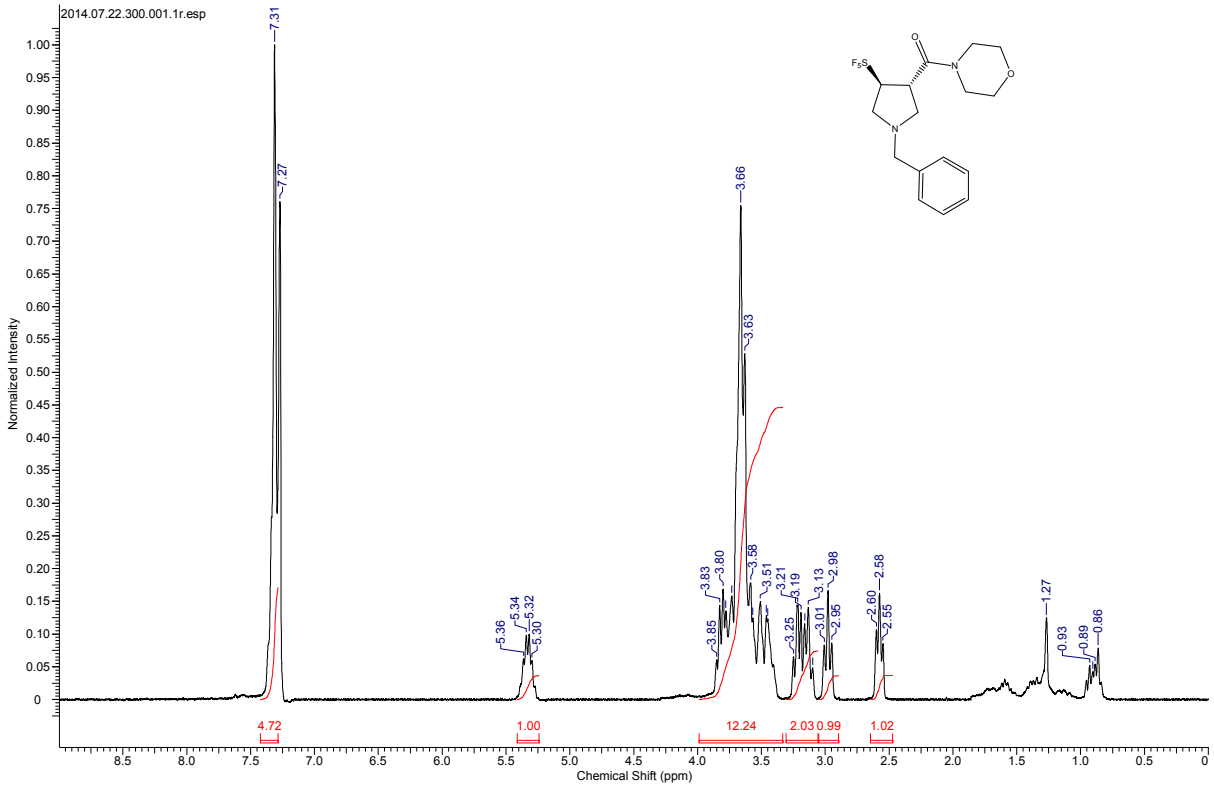

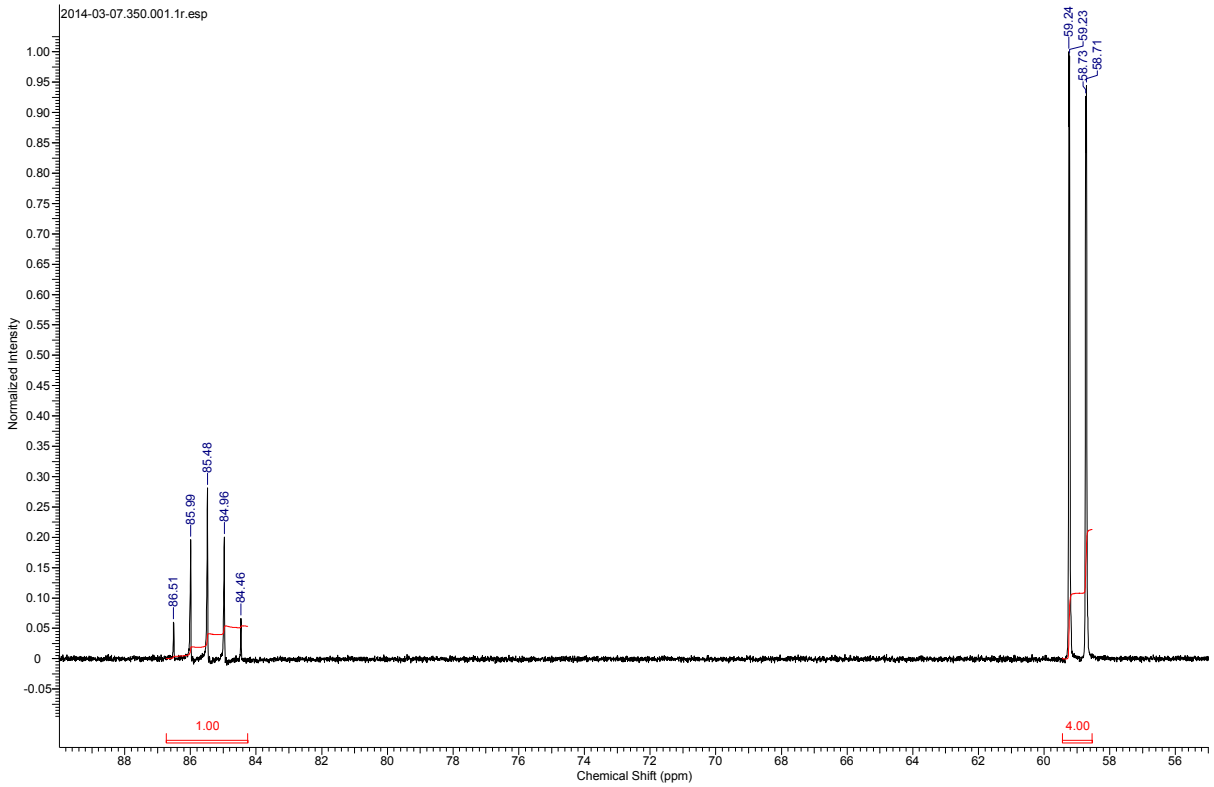

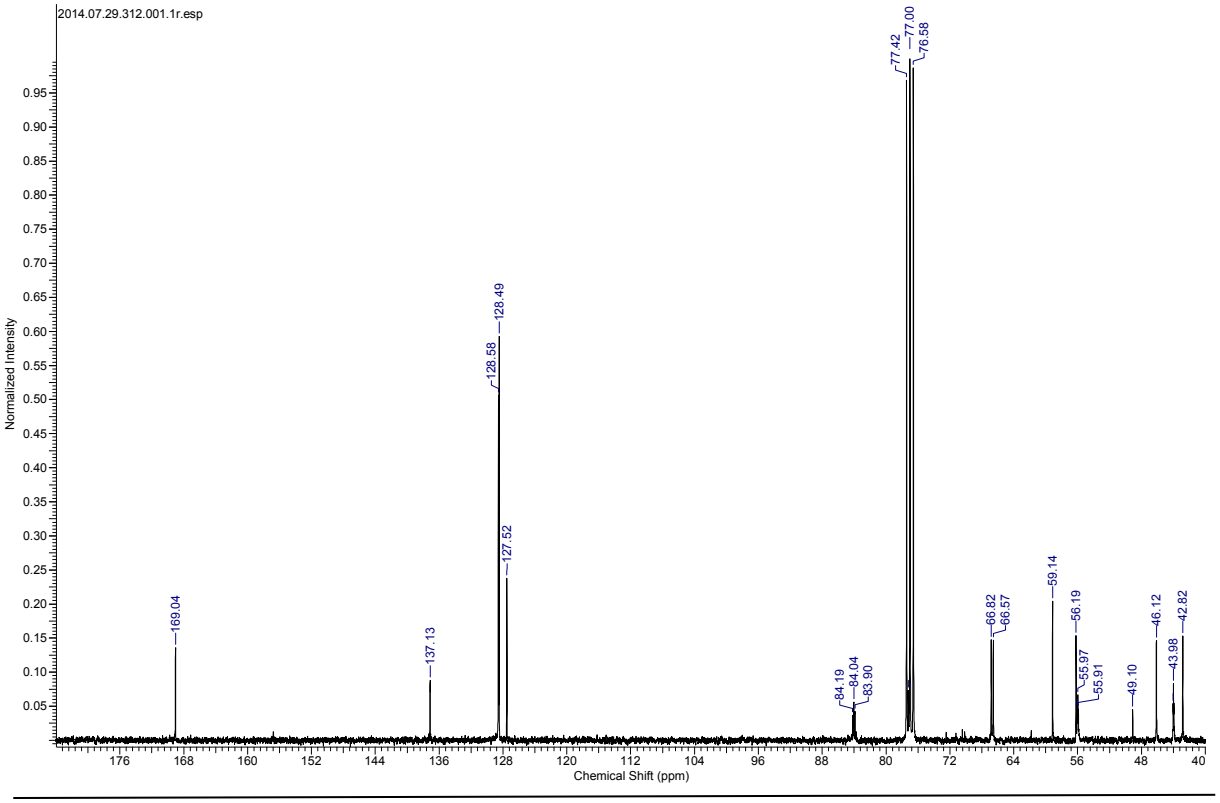
2014.07.29.312.001.1r.esp
Normalized Intensity
Chemical Shift (ppm)
169.04
137.13
128.58
128.49
127.52
84.19
84.04
83.90
77.42
77.00
76.58
66.82
66.57
59.14
56.19
55.97
55.91
49.10
46.12
43.98
42.82

^{1}H, ^{19}F and ^{13}C NMR ($CDCl_3$) spectra of **5i**

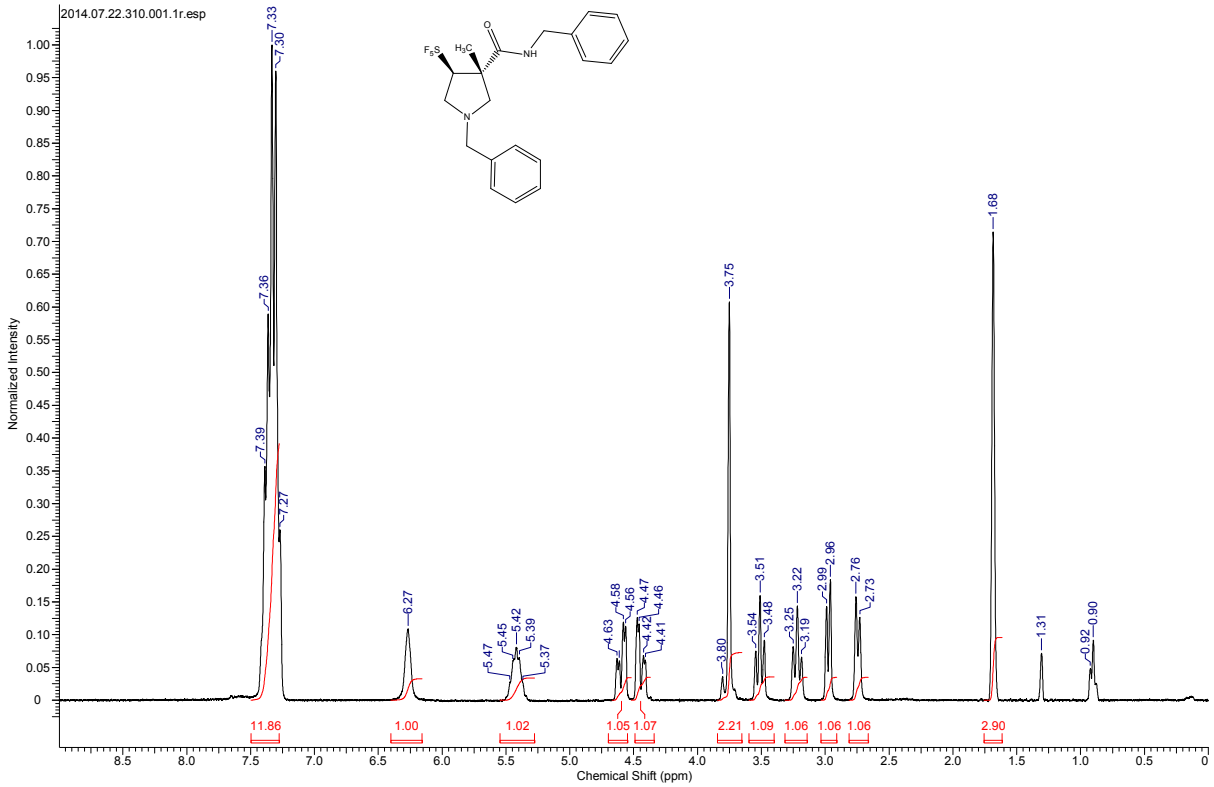

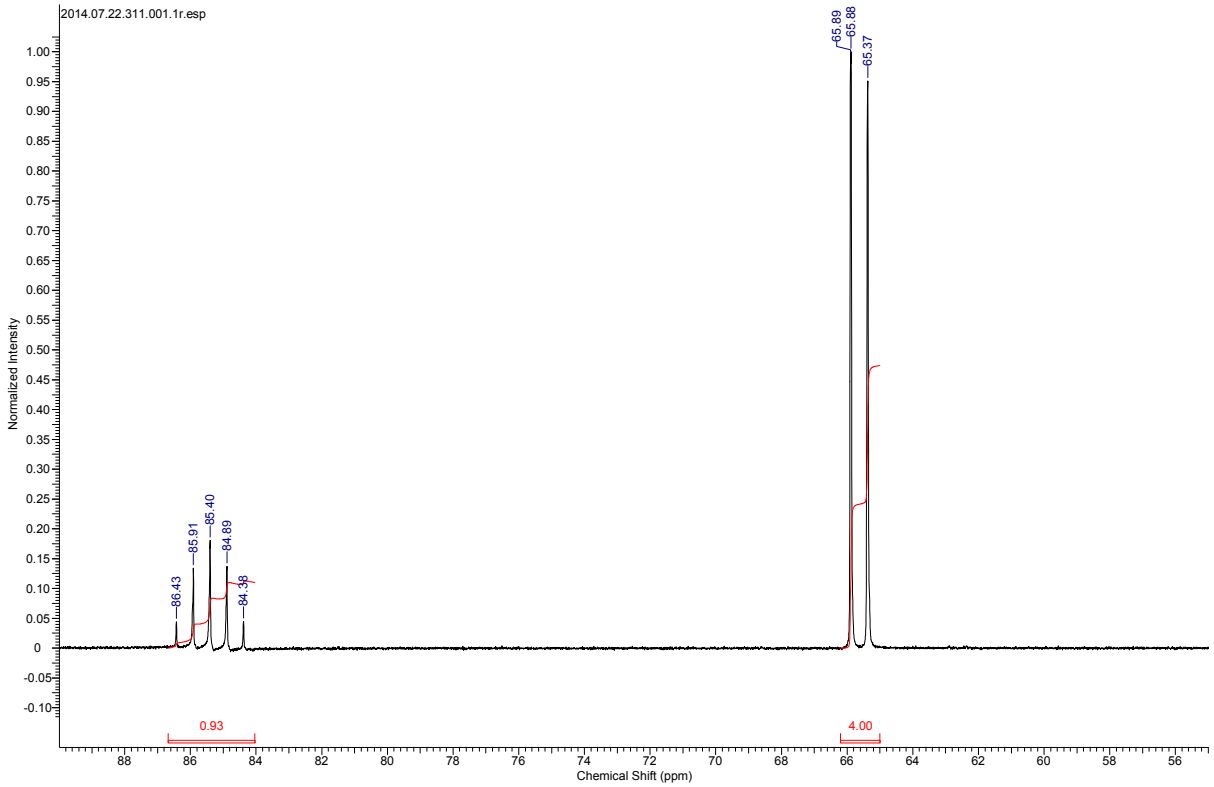

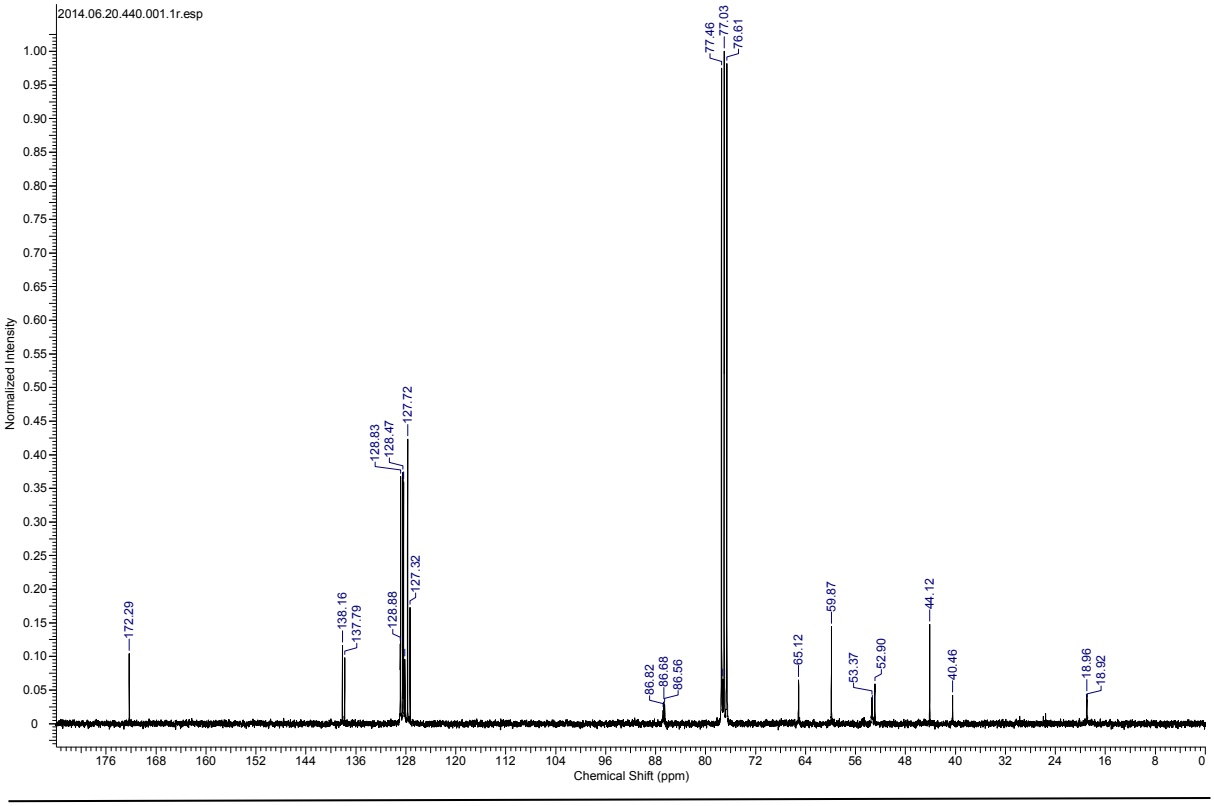
2014.06.20.440.001.1r.esp
Normalized Intensity
Chemical Shift (ppm)
172.29
138.16
137.79
128.88
128.83
128.47
127.72
127.32
86.82
86.68
86.56
77.46
77.03
76.61
65.12
59.87
53.37
52.90
44.12
40.46
18.96
18.92

^{1}H, ^{19}F and ^{13}C NMR ($CDCl_3$) spectra of **5j**

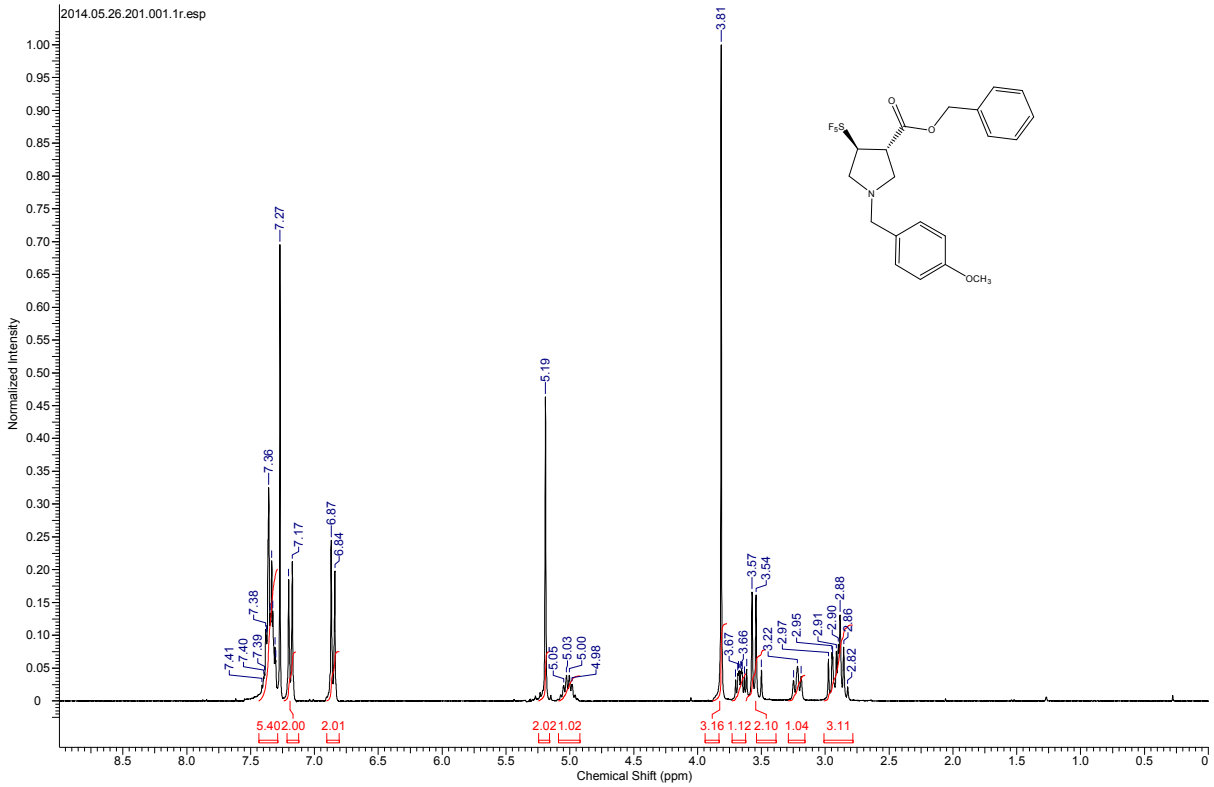

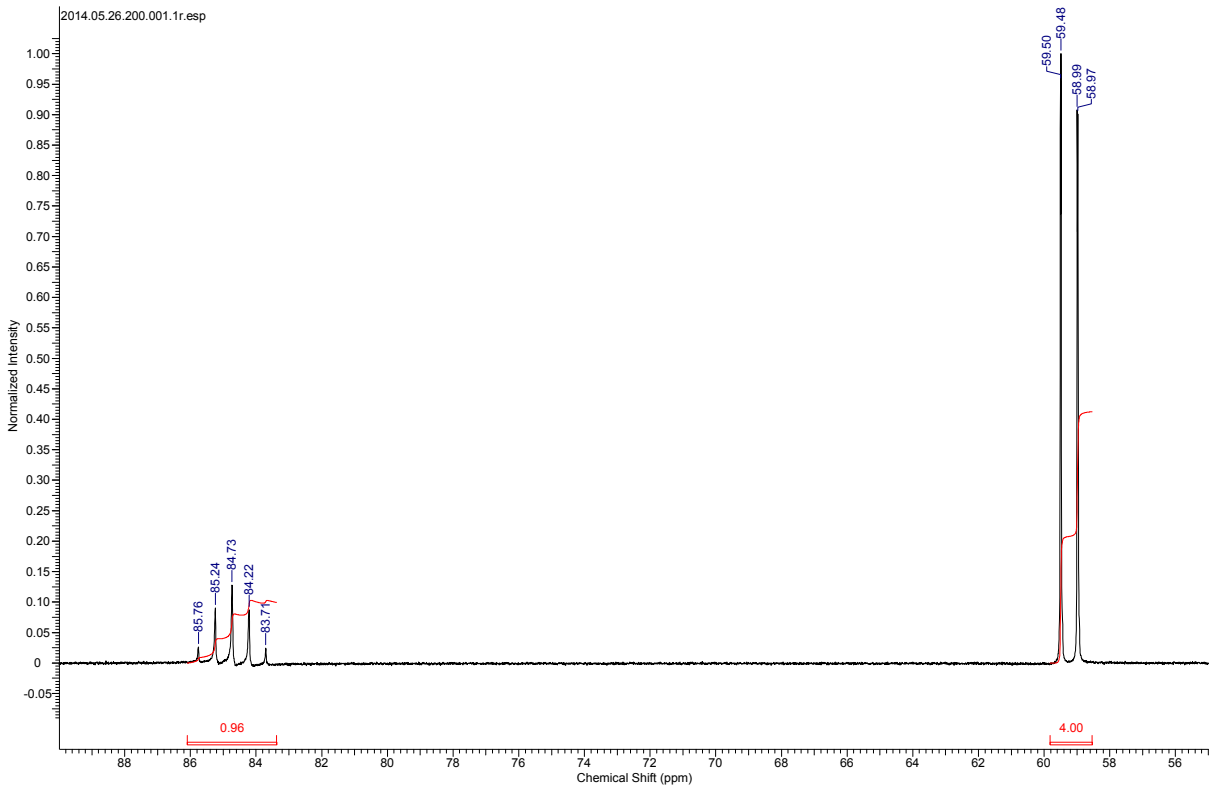

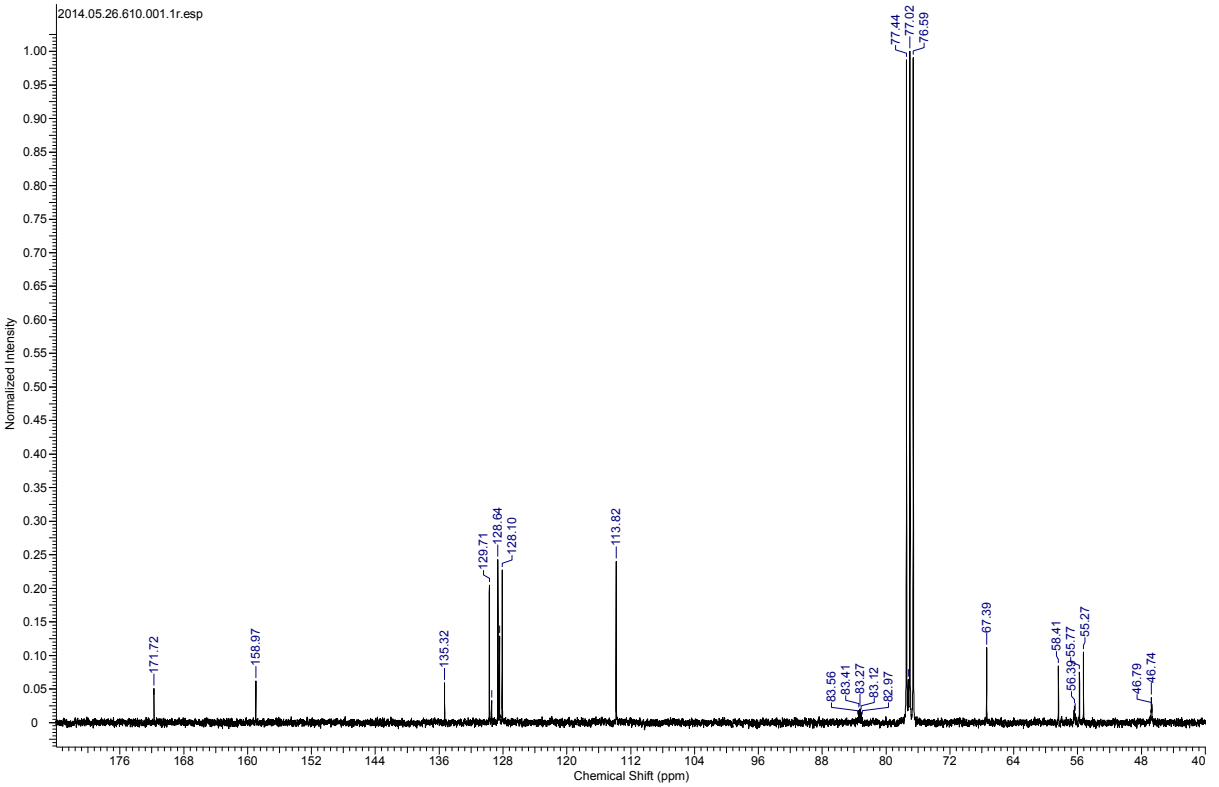

^{1}H, ^{19}F and ^{13}C RMN ($CDCl_3$) spectra of **5k**

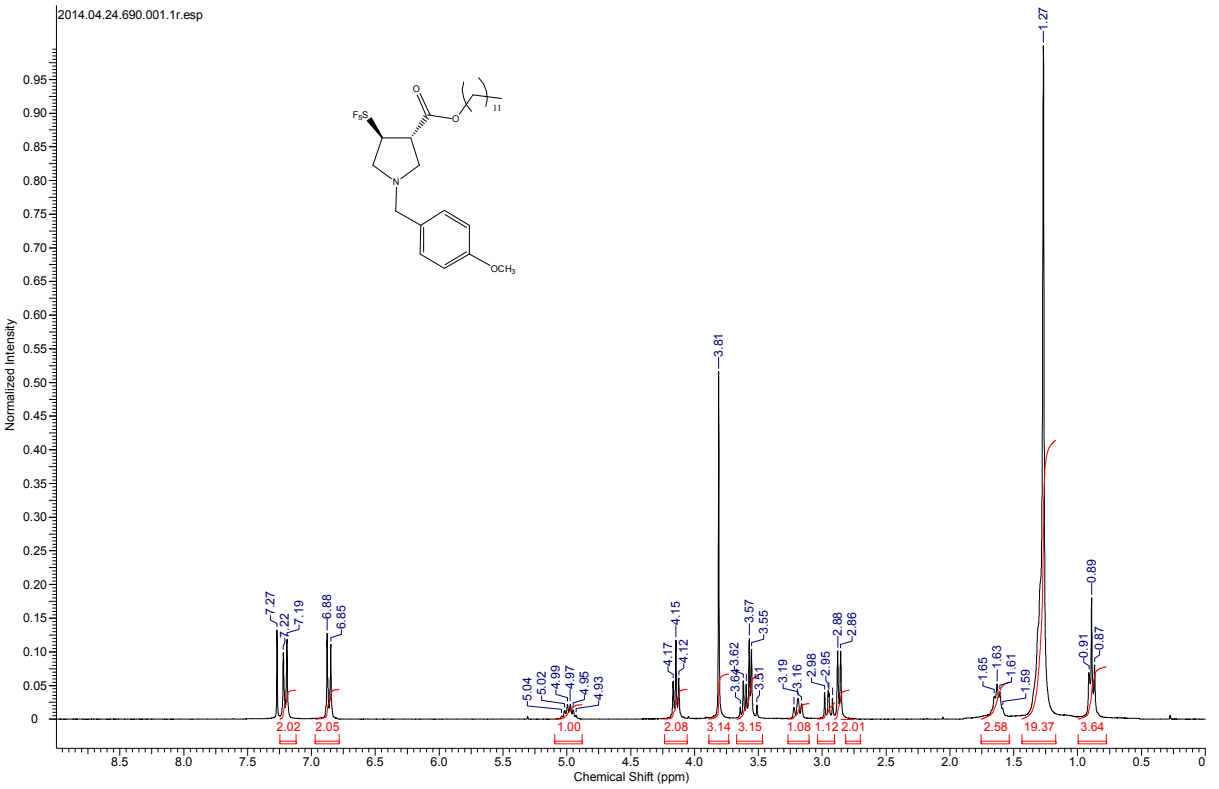

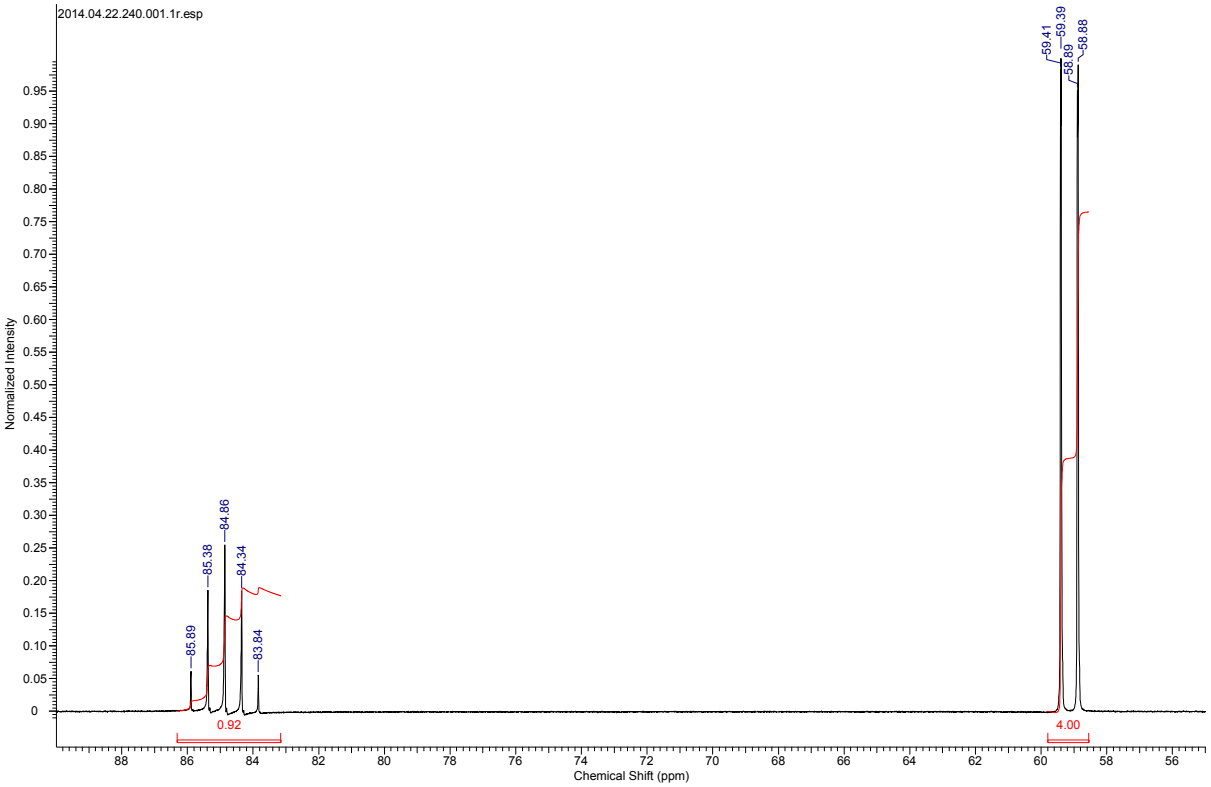
2014.04.22.240.001.1r.esp
Normalized Intensity
Chemical Shift (ppm)
85.89
85.38
84.86
84.34
83.84
59.41
59.39
58.89
58.88
0.92
4.00

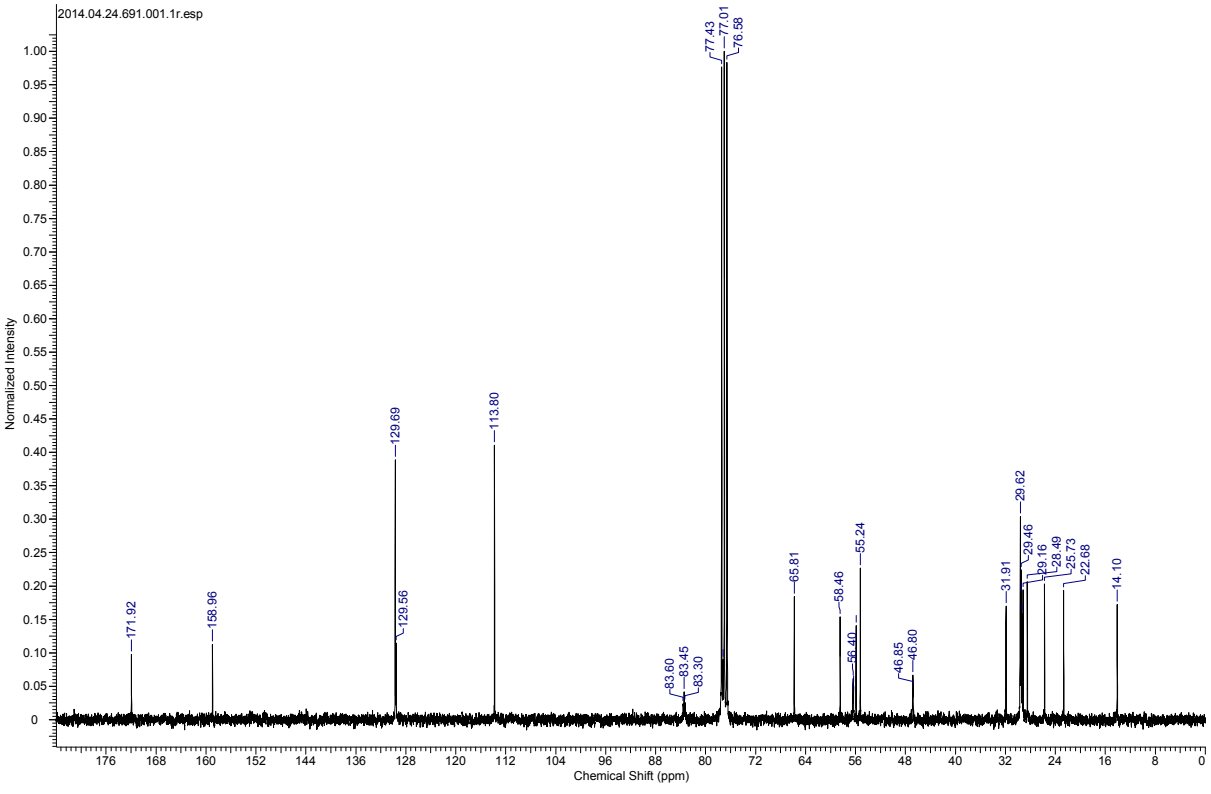
2014.04.24.691.001.1r.esp
Normalized Intensity
Chemical Shift (ppm)
171.92
158.96
129.69
129.56
113.80
83.60
83.45
83.30
77.43
77.01
76.58
65.81
58.46
56.40
55.24
46.85
46.80
31.91
29.62
29.46
29.16
28.49
25.73
22.68
14.10

^{1}H, ^{19}F and ^{13}C NMR ($CDCl_3$) spectra of **5l** (**5l** was contaminated by ~5% of the starting product)

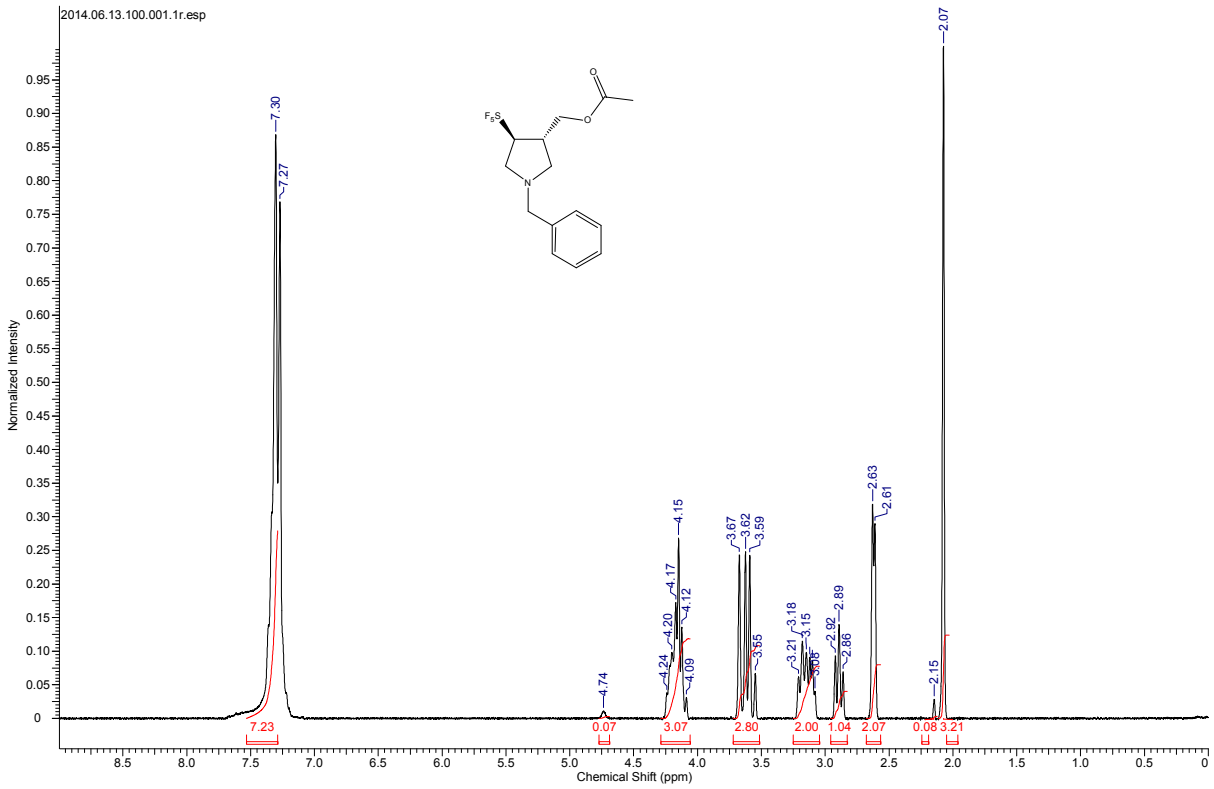

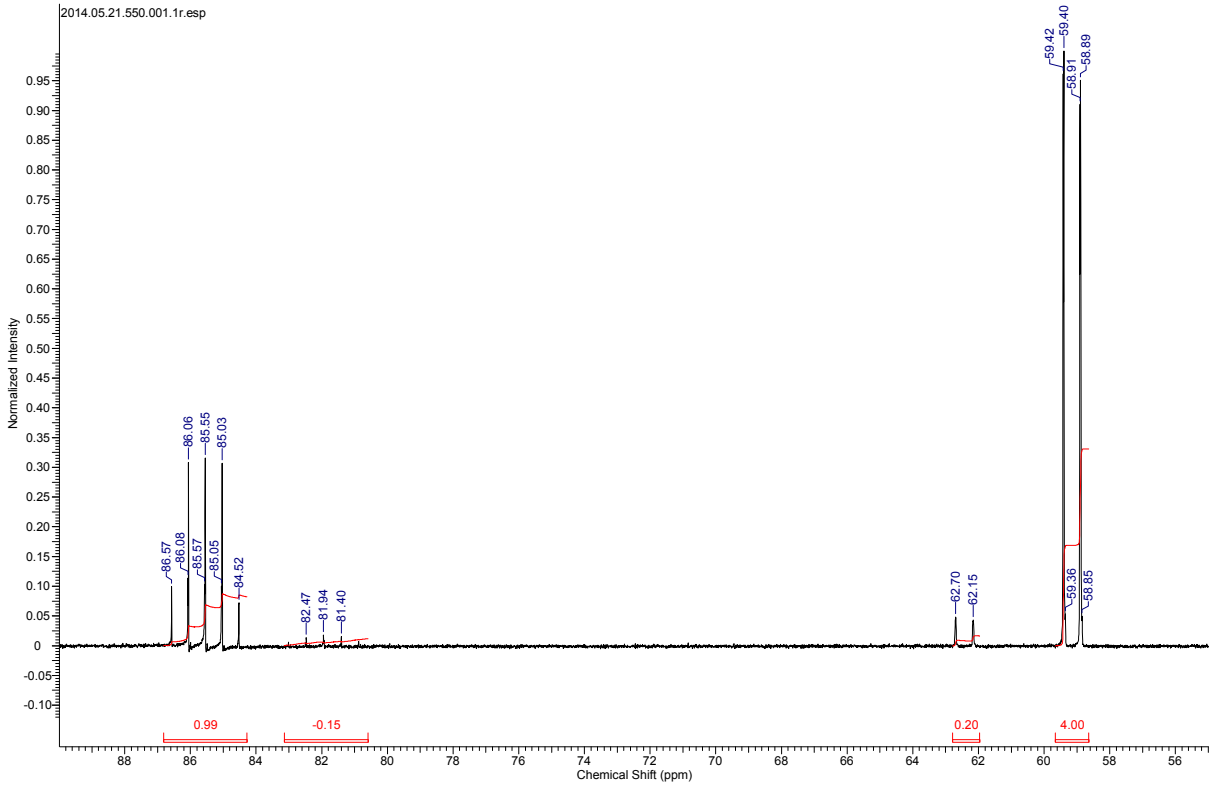

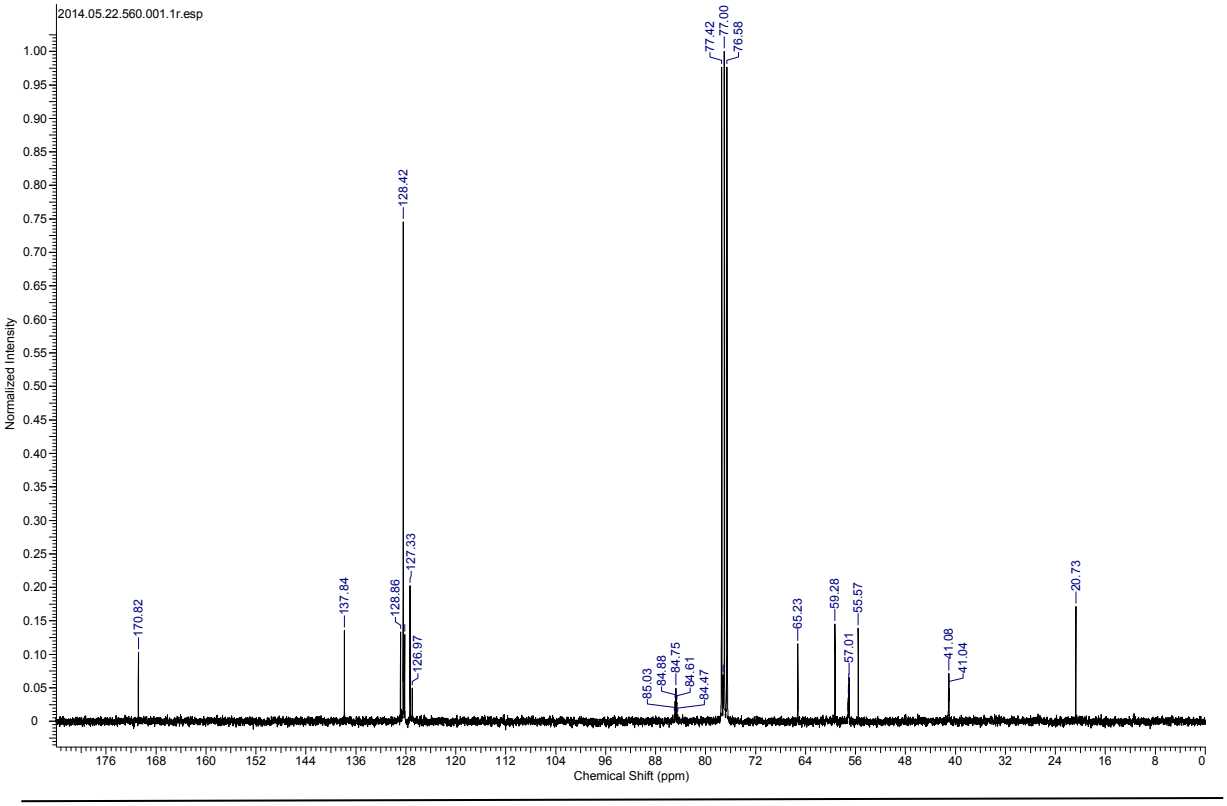
2014.05.22.560.001.1r.esp
Normalized Intensity
Chemical Shift (ppm)
170.82
137.84
128.86
128.42
127.33
126.97
85.03
84.88
84.75
84.61
84.47
77.42
77.00
76.58
65.23
59.28
57.01
55.57
41.08
41.04
20.73

^{1}H, ^{19}F and ^{13}C NMR ($CDCl_3$) spectra of **8**

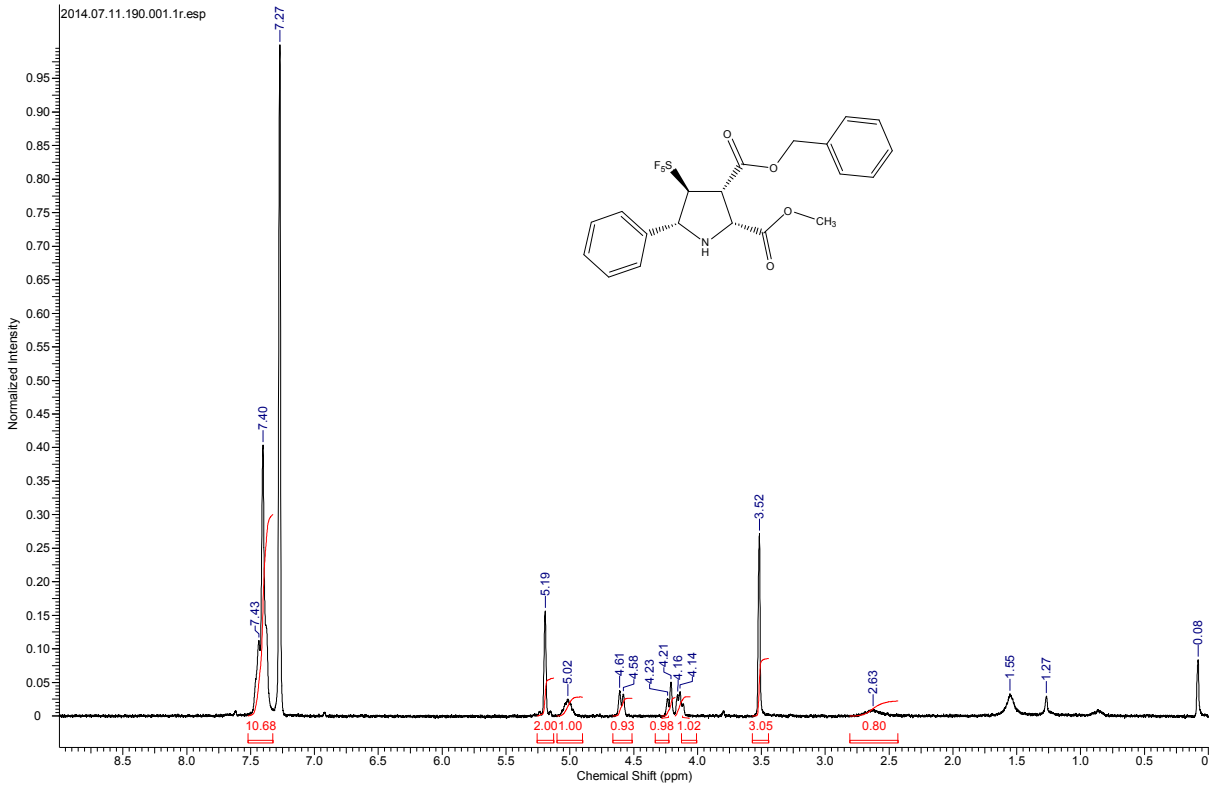

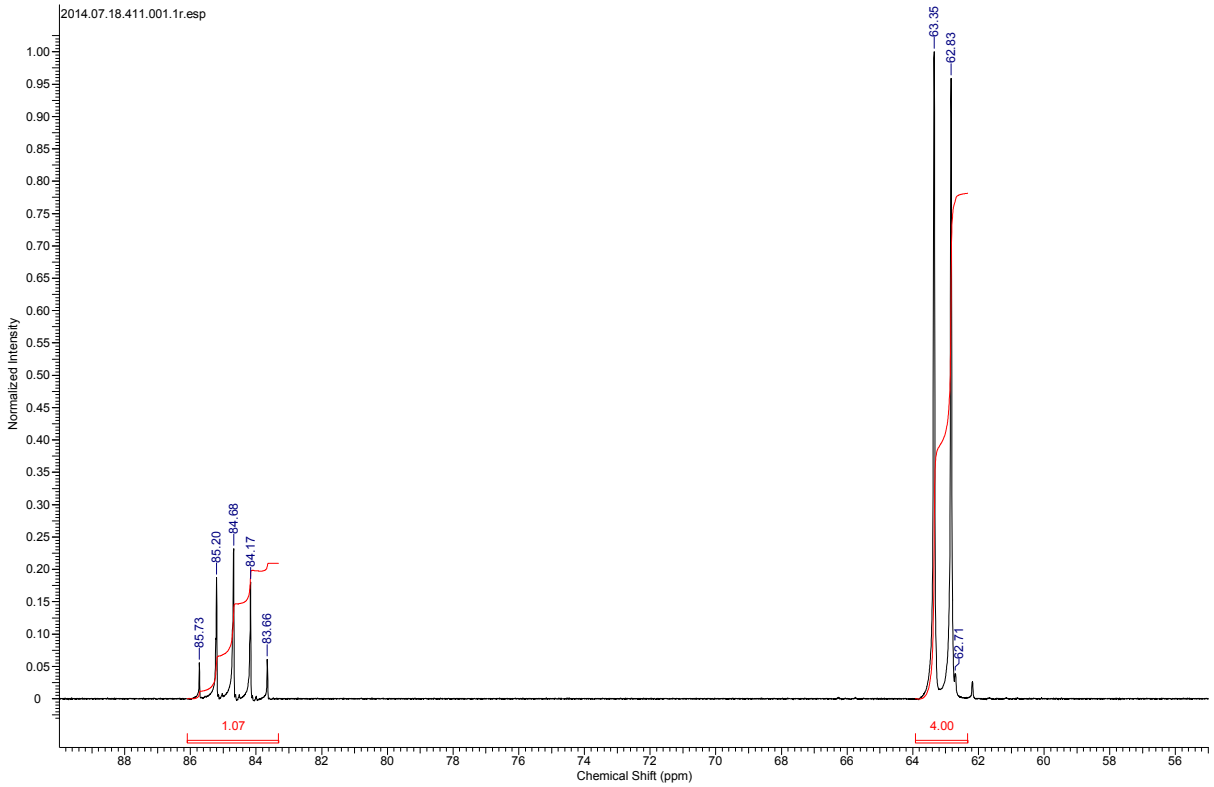

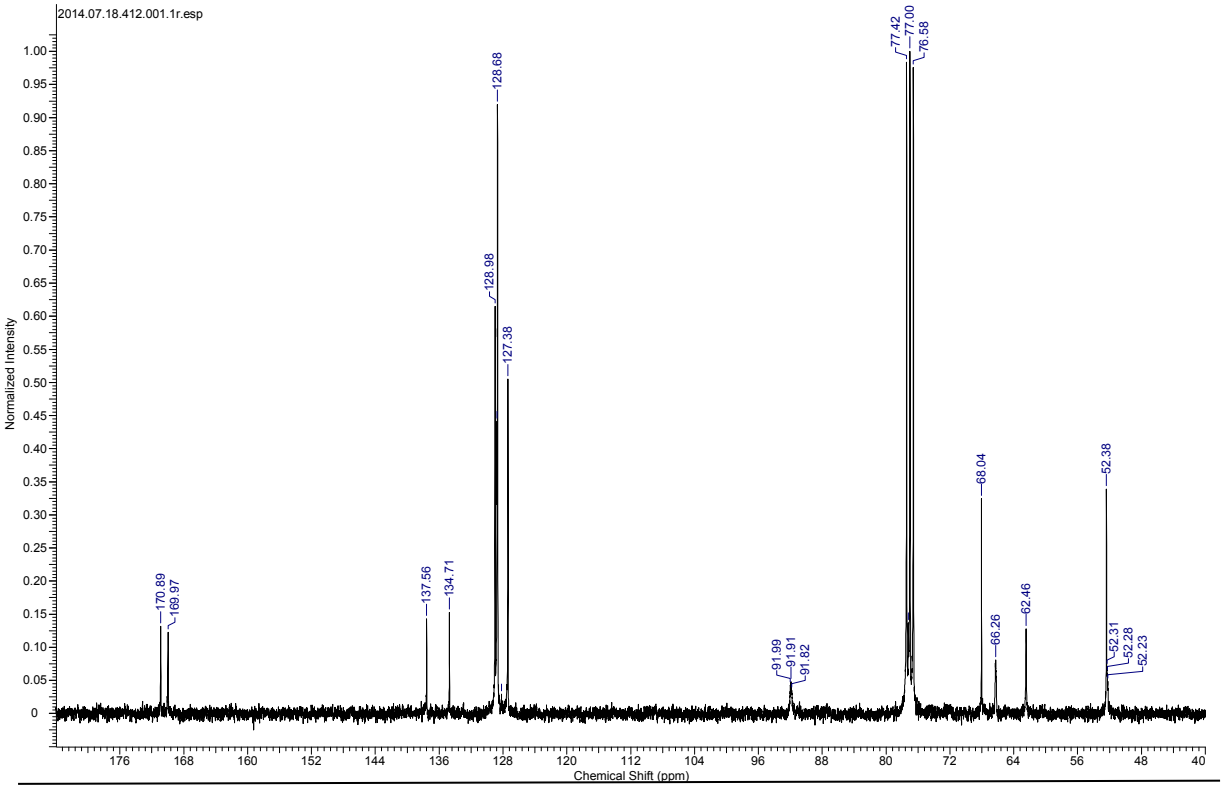
2014.07.18.412.001.1r.esp
Normalized Intensity
Chemical Shift (ppm)
170.89
169.97
137.56
134.71
128.98
128.68
127.38
91.99
91.91
91.82
77.42
77.00
76.58
68.04
66.26
62.46
52.38
52.31
52.28
52.23

^{1}H NMR, ^{19}F and ^{13}C ($CDCl_3$) spectra of **8'**

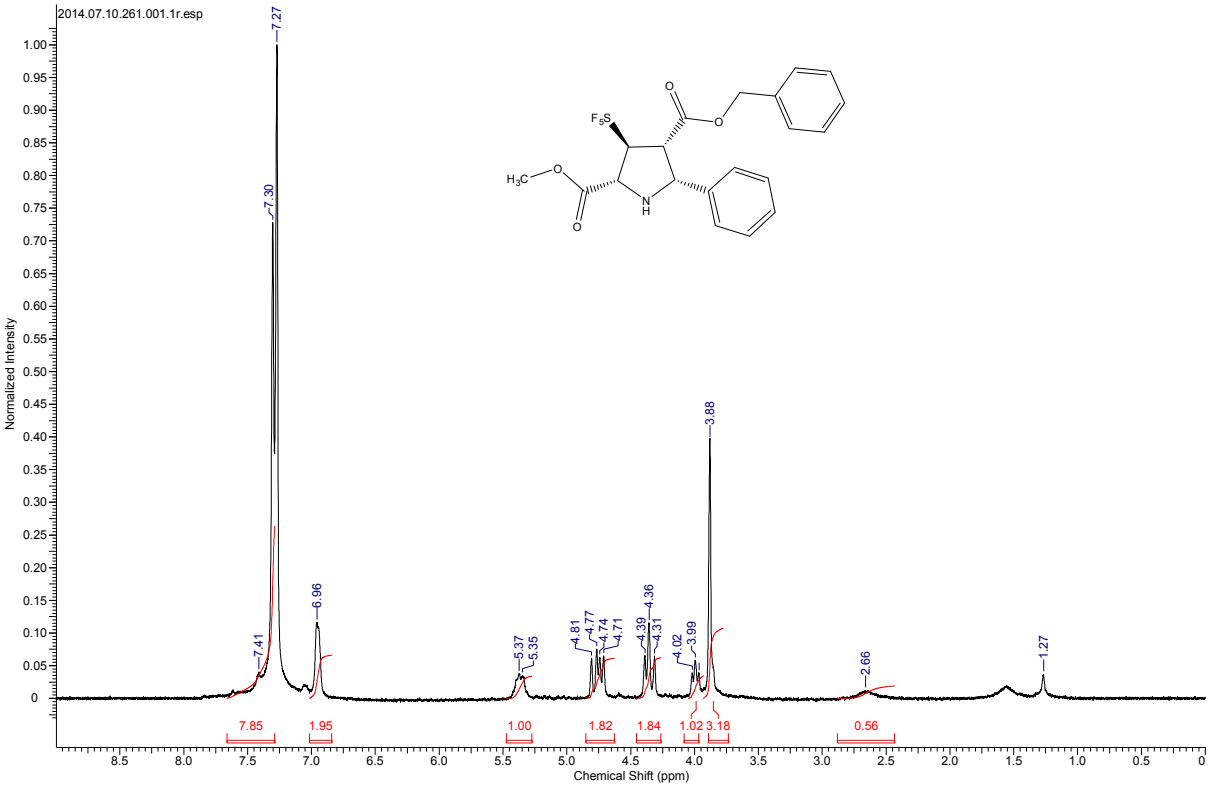

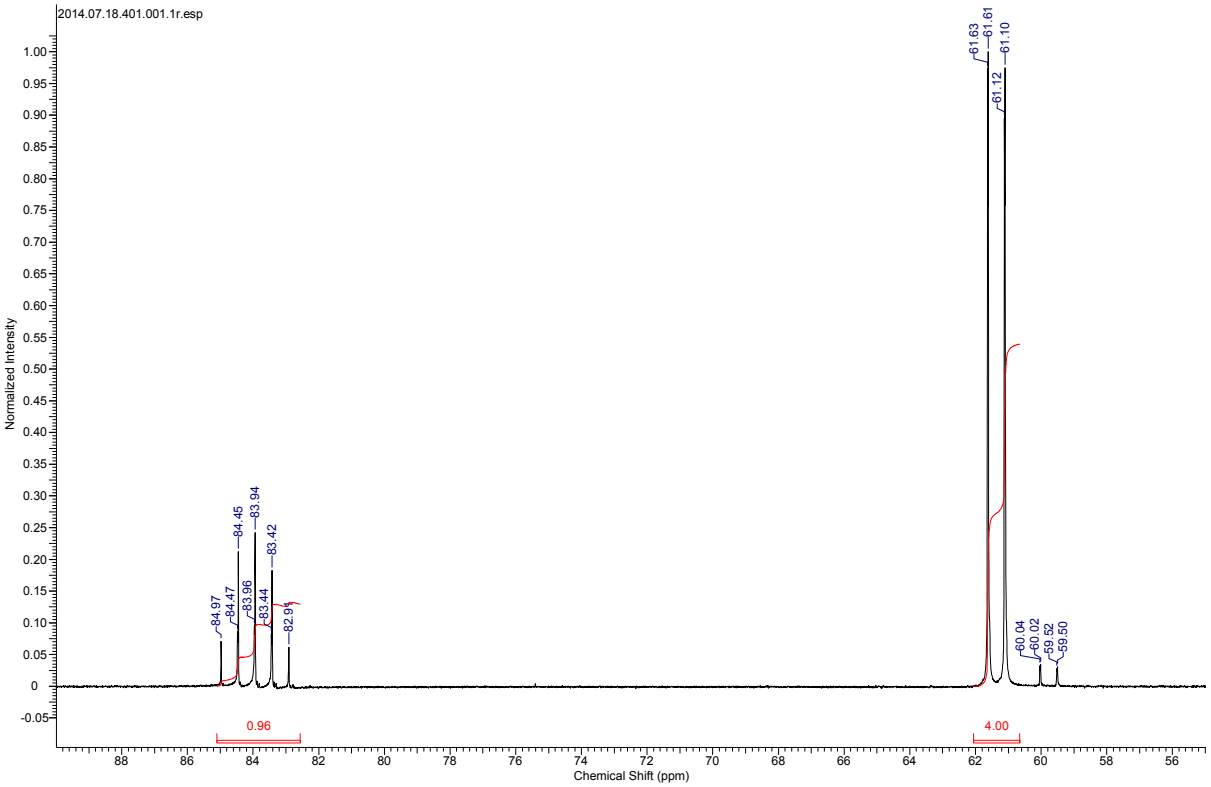

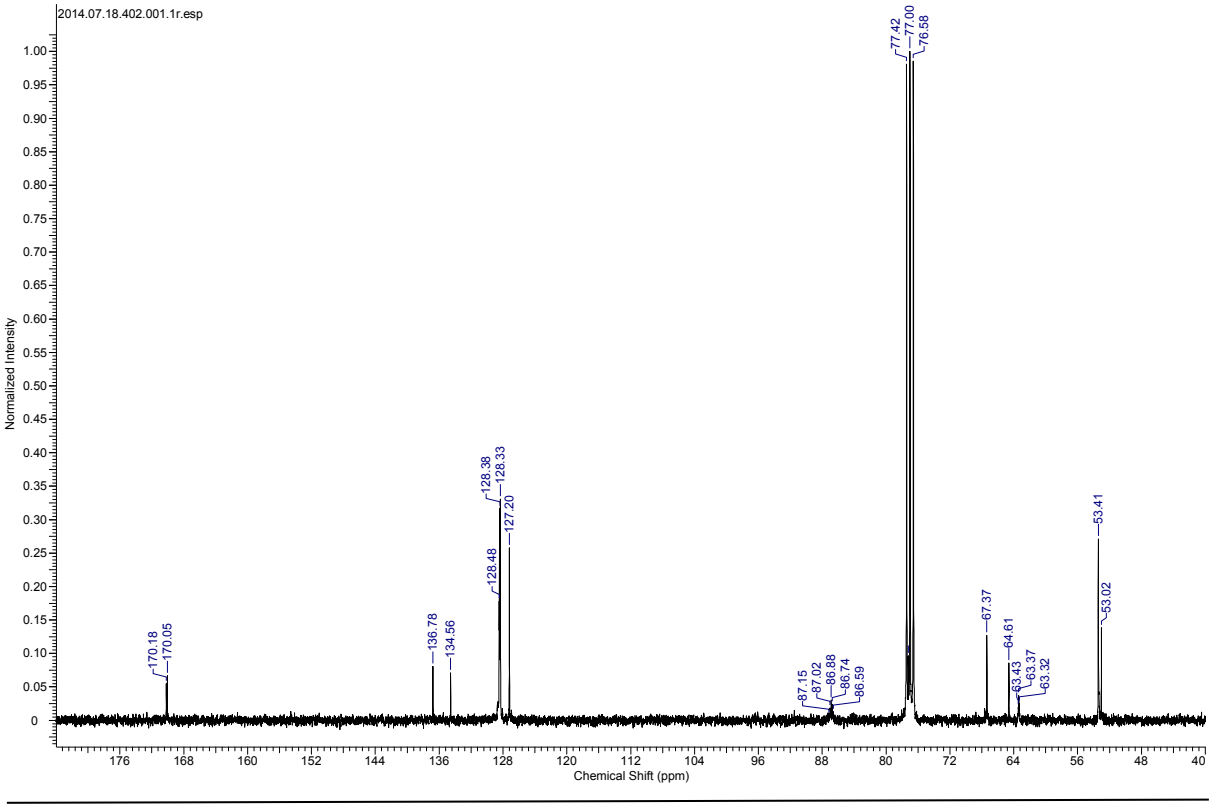
2014.07.18.402.001.1r.esp
Normalized Intensity
Chemical Shift (ppm)
170.18
170.05
136.78
134.56
128.48
128.38
128.33
127.20
87.15
87.02
86.88
86.74
86.59
77.42
77.00
76.58
67.37
64.61
63.43
63.37
63.32
53.41
53.02

^{1}H and ^{19}F NMR ($CDCl_3$) spectra of **9** (slightly contaminated with **9'**)

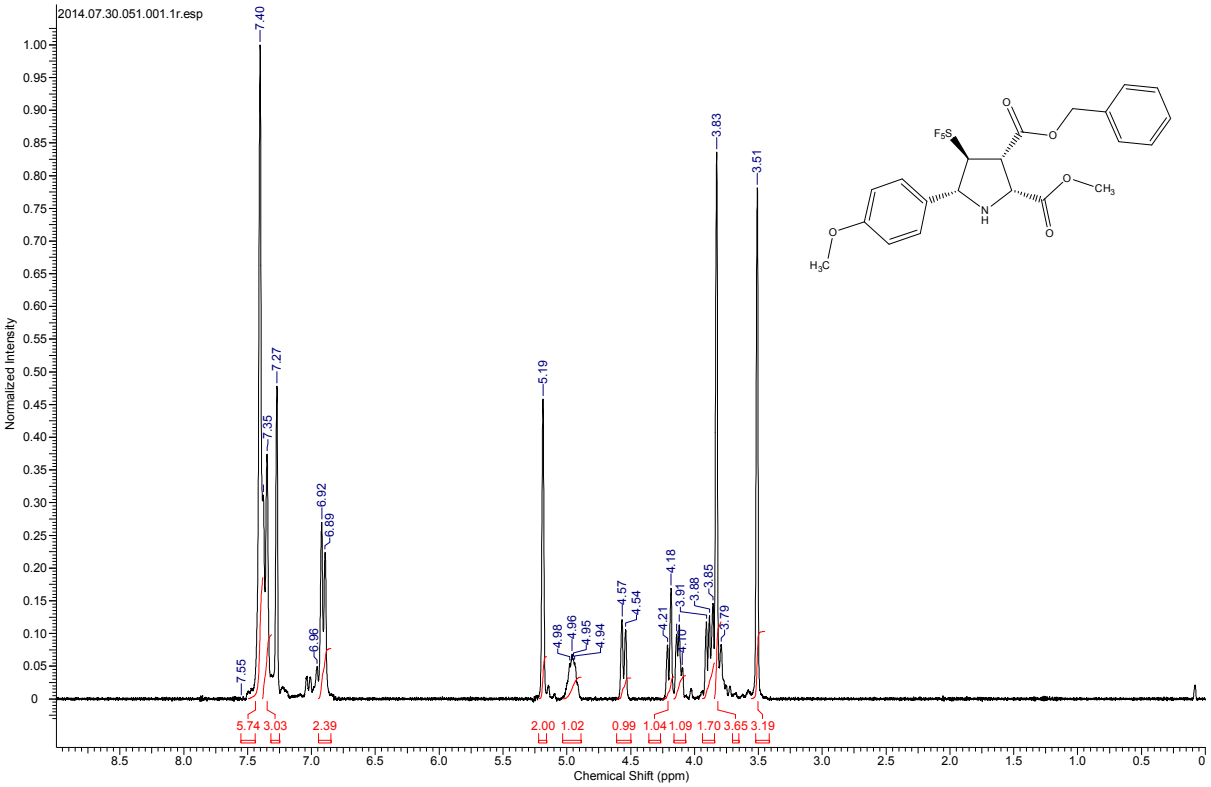

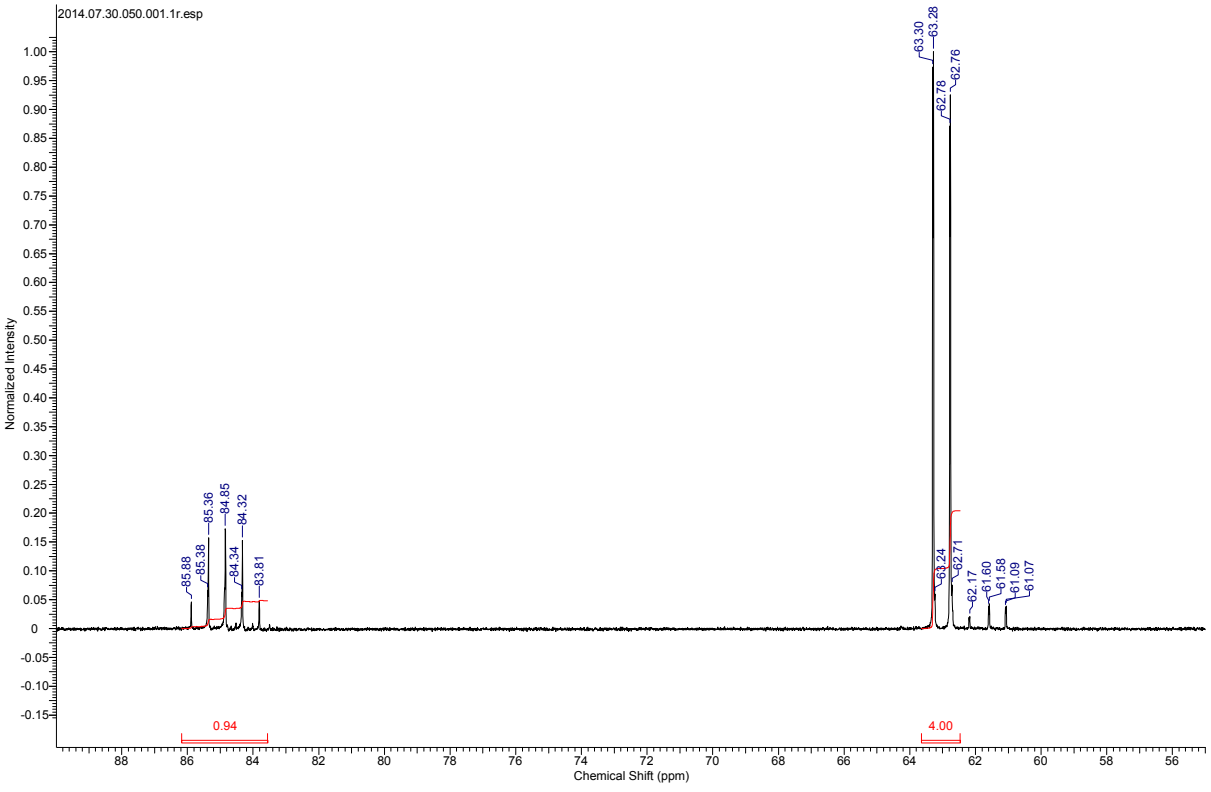

^{1}H and ^{19}F NMR ($CDCl_3$) spectra of **9'**

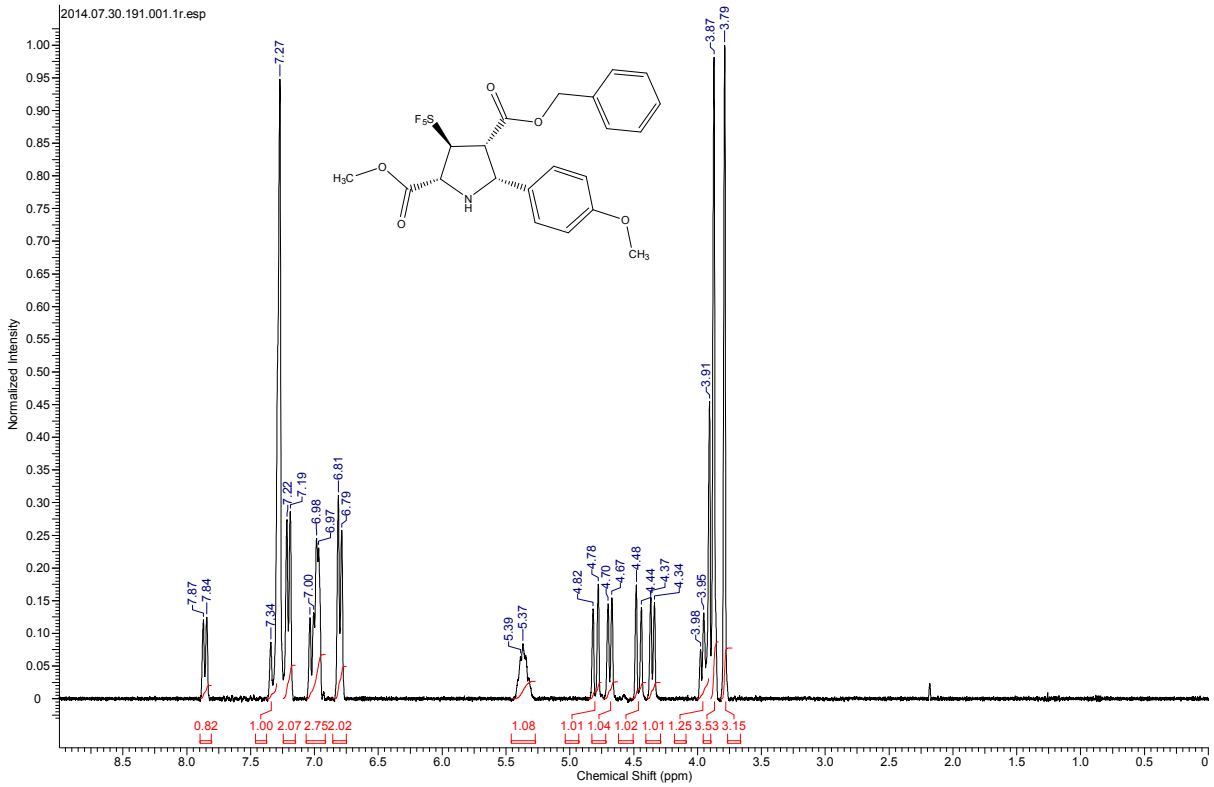

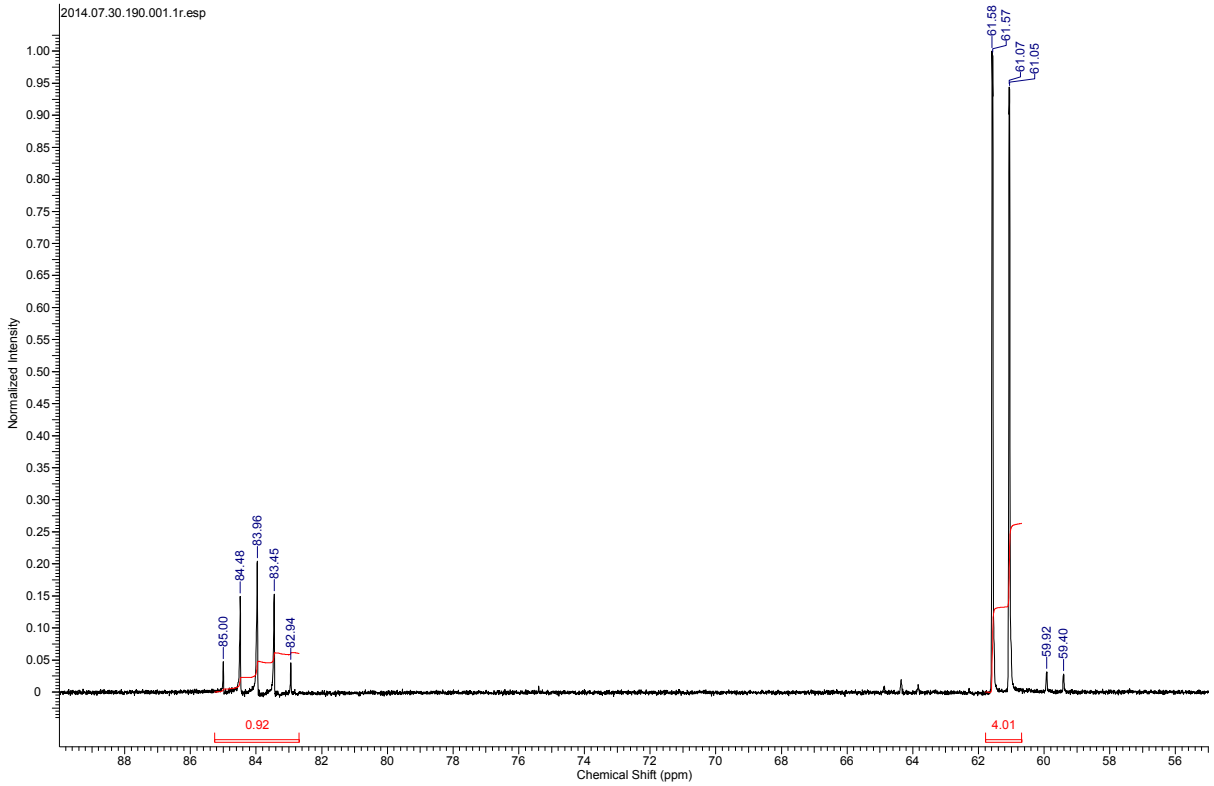

^{1}H, ^{19}F and ^{13}C NMR ($CDCl_3$) spectra of **10**

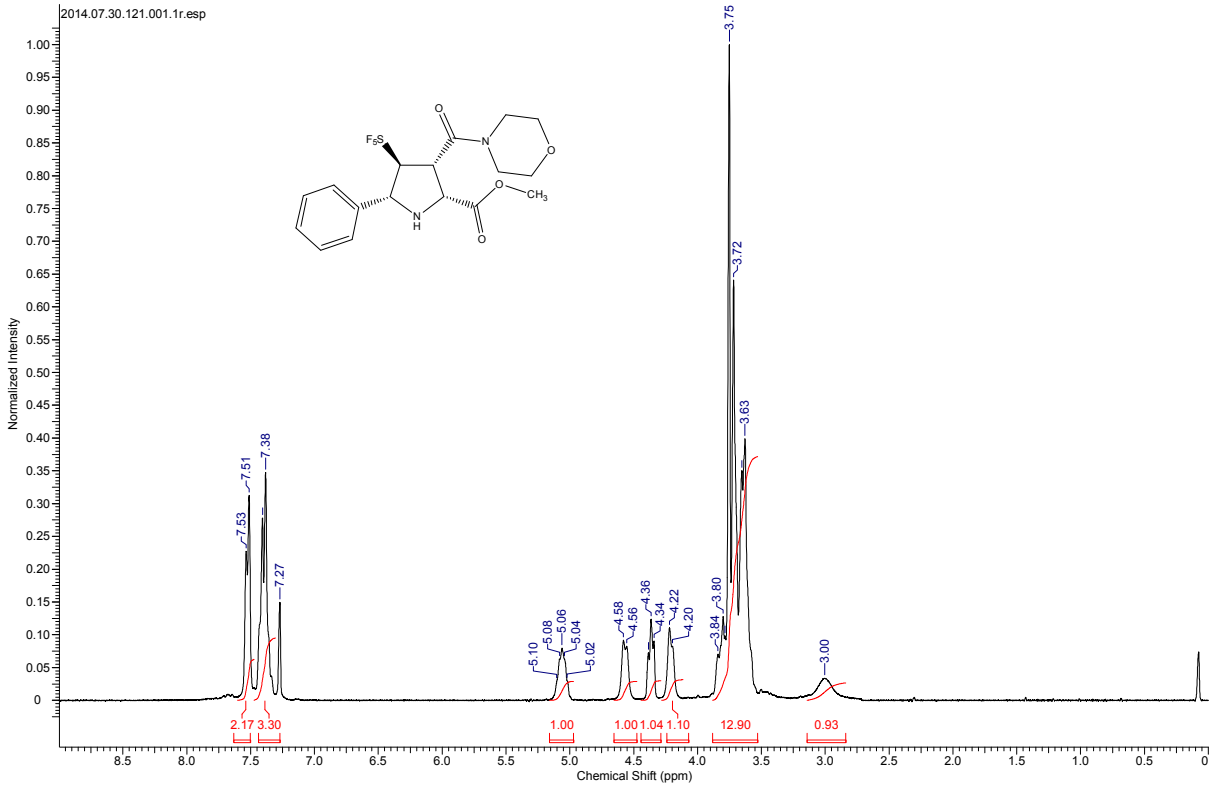

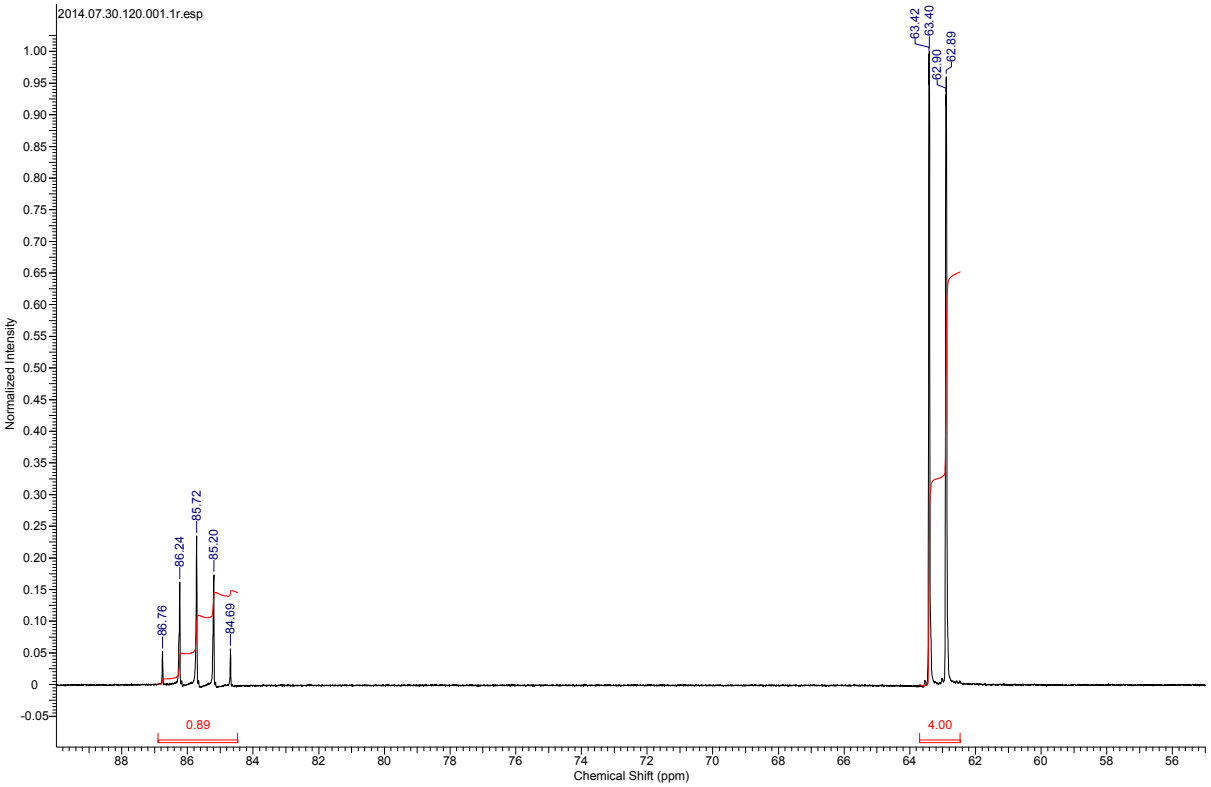
2014.07.30.120.001.1r.esp
Normalized Intensity
Chemical Shift (ppm)
63.42
63.40
62.90
62.89
86.24
85.72
85.20
86.76
84.69
0.89
4.00

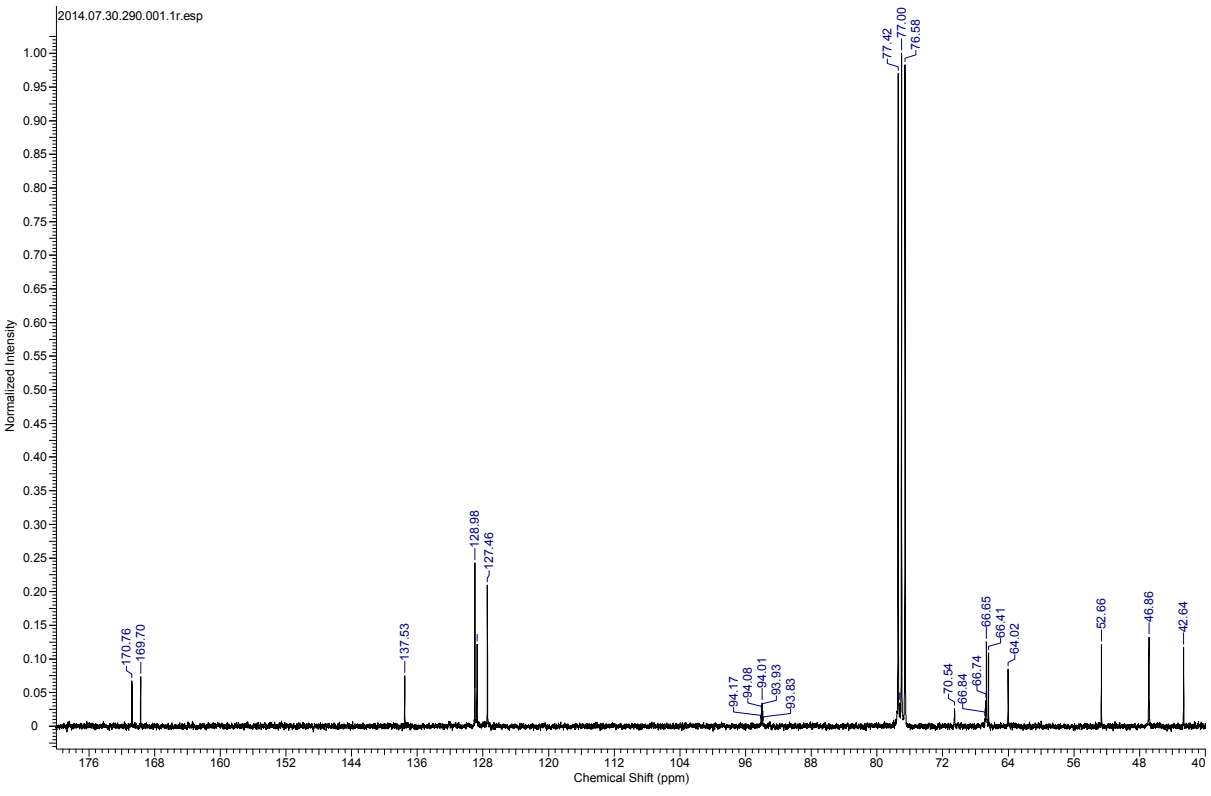
2014.07.30.290.001.1r.esp
Normalized Intensity
Chemical Shift (ppm)
77.42
77.00
76.58
128.98
127.46
170.76
169.70
137.53
94.17
94.08
94.01
93.93
93.83
70.54
66.84
66.74
66.65
66.41
64.02
52.66
46.86
42.64

^{1}H, ^{19}F and ^{13}C NMR ($CDCl_3$) spectra of **10'** (slightly contaminated with **10**)

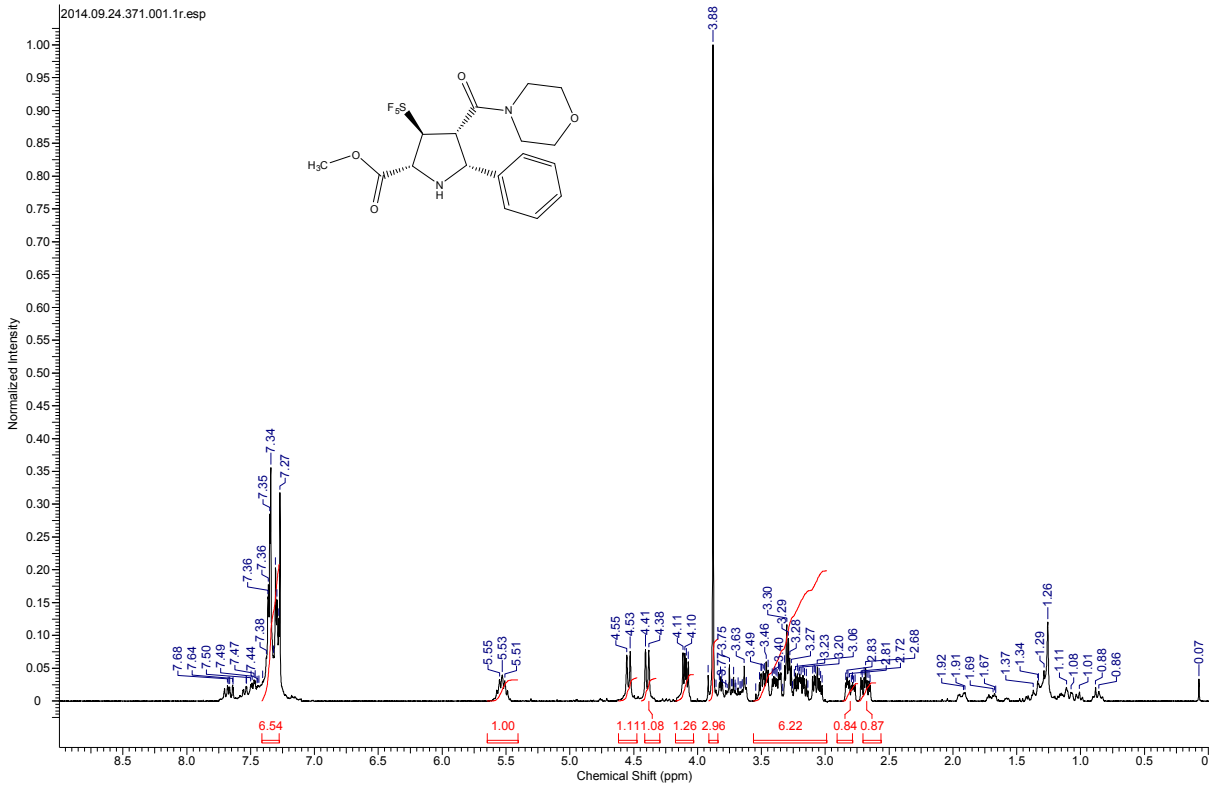

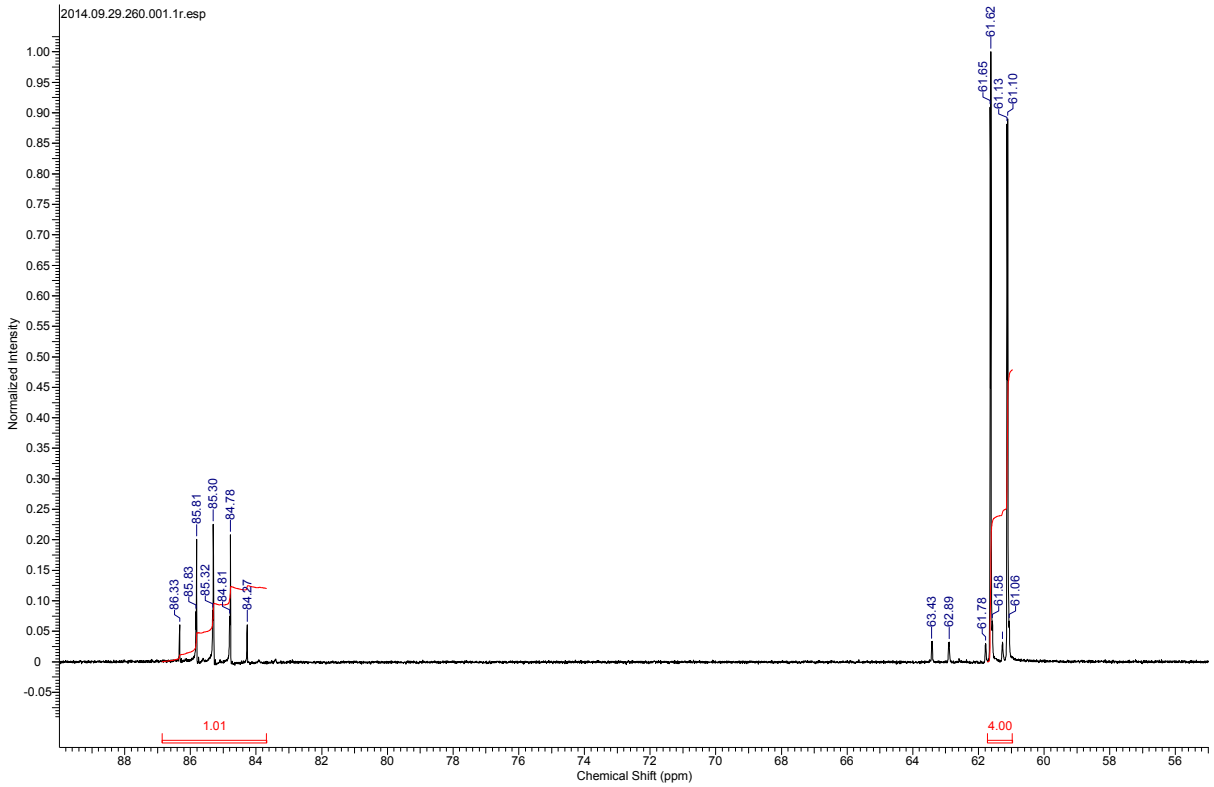

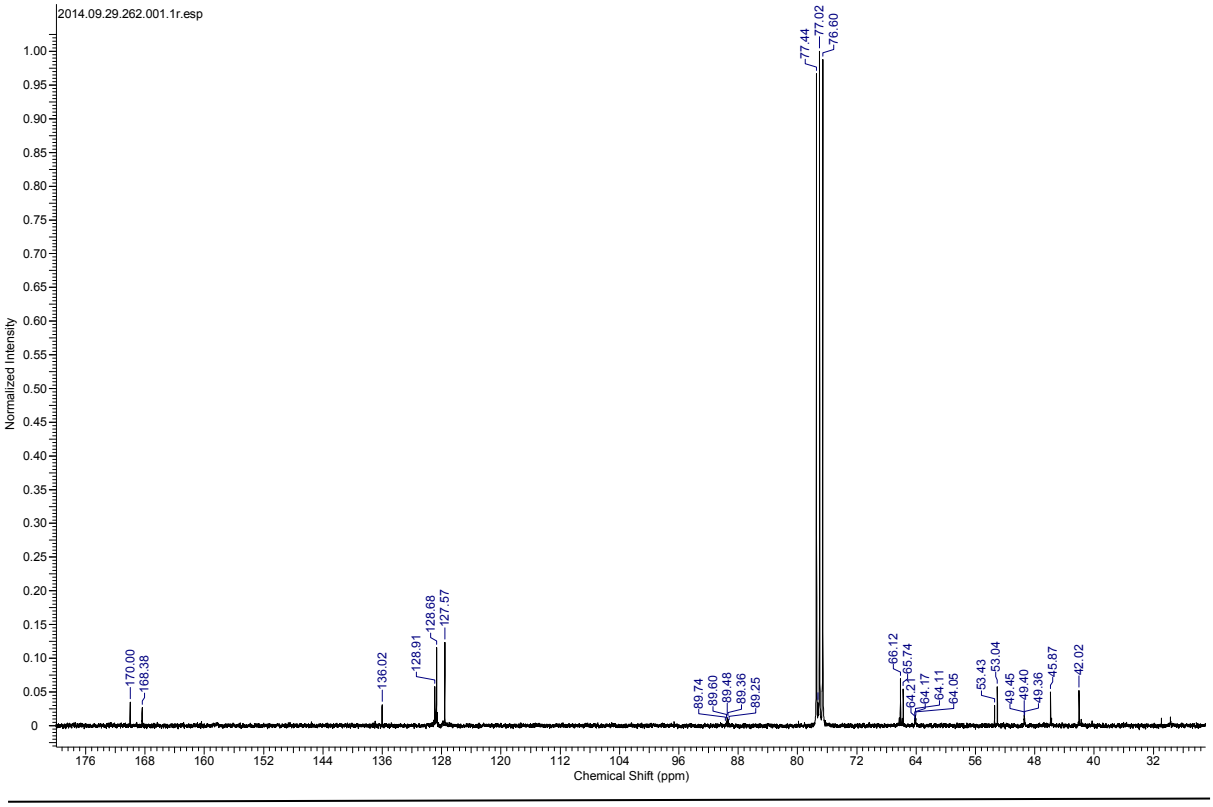
2014.09.29.262.001.1r.esp
Normalized Intensity
Chemical Shift (ppm)
77.44
77.02
76.60
170.00
168.38
136.02
128.91
128.68
127.57
89.74
89.60
89.48
89.36
89.25
66.12
65.74
64.21
64.17
64.11
64.05
53.43
53.04
49.45
49.40
49.36
45.87
42.02

NOESY Experiments of compound **8'**

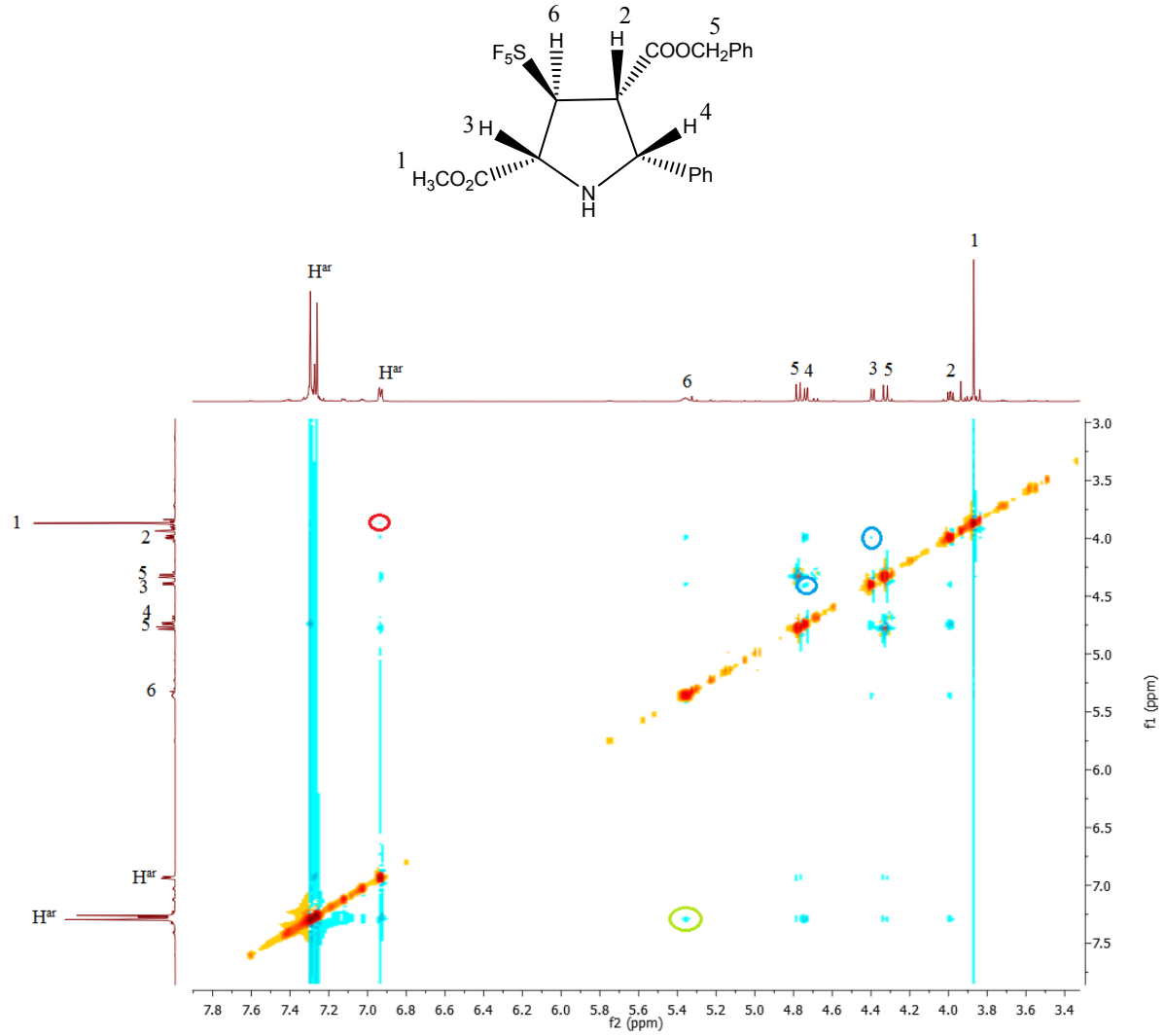

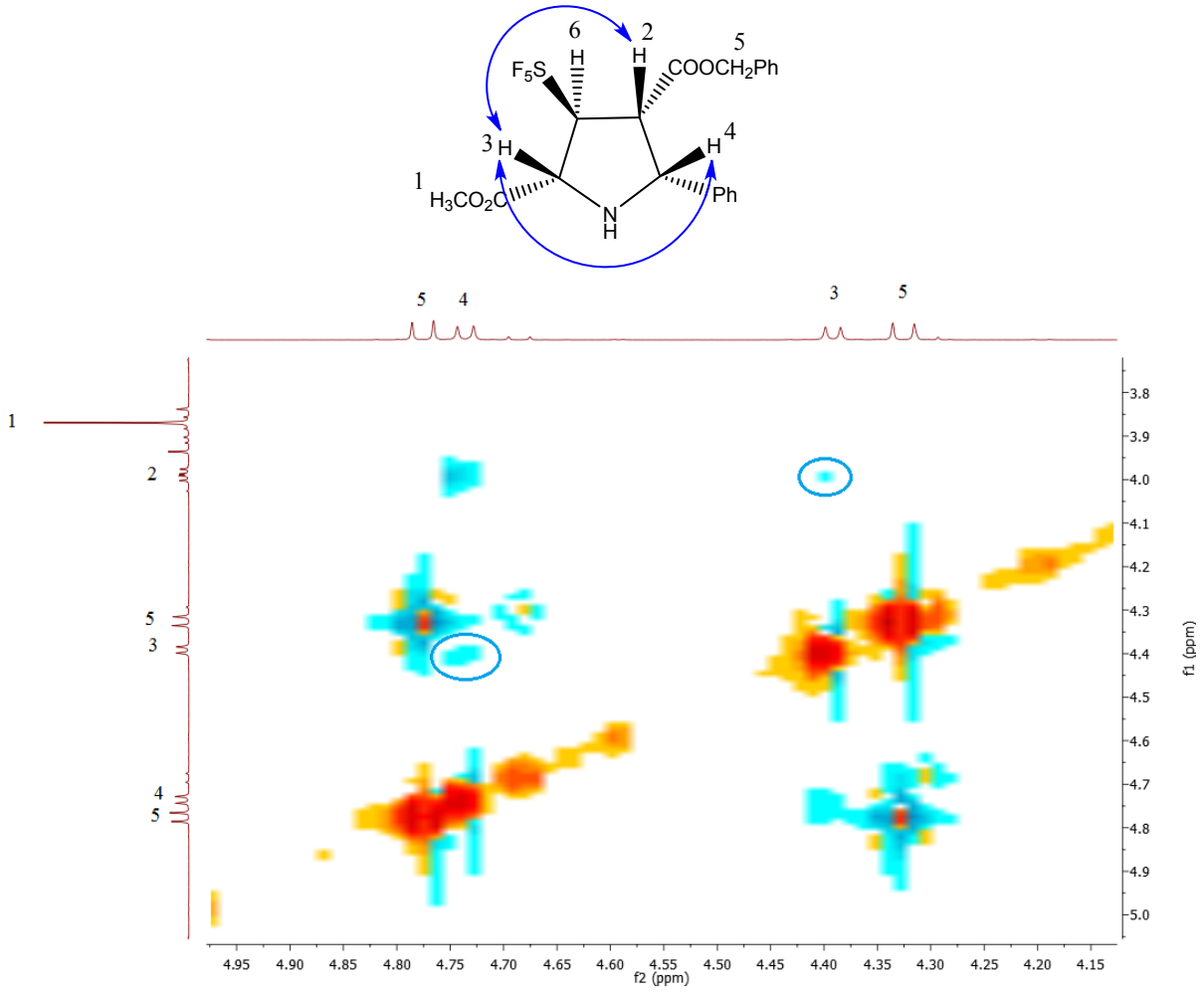
6
H
2
H
5
COOCH2Ph
F5S
3
H
4
H
1
H3CO2C
Ph
N
H
5
4
3
5
1
2
5
3
4
5
f2 (ppm)
f1 (ppm)

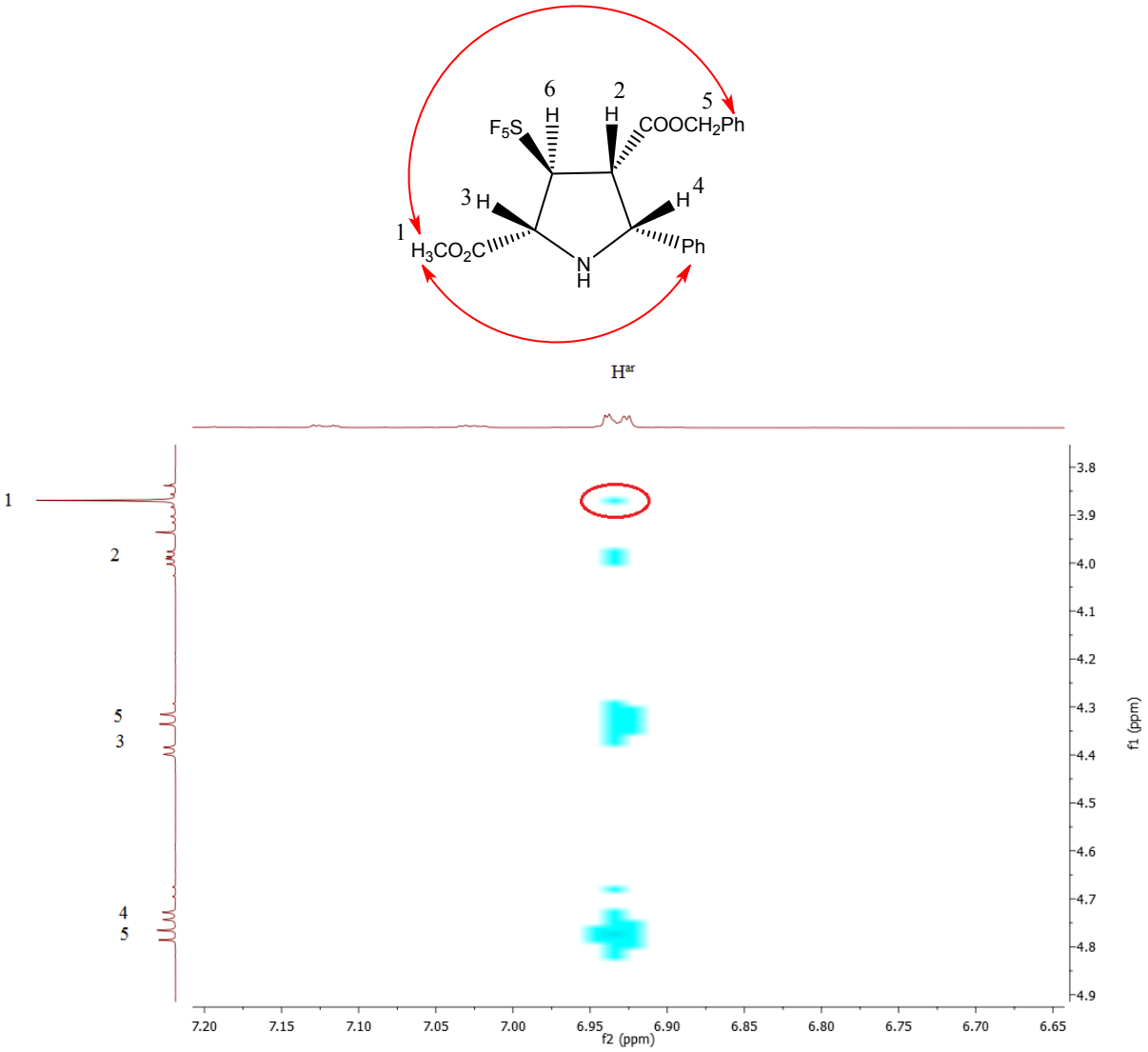
6
2
5
F5S
H
H
COOCH2Ph
3 H
H 4
1
H3CO2C
Ph
N
H
Har
1
2
5
3
4
5
7.20
7.15
7.10
7.05
7.00
6.95
6.90
6.85
6.80
6.75
6.70
6.65
f2 (ppm)
3.8
3.9
4.0
4.1
4.2
4.3
4.4
4.5
4.6
4.7
4.8
4.9
f1 (ppm)

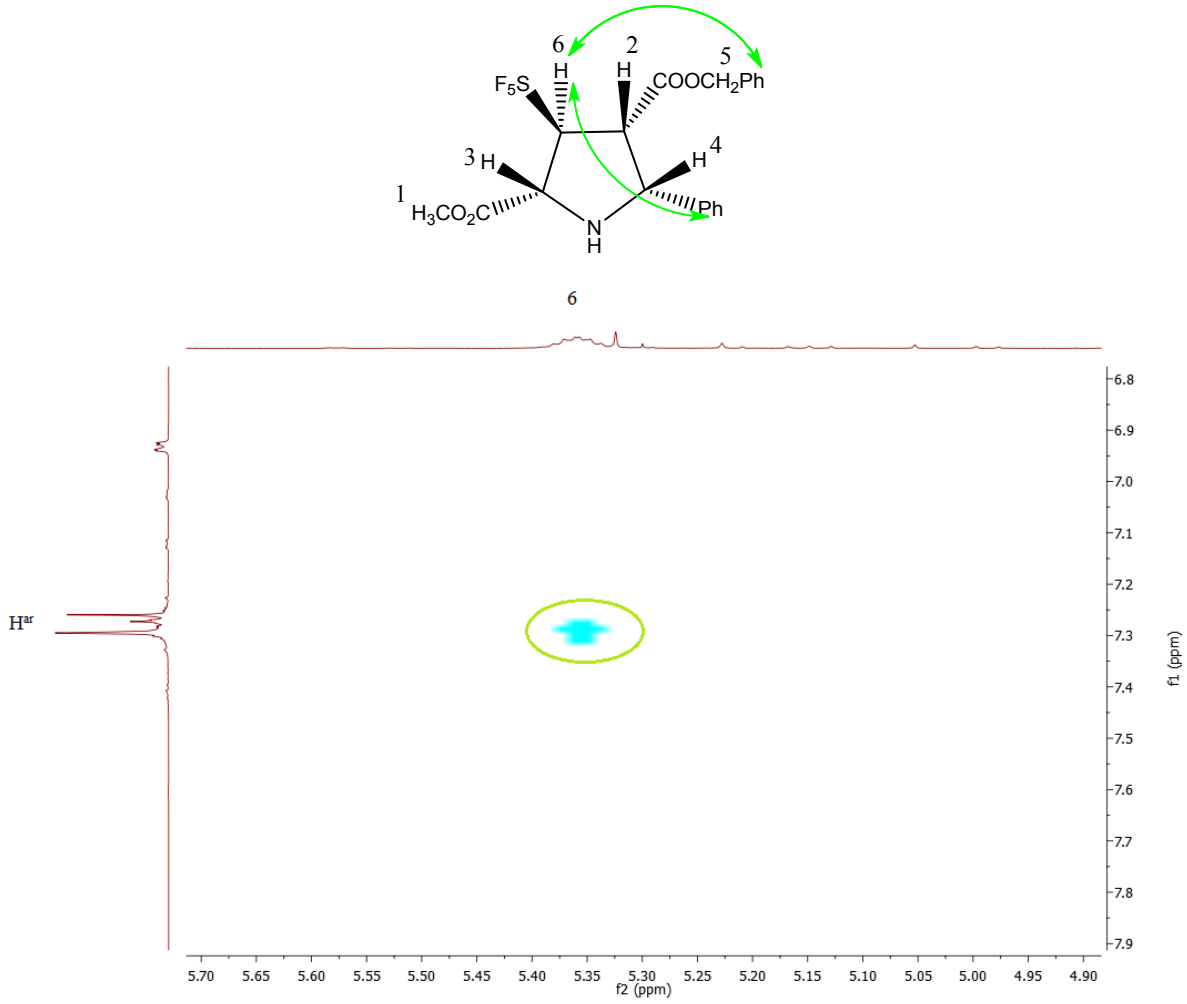
6
2
5
H
H
F5S
COOCH2Ph
3 H
H 4
1
H3CO2C
Ph
N
H
6
Har
6.8
6.9
7.0
7.1
7.2
7.3
7.4
7.5
7.6
7.7
7.8
7.9
f1 (ppm)
5.70
5.65
5.60
5.55
5.50
5.45
5.40
5.35
5.30
5.25
5.20
5.15
5.10
5.05
5.00
4.95
4.90
f2 (ppm)

7 References

(1) M. J. Frisch, et al. Gaussian 09 Revision D.01., Gaussian Inc., Wallingford, CT, 2009.

(2) J.-D. Chai, M. Head-Gordon, *Phys. Chem. Chem. Phys.*, 2008, **10**, 6615.

(3) P. J. Hay, W. R. Wadt, *J. Chem. Phys.*, 1985, **82**, 270.

(4) G. Scalmani, M. J. Frisch, *J. Chem. Phys.*, 2010, **132**, 114110.

(5) K. Fukui, *Acc. Chem. Res.*, 1981, **14**, 363.

(6) R. F. W. Bader, Atoms in Molecules: A Quantum Theory, Oxford University Press, 1990.

(7) T. A. Keith, AIMAll version 14.04.17, 2014, see aim.tkgristmill.com.

(8) V. Tognetti, C. Morell, P. W. Ayers, L. Joubert, H. Chermette, *Phys. Chem. Chem. Phys.*, 2013, **15**, 14465.

(9) (a) A. Toro-Labbé, *J. Phys. Chem. A*, 1999, **103**, 4398. (b) V. Labet, C. Morell, A. Toro-Labbé, A. Grand, *Phys. Chem. Chem. Phys*., 2010, **12**, 4142.

(10) P. Geerlings, F. De Proft, W. Langenaeker, *Chem. Rev.*, 2003, **103**, 1793.

(11) F. Zielinski, V. Tognetti, L. Joubert, *Chem Phys. Lett.*, 2012, **527**, 67.

(12) W. Yang, W. J. Mortier, *J. Am. Chem. Soc.*, 1986, **108**, 5708.

(13) L.-A. Jouanno, V. Di Mascio, V. Tognetti, L. Joubert, C. Sabot, P.-Y. Renard, *J. Org. Chem.*, 2014, **79**, 1303.

(14) SMART for WNT/2000 V5.622 (2001), Smart software reference manual, Bruker Advanced X Ray Solutions, Inc., Madison, Wisconsin, USA.

(15) SAINT+ V6.02 (1999), Saint software reference manual, Bruker Advanced X Ray Solutions, Inc., Madison, Wisconsin, USA.

(16) WinGX: Version 1.70.01: An integrated system of Windows Programs for the solution, refinement and analysis of Single Crystal X-Ray Diffraction Data, L. J. Farrugia, Dept. of chemistry, University of Glasgow. L. J. Farrugia, *J. Appl. Cryst.,* 1999, **32**, 837.

(17) SHELXS-97: A program for crystal structure refinement, G. M. Sheldrick, University of Goettingen, Germany, 1997. G. M. Sheldrick, *Acta Cryst*., 1990, **A46**, 467.